Supporting Information for

# Catalyst Halogenation Enables Rapid and Efficient Polymerizations with Visible to Near-Infrared Light

Alex Stafford,[a] Dowon Ahn,[a] Emily K. Raulerson,[a] Kun-You Chung,[a] Kaihong Sun,[a] Danielle M. Cadena,[a] Elena M. Forrister,[b] Shane R. Yost,[b] Sean T. Roberts,[a] and Zachariah A. Page*[a]

[a]Department of Chemistry, The University of Texas at Austin, Austin, Texas 78712, USA.

[b]Department of Chemistry and Biochemistry, Texas State University, San Marcos, TX 78666, USA.

*email: zpage@utexas.edu

## Table of Contents

## EXPERIMENTAL DETAILS

### *Materials*

*Chemicals*: *2,4-Dimethyl-1H-pyrrole 97%* and *1-chloropyrrolidine-2,5-dione (NCS) 97%* were purchased from Ark Pharm. *2,4,6-trimethyl-benzaldehyde 97%*, *dichloromethane (DCM)* 99.9%, anhydrous, *potassium hydroxide (KOH)* (certified ACS), *methanol (MeOH)* (certified ACS), and *toluene* (Certified ACS) were purchased from Fisher Scientific. *Trifluoroacetic acid (TFA) >99.9%*, *2,3-dichloro-5,6-dicyano-1,4-benzoquinone (DDQ) 99.15%*, *N-bromosuccinimide (NBS) 99.98%* were purchased from Chem-Impex. *Triethylamine ≥99.5%*, *3,4,5-trimethoxybenzaldehyde 98%, and Uvasol® acetonitrile for spectroscopy* was purchased were purchased from Sigma-Aldrich. *Boron trifluoride diethyl etherate 98%* was purchased from Oakwood Chemical. *N-iodosuccinimide (NIS)* was purchased from Combi-Blocks. *4'-tert-butylacetophenone 95%* was purchased from Matrix Scientific**.** *Nitromethane >98%* was purchased from TCI Chemicals. *Ammonium acetate ≥97.0%* was purchased from Alfa Aesar. *Rhodamine 6G*, 99%, pure, laser grade, was purchased from ACROS Organics. *H-Nu 254, Onium Salt* and *Borate V* were purchased from Spectra Group Limited, Inc. *$CDCl_3$ 99.8%* was purchased from Cambridge Isotope Laboratories. All chemicals were used as received without additional purification, unless otherwise noted.

### *Equipment and Instrumentation*

*Nuclear Magnetic Resonance (NMR) Spectroscopy*
NMR spectra were recorded on an Agilent MR 400 MHz spectrometer utilizing $CDCl_3$ as the solvent. $^{1}H$ NMR were carried out coupled and referenced to the $CDCl_3$ chemical shift at 7.26 ppm. $^{13}C$ NMR were carried out decoupled and referenced to the $CDCl_3$ chemical shift at 77.16 ppm.

*High Resolution Mass Spectrometry (HRMS)*
HRMS was performed on an Agilent Technologies 6530 Accurate-Mass Q-TOF LC/MS using ESI and the data was subsequently analyzed using Agilent MassHunter Qualitative Analysis Software.

*Real-Time Fourier-Transform Infrared Spectroscopy (RT-FTIR)*
RT-FTIR was recorded utilizing an INVENIO-R FT-IR Spectrometer from Bruker (**Figure S1**) and controlled via OPUS Spectroscopy Software. A liquid nitrogen cooled (LN-MCT Mid) detector was used for measurements. A modified GladiATR Illuminate ATR accessory[1] from PIKE Technologies was used to analyze chemical composition and monitor photocuring of liquid resins upon exposure to light. Collimated LED light sources (530 nm-P/N LCS-0530-15-22, 656 nm-P/N LCS-0656-07-22, and 740 nm-P/N LCS-0740-10-22) from Mightex Systems along with Lightguide Adapters were utilized to irradiate resins with visible light (see photopolymerization procedure for more details). LED Controller M/N SLC-MA02-U was used with a 3 mm liquid light guide (LLG-3-4H).

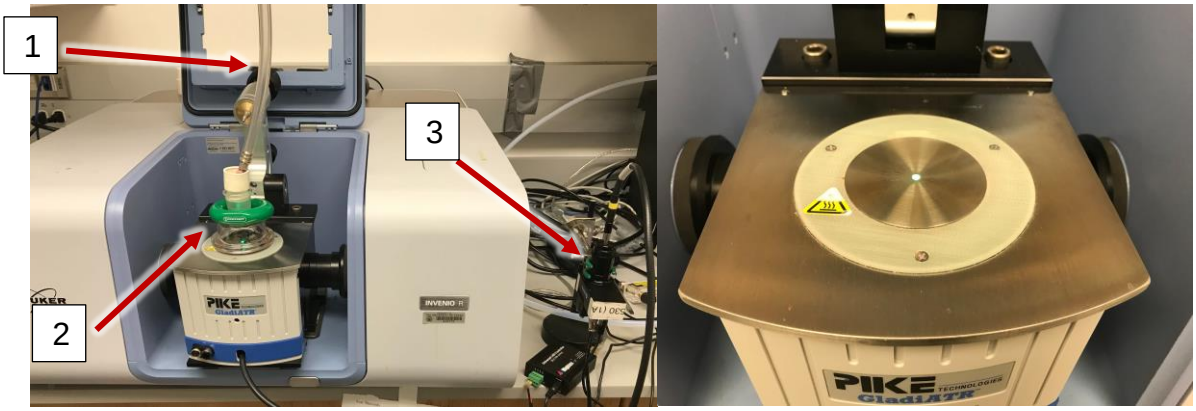


**Figure S1**. Photo-ATR FTIR Setup (1) Argon/Nitrogen gas line (2) Custom glass top with O-ring to create oxygen free atmosphere (3) LED and liquid light guide. Close-up image of custom ATR accessory with green LED on.

*Steady-State Optical Characterization*

UV-visible absorption spectra were recorded on an Ocean Optics QE PRO-ABS Fiber Optic Spectrometer utilizing deuterium-tungsten halogen light sources (DH-2000-BAL). 600 µm fiber-optic cables (QP600-025-SR) were coupled to the detector with a slit width of 5 µm. Dilute absorption data was collected in acetonitrile utilizing quartz cuvettes and a qpod sample holder (QNW qpod2e). Thin-film absorption data was collected in the resin formulation (see photopolymerization conditions) utilizing the Ocean Optics Stage RTL-T.

*Transient Absorption Characterization*

1) Femtosecond time-resolved experiments: Transient absorption (TA) spectra that monitored photoexcited sample dynamics on femtosecond to sub-nanosecond timescales were performed using an experimental layout described in prior work.[2,3] Briefly, excitation and probe pulses were derived from the output of a Ti:sapphire regenerative amplifier (Coherent Legend Elite Duo: 3 kHz repetition rate, ~4.2 mJ, ~90 fs). Excitation pulses centered at 525 nm used to photoexcite Mes-BODIPY derivatives were produced by using the Ti:sapphire laser to pump a home-built noncollinear optical parametric amplifier (NOPA). Pulses centered at 645 nm used to excite **aza-H** and **aza-Br** were created by using a β-barium borate (BBO) crystal to frequency double signal output of a commercial optical parametric amplifier (Light Conversion, TOPAS-prime). Spectrally-broad probe pulses (450 – 800 nm) were derived via self-phase modulation by focusing a small portion of the Ti:sapphire output into a 3 mm thick c-cut sapphire window. A computer controlled optical delay stage (Newport ILS300LM) was used to scan the time of arrival of the probe at the sample with respect to the pump. Pump-induced changes in probe transmission through each sample solution were detected using a Si CCD (Princeton Instruments, PyLoN 100BR) interfaced with a Czerny-Turner spectrometer (Acton Instruments SP-2556). Sample solutions were prepared by dissolving dry powder of each compound in acetonitrile. Sample solutions were housed in 1 mm path length quartz cuvettes and degassed using nitrogen prior to experiments.
2) Nanosecond time-resolved experiments: For experiments that probed the photoexcited dynamics of **Mes-Cl**, **Mes-Br**, and **Mes-I** over nanosecond-to-microsecond timescales, the probe pulse and detection setup were identical to that used for femtosecond resolution experiments. However, the excitation pulse was replaced by the frequency-doubled output of a Q-switched Nd:YAG laser (Alphalas Pulselas-A: 532 nm, <1 ns, 8.7 µJ). Scanning of the time delay between the pump and probe was achieved by using an electronic delay generator (Stanford Research Systems DG535) to synchronize the operation of the Ti:sapphire and Q-switched Nd:YAG lasers.

*Fluorescence Measurements*

All fluorescence measurements were recorded on an Agilent Cary Eclipse Fluorescence Spectrophotometer. The fluorometer is equipped with a Unique Agilent Xenon flash lamp (190 nm – 1100 nm) as the light source, and a high performance R928 photomultiplier (PMT) (200 nm – 900 nm) detector. The sensitivity of this system is >4000:1 RMS (350 nm) and >1400:1 RMS (500 nm) after the calibration.

*Electronic Characterization*

Cyclic voltammetry (CV) was performed in an argon-filled MBraun glovebox using the CHI 660D Electrochemistry Workstation housed within the Center for Electrochemistry at The University of Texas at Austin. A single-compartment three-electrode cell was used with glassy carbon as the working electrode, a platinum wire as the counter electrode, and an $Ag/AgNO_3$ (0.01 M) non-aqueous reference electrode calibrated versus Fc/Fc+ in 0.1 M tetrabutylammonium hexafluorophosphate ($TBAPF_6$) acetonitrile solutions ($E_{½}$(Fc/Fc+) = 0.1 V vs Ag/Ag+) with a 0.1 V/s scan rate. Oxidation onsets were utilized to calculate the highest occupied molecular orbital (HOMO) energy levels -(4.8 eV $-E_{oxFerrocene} + E_{ox}$) and reduction onsets to calculate the lowest unoccupied molecular orbital (LUMO) energy levels -(4.8 eV $-E_{oxFerrocene} + E_{red}$)[4].

*LED Light Sources*

All LEDs used were purchased from the Mightex Systems. The product numbers for the three LEDs listed are LCS-530-15-xx, LCS-656-07-xx, and LCS-740-10-xx. The emission profile for each LED was measured using a calibrated UV-Vis Ocean Insight system (**Figure S2**). Intensity measurements were recorded with a QE pro spectrometer, in which the LED was connected to the fiber optic system using a 3 mm liquid lightguide from Mightex Systems (serial #: LLG-03-59-340-0800-1).

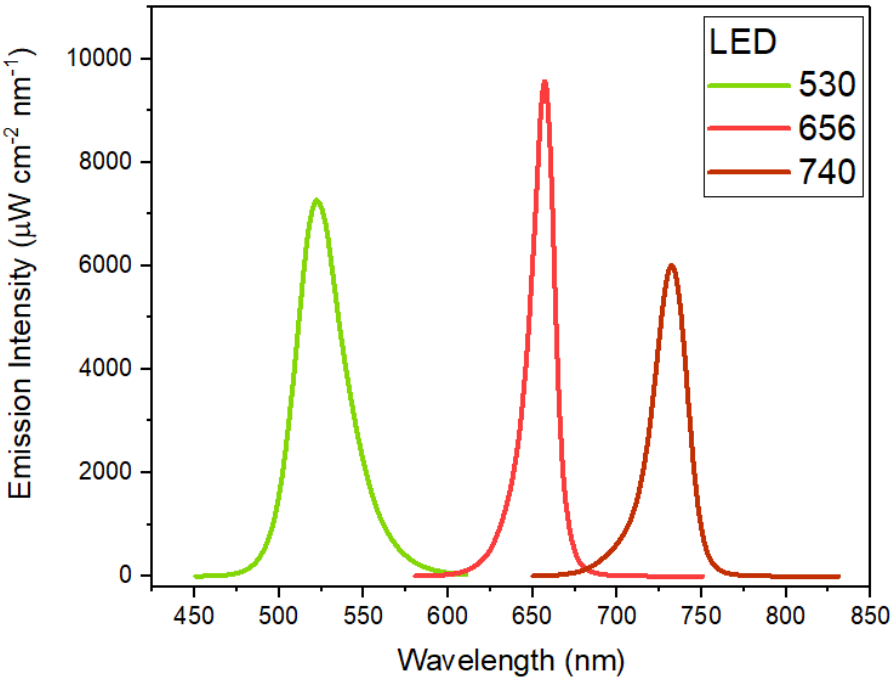


**Figure S2**. The emission intensity profile of the three LEDs. The input current for all three LEDs were 50 mA.

***Synthesis***

The syntheses of Mes-BODIPY derivatives were accomplished in an analogous fashion to that previously reported in literature (**Scheme S1**).[5,6]

**Scheme S1**. Synthesis of Mesityl BODIPYs

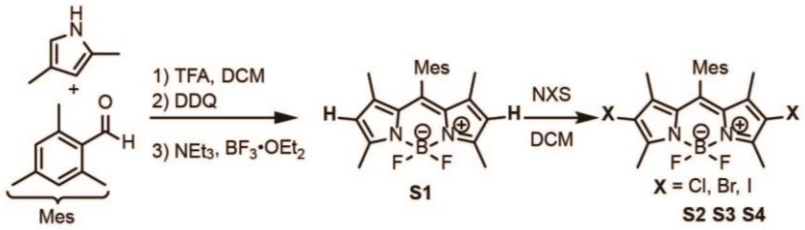


**5,5-difluoro-10-mesityl-1,3,7,9-tetramethyl-5H-4l4,5l4-dipyrrolo[1,2-c:2',1'-f][1,3,2]diazaborinine (S1).** 2,4-dimethyl-1H-pyrrole (1.18 g, 1.28 mL, 1 Eq, 12.4 mmol) was added to 250 mL of DCM in a dry 500 mL 2-neck round bottom flask in a nitrogen filled glovebox. 2,4,6-trimethylbenzaldehyde (0.73 g, .73 mL, 0.40 Eq, 5.0 mmol) was added to the solution. The round bottom was removed from the glovebox and placed under $N_2$. 50 µL of TFA in 2.5 mL of dry DCM was added slowly to the reaction flask while stirring and after complete addition the reaction was stirred for 3 hr. The reaction was monitored via thin layer chromatography (TLC) (1:1 DCM:hexane). After reaction completion, the round bottom was placed in an ice bath and 1.13 g of DDQ (0.40 Eq, 5.0 mmol) was added to the flask and stirred for 10 min while on ice then 1 hr at room temp. 10 mL of $NEt_3$ (5.8 Eq, 72 mmol) was added to the reaction mixture and stirred for 10 min. 10 mL of $BF_3$•$OEt_2$ (6.5 Eq, 81 mmol) was added slowly to the reaction flask and stirred for 2 hr. Crude product was washed with sat. $Na_2CO_3$ (3 x 50mL) and the organic layer subsequently dried with anh. $MgSO_4$, filtered, concentrated under reduced pressure using rotary evaporation, and purified via column chromatography (1:1 DCM:hexane) to yield the desired product as an orange solid (1.170 g, 65%). $^1$H NMR (400 MHz, $CDCl_3$) δ 6.94 (s, 2H), 5.96 (s, 2H), 2.56 (s, 6H), 2.33 (s, 3H), 2.09 (s, 6H), 1.38 (s, 6H); $^{13}$C NMR (100 MHz, $CDCl_3$) δ 155.0, 142.3, 141.6, 138.5, 134.9, 131.1, 130.6, 128.9, 120.8, 21.2, 19.5, 14.6, 13.4; IR (ATR): 2950, 2918, 2858, 1537, 1501, 1463, 1435, 1406, 1362, 1303, 1187, 1152, 1122, 1103, 1083, 1061, 1046, 970, 702 cm$^{-1}$; HRMS (ESI): exact mass calculated for $C_{22}H_{25}BF_2N_2$ $[M+Na]^+$ 389.1976, found 389.1980

**2,8-dichloro-5,5-difluoro-10-mesityl-1,3,7,9-tetramethyl-5H-4l4,5l4-dipyrrolo[1,2-c:2',1'-f][1,3,2]diazaborinine (S2, Mes-Cl).** 5,5-difluoro-10-mesityl-1,3,7,9-tetramethyl-5H-4l4,5l4-dipyrrolo[1,2-c:2',1'-f][1,3,2]diazaborinine (**S1**) (100 mg, 1 Eq, 273 µmol) was dissolved in 10 mL of dry DCM in a 100 mL 2-neck round bottom. 1-chloropyrrolidine-2,5-dione (80.2 mg, 2.2 Eq, 601 µmol) in 5 mL of DCM was added to the flask under $N_2$ at room temp. The reaction was monitored via TLC (1:1 DCM:hexane) until completion. The crude product was washed with 1M NaOH (3 x 10mL) and the organic layer was subsequently dried with anh. $MgSO_4$, filtered, concentrated under reduced pressure using rotary evaporation, and purified via column chromatography (1:1 DCM:hexane) to yield the desired product as a red-orange solid (69 mg, 58%).$^1$H NMR (400 MHz, $CDCl_3$) δ 6.97 (s, 2H), 2.58 (s, 6H), 2.35 (s, 3H), 2.07 (s, 6H), 1.37 (s, 6H); $^{13}$C NMR (100 MHz, $CDCl_3$) δ 152.3, 142.8, 139.4, 137.3, 134.9, 130.4, 129.4, 129.0, 122.3, 21.4, 19.6, 12.6, 11.0; IR (ATR): 2962, 2922, 2852, 1531, 1500, 1466, 1405, 1382, 1350, 1309, 1166, 1122, 1085, 1062, 994, 923, 774, 702, 604 cm$^{-1}$; HRMS (ESI): exact mass calculated for $C_{22}H_{23}BCl_2F_2N_2$ $[M+Na]^+$ 457.1196, found 457.1202

**2,8-dibromo-5,5-difluoro-10-mesityl-1,3,7,9-tetramethyl-5H-4l4,5l4-dipyrrolo[1,2-c:2',1'-f][1,3,2]diazaborinine (S3, Mes-Br).** 5,5-difluoro-10-mesityl-1,3,7,9-tetramethyl-5H-4l4,5l4-dipyrrolo[1,2-c:2',1'-f][1,3,2]diazaborinine (**S1**) (200 mg, 1 Eq, 0.27 mmol) was dissolved in 20 mL of dry DCM in a 100 mL 2-neck round bottom. NBS (214 mg, 2.2 Eq, 1.20 mmol) in 5 mL of dry DCM was added to the flask under $N_2$ at room temp. The reaction was monitored via TLC (1:1 DCM:hexane). The crude product was washed with 1M NaOH (3 x 10mL), and the organic layer was dried with anh. $MgSO_4$, filtered, concentrated under reduced pressure using rotary evaporation, and purified via column chromatography (1:1 DCM:hexane) to yield the desired product as a red solid (150mg, 52%). $^1$H NMR (400 MHz, $CDCl_3$) δ 6.98 (s, 2H), 2.61 (s, 6H), 2.36 (s, 3H), 2.07 (s, 6H), 1.38 (s, 6H); $^{13}$C NMR (100 MHz, $CDCl_3$) δ 153.6, 142.4, 139.8, 139.3, 134.8, 130.5, 129.6, 129.3, 111.4, 21.2, 19.5, 13.7, 12.6; IR (ATR): 2956, 2919, 2854, 1529, 1462, 1400, 1383, 1345, 1314, 1175, 1118, 1099, 1084, 1060, 996, 851, 774, 701, 592 cm$^{-1}$; HRMS (ESI): exact mass calculated for $C_{22}H_{23}BBr_2F_2N_2$ $[M+Na]^+$ 545.0186, found 545.0189

**5,5-difluoro-2,8-diiodo-10-mesityl-1,3,7,9-tetramethyl-5H-4l4,5l4-dipyrrolo[1,2-c:2',1'-f][1,3,2]diazaborinine (S4, Mes-I).** 5,5-difluoro-10-mesityl-1,3,7,9-tetramethyl-5H-4l4,5l4-dipyrrolo[1,2-c:2',1'-f][1,3,2]diazaborinine (**S1**) (100 mg, 1 Eq, 273 µmol) was dissolved in 10 mL of DCM in a 100 mL 2-neck round bottom. NIS (135 mg, 2.2 Eq, 601 µmol) in 10 mL of methanol was added to the flask under $N_2$ at room temp. The reaction was monitored via TLC (1:1 DCM:hexane). The crude product was washed with 1M NaOH (3 x 10mL) and the organic layer was dried with anh. MgSO4, filtered, concentrated under reduced pressure using rotary evaporation, and purified via column chromatography (1:1 DCM:hexane) to yield the desired product as a purple solid (110 mg, 65%).$^1$H NMR (400 MHz, $CDCl_3$) δ 6.97 (s, 2H), 2.65 (s, 6H), 2.36 (s, 3H), 2.06 (s, 6H), 1.40 (s, 6H); $^{13}$C NMR (100 MHz, $CDCl_3$) δ 156.4, 144.6, 141.7, 139.3, 134.8, 130.8, 130.5, 129.3, 85.3, 21.2, 19.5, 16.0, 15.8; IR (ATR): 2953, 2917, 2852, 1519, 1475, 1455, 1397, 1340, 1308, 1176, 1135, 1115, 1092, 1080, 993, 850, 775, 701, 586 cm$^{-1}$; HRMS (ESI): exact mass calculated for $C_{22}H_{23}BF_2I_2N_2$ $[M+Na]^+$ 640.9909, found 640.9908

The syntheses of aza-BODIPY derivatives were accomplished in an analogous fashion to that previously reported in literature (**Scheme S2**).[7,8]

**Scheme S2**. Synthesis of Aza-H & Aza-Br BODIPYs

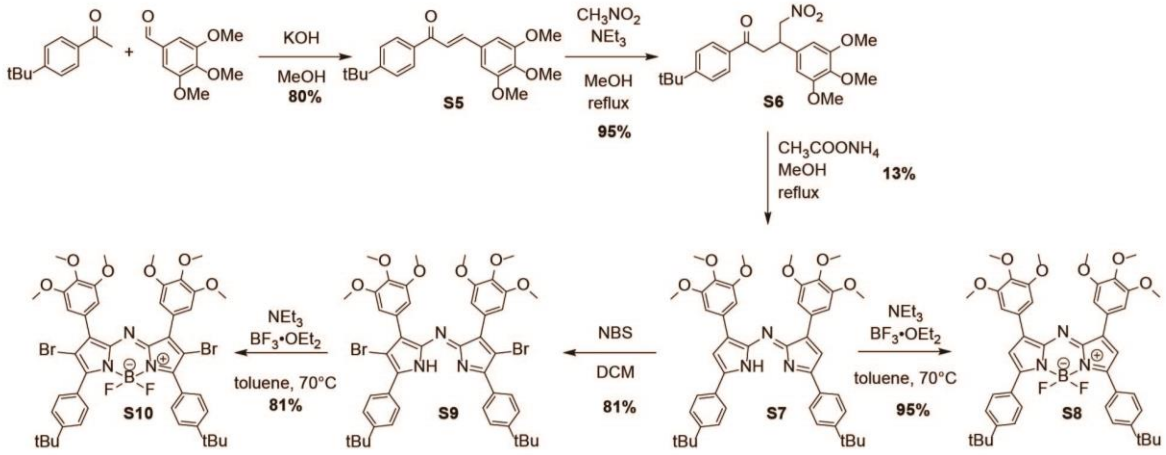


**(*E*)-1-(4-(tert-butyl)phenyl)-3-(3,4,5-trimethoxyphenyl)prop-2-en-1-one (S5).** 1-(4-(tert-butyl)phenyl)ethan-1-one (8.00 g, 8.30 mL, 1 Eq, 45.4 mmol) and potassium hydroxide (9.00 g, 3.53 Eq, 160 mmol) in 30 mL of methanol was slowly added to 3,4,5-trimethoxybenzaldehyde

(8.00 g, 0.898 Eq, 40.8 mmol) in 20 mL of methanol. The mixture was stirred at room temperature for 1 h and filtered under vacuum. The resultant faint yellow solid was collected and washed twice with methanol and water to yield the desired product as a faint yellow solid (12.880 g, 89%).$^{1}$H NMR (400 MHz, $CDCl_3$) δ 7.95-7.98 (d, *J* = 8.8 Hz, 2H), 7.69-7.73 (d, *J* = 15.6 Hz, 1H), 7.51-7.53 (d, *J* = 8.8 Hz, 2H), 7.39-7.43 (d, *J* = 15.6 Hz, 1H), 6.86 (s, 2H), 3.92 (s, 6H), 3.90 (s, 3H), 1.36 (s, 9H); $^{13}$C NMR (100 MHz, $CDCl_3$) δ 190.1, 156.5, 153.4, 144.5, 140.3, 135.6, 130.5, 128.5, 125.6, 121.6, 105.6, 60.9, 56.2, 35.1, 31.1; IR (ATR): 2962, 2938, 2905, 1651, 1580, 1501, 1451, 1417, 1327, 1318, 1278, 1245, 1218, 1191, 1153, 1004, 825, 525, 516 cm$^{-1}$; HRMS (ESI): exact mass calculated for $C_{22}H_{26}O_4$ $[M+H]^+$ 355.1909, found 355.1904

**1-(4-(tert-butyl)phenyl)-4-nitro-3-(3,4,5-trimethoxyphenyl)butan-1-one (S6).** (*E*)-1-(4-(tert-butyl)phenyl)-3-(3,4,5-trimethoxyphenyl)prop-2-en-1-one (**S5**) (10.796 g, 1 Eq, 30.458 mmol), triethylamine (13 g, 18 mL, 4.2 Eq, 0.13 mol), and nitromethane (11 g, 10 mL, 6.1 Eq, 0.19 mol) were dissolved in 80 mL of MeOH. The reaction mixture was refluxed at 65°C overnight. Upon cooling the reaction, solvent was removed under reduced pressure using rotary evaporation, followed by recrystallization of the crude product in MeOH to yield the desired product as a white solid (12.035 g, 95%).$^{1}$H NMR (400 MHz, $CDCl_3$) δ 7.85-7.87 (d, *J* = 8.8 Hz, 2H), 7.46-7.48 (d, *J* = 8.8 Hz, 2H), 6.46 (s, 2H), 4.79-4.84 (dd, *J* = 12.5, 6.6 Hz, 1H), 4.65-4.70 (dd, *J* = 12.5, 8.1 Hz, 1H), 4.12-4.21 (m, 1H), 3.84 (s, 6H), 3.81 (s, 3H), 3.32-3.47 (qd, *J* = 17.5, 6.9 Hz, 2H), 1.33 (s, 9H); $^{13}$C NMR (100 MHz, $CDCl_3$) δ 196.9, 157.6, 153.5, 137.5, 134.9, 133.9, 128.1, 125.8, 104.6, 79.5, 60.8, 56.2, 50.6, 41.6, 39.8, 35.2, 31.0; IR (ATR): 2959, 2841, 1681, 1592, 1545, 1513, 1462, 1427, 1406, 1378, 1358, 1321, 1272, 1251, 1236, 1159, 993, 826, 658 cm$^{-1}$; HRMS (ESI): exact mass calculated for $C_{23}H_{29}NO_6$ $[M+Na]^+$ 438.1892, found 438.1894

**(*Z*)-5-(4-(tert-butyl)phenyl)-N-(5-(4-(tert-butyl)phenyl)-3-(3,4,5-trimethoxyphenyl)-1H-pyrrol-2-yl)-3-(3,4,5-trimethoxyphenyl)-2H-pyrrol-2-imine (S7).** 1-(4-(tert-butyl)phenyl)-4-nitro-3-(3,4,5-trimethoxyphenyl)butan-1-one (**S6**) (2.00 g, 1 Eq, 4.81 mmol) and ammonium acetate (5.94 g, 16 Eq, 77.0 mmol) were dissolved in 100 mL of methanol and refluxed for 24 h. After cooling down to room temperature, the reaction mixture was filtered under reduced pressure to give a metallic dark black solid, which was washed with methanol followed by water to yield the desired product as a black solid (422 mg, 12%).$^{1}$H NMR (400 MHz, $CDCl_3$) δ 7.90-7.92 (d, *J* = 8.5 Hz, 4H), 7.57-7.59 (d, *J* = 8.5 Hz, 4H), 7.16 (s, 4H), 7.11 (s, 2H), 3.91 (s, 6H), 3.72 (s, 12H), 1.42 (s, 18H); $^{13}$C NMR (100 MHz, $CDCl_3$) δ 154.9, 153.8, 153.1, 149.4, 142.7, 138.1, 129.7, 129.4, 126.5, 126.3, 114.9, 106.4, 61.0, 56.0, 35.1, 31.3; IR (ATR): 2998, 2962, 2825, 1567, 1545, 1493, 1461, 1411, 1363, 1321, 1306, 1281, 1264, 1239, 1186, 1031, 796, 713, 650 cm$^{-1}$; HRMS (ESI): exact mass calculated for $C_{46}H_{51}N_3O_6$ $[M+H]^+$ 742.3856, found 742.3854

**3,7-bis(4-(tert-butyl)phenyl)-5,5-difluoro-1,9-bis(3,4,5-trimethoxyphenyl)-5H-4l4,5l4-dipyrrolo[1,2-c:2',1'-f][1,3,5,2]triazaborinine (S8, aza-H).** (*Z*)-5-(4-(tert-butyl)phenyl)-N-(5-(4-(tert-butyl)phenyl)-3-(3,4,5-trimethoxyphenyl)-1H-pyrrol-2-yl)-3-(3,4,5-trimethoxyphenyl)-2H-pyrrol-2-imine (**S7**) (250 mg, 1 Eq, 337 µmol) was dissolved in 20 mL of toluene in a 100 mL 2-neck RB flask under $N_2$. Triethylamine (6.82 g, 9.40 mL, 200 Eq, 67.4 mmol) was added to the reaction mixture followed by dropwise addition of boron trifluoride diethyl etherate (11.0 g, 9.56 mL, 230 Eq, 77.5 mmol). The reaction mixture was then heated to 70°C for 2 hrs and monitored via TLC (100% DCM). The solvent was concentrated under reduced pressure using rotary evaporation, and the crude product was purified via column chromatography (100% DCM) to yield the desired product as a black solid (252 mg, 95%).$^{1}$H NMR (400 MHz, $CDCl_3$) δ 8.03-8.05 (d, *J* = 8.9 Hz, 4H), 7.51-7.53 (d, *J* = 8.8 Hz, 4H), 7.19 (s, 4H), 6.98 (s, 2H), 3.92 (s, 6H), 3.77 (s, 12H), 1.37 (s, 18H); $^{13}$C NMR (100 MHz, $CDCl_3$) δ 158.9, 154.6, 153.4, 145.6, 143.9, 139.6, 129.6, 128.8, 128.3, 125.9, 119.0, 106.8, 61.2, 56.1, 35.2, 31.3; IR (ATR): 2950, 2904, 2868, 2830, 1605, 1578, 1492, 1464, 1415, 1385, 1337, 1311, 1270, 1242, 1208, 1085, 1005, 810, 717 cm$^{-1}$; HRMS (ESI): exact mass calculated for $C_{46}H_{50}BF_2N_3O_6$ $[M+Na]^+$ 812.3658, found 812.3666

**(*Z*)-4-bromo-N-(4-bromo-5-(4-(tert-butyl)phenyl)-3-(3,4,5-trimethoxyphenyl)-1H-pyrrol-2-yl)-5-(4-(tert-butyl)phenyl)-3-(3,4,5-trimethoxyphenyl)-2H-pyrrol-2-imine (S9).** (*Z*)-5-(4-(tert-butyl)phenyl)-N-(5-(4-(tert-butyl)phenyl)-3-(3,4,5-trimethoxyphenyl)-1H-pyrrol-2-yl)-3-(3,4,5-trimethoxyphenyl)-2H-pyrrol-2-imine (**S7**) (150 mg, 1 Eq, 202 µmol) was dissolved in 20 mL of dry DCM in a 100 mL 2-neck round bottom. N-bromosuccinimide (72.0 mg, 2 Eq, 404 µmol) in 5 mL of dry DCM was added to the flask under $N_2$ at room temp and the reaction was monitored via TLC (DCM). The crude reaction mixture was washed with DI water (3x20mL) and the organic layer was dried over anh. $MgSO_4$, filtered, concentrated under reduced pressure using rotary evaporation, and purified via column chromatography (DCM) to yield the desired product as a black solid (147 mg, 81%).$^1$H NMR (400 MHz, $CDCl_3$) δ 7.98-8.00 (d, *J* = 8.1 Hz, 4H), 7.56-7.58 (d, *J* = 8.0 Hz, 4H), 7.00 (s, 4H), 3.95 (s, 6H), 3.60 (s, 12H), 1.41 (s, 18H); $^{13}$C NMR (100 MHz, $CDCl_3$) δ 153.9, 152.9, 152.4, 147.6, 140.4, 138.1, 128.9, 128.5, 127.1, 125.7, 108.3, 106.9, 60.8, 55.8, 35.0, 31.2; IR (ATR): 2956, 2902, 2866, 2829, 1578, 1546, 1498, 1451, 1411, 1322, 1260, 1230, 1186, 1161, 1122, 975, 877, 760, 666 cm$^{-1}$; HRMS (ESI): exact mass calculated for $C_{46}H_{49}Br_2N_3O_6$ $[M+H]^+$ 898.2066, found 898.2056

**2,8-dibromo-3,7-bis(4-(tert-butyl)phenyl)-5,5-difluoro-1,9-bis(3,4,5-trimethoxyphenyl)-5H-4l4,5l4-dipyrrolo[1,2-c:2',1'-f][1,3,5,2]triazaborinine (S10, aza-Br).** (*Z*)-4-bromo-N-(4-bromo-5-(4-(tert-butyl)phenyl)-3-(3,4,5-trimethoxyphenyl)-1H-pyrrol-2-yl)-5-(4-(tert-butyl)phenyl)-3-(3,4,5-trimethoxyphenyl)-2H-pyrrol-2-imine (**S9**) (250 mg, 1 Eq, 278 µmol) was dissolved in 20 mL of toluene in a 100 mL 2-neck RB flask under $N_2$. Triethylamine (5.62 g, 7.75 mL, 200 Eq, 55.6 mmol) was added to the reaction mixture followed by dropwise addition of boron trifluoride diethyl etherate (9.07 g, 7.89 mL, 230 Eq, 63.9 mmol). The reaction mixture was then heated to 70°C for 2 hrs and monitored via TLC (100% DCM). The solvent was removed under reduced pressure using rotary evaporation and the crude product was purified via column chromatography (100% DCM) to yield the desired product as a black solid (214 mg, 81%).$^1$H NMR (400 MHz, $CDCl_3$) δ 7.68-7.70 (d, *J* = 8.4 Hz, 4H), 7.48-7.50 (d, *J* = 8.5 Hz, 4H), 7.11 (s, 4H), 3.94 (s, 6H), 3.69 (s, 12H), 1.35 (s, 18H); $^{13}$C NMR (100 MHz, $CDCl_3$) δ 158.4, 154.3, 152.8, 144.2, 142.2, 139.6, 130.3, 126.6, 126.2, 125.1, 109.9, 108.5, 61.1, 56.1, 35.1, 31.3; IR (ATR): 2958, 2905, 2867, 2833, 1579, 1491, 1464, 1411, 1377, 1336, 1290, 1269, 1240, 1168, 1121, 1063, 1015, 837, 713 cm$^{-1}$; HRMS (ESI): exact mass calculated for $C_{46}H_{48}BBr_2F_2N_3O_6$ $[M+Na]^+$ 968.1868, found 968.1868

***Thin-Film Absorption***

The absorption data for the BODIPY dyes was acquired using the following general resin formulation: 0.1 mol% BODIPY, 0.1 mol% Borate V (Donor), and 1.0 mol% H-Nu 254 (Acceptor) in order to more accurately represent the conditions used during photopolymerization measurements. Plastic shims were used as spacers to create a gap of known thickness between two glass slides. Due to the high extinction coefficient of the BODIPY dyes the samples were measured within a thickness range from 13-100 µm on an Ocean Optics Stage RTL-T. All absorption data was collected within the limits of Beer's Law with respect to the max emission peak for each corresponding LED (i.e., 530 nm for the green LED). The extinction coefficient values determined from this data were used to calculate the number of equivalent photons between samples in order to normalize the number of photons absorbed (see "normalizing photons absorbed" section for more details).

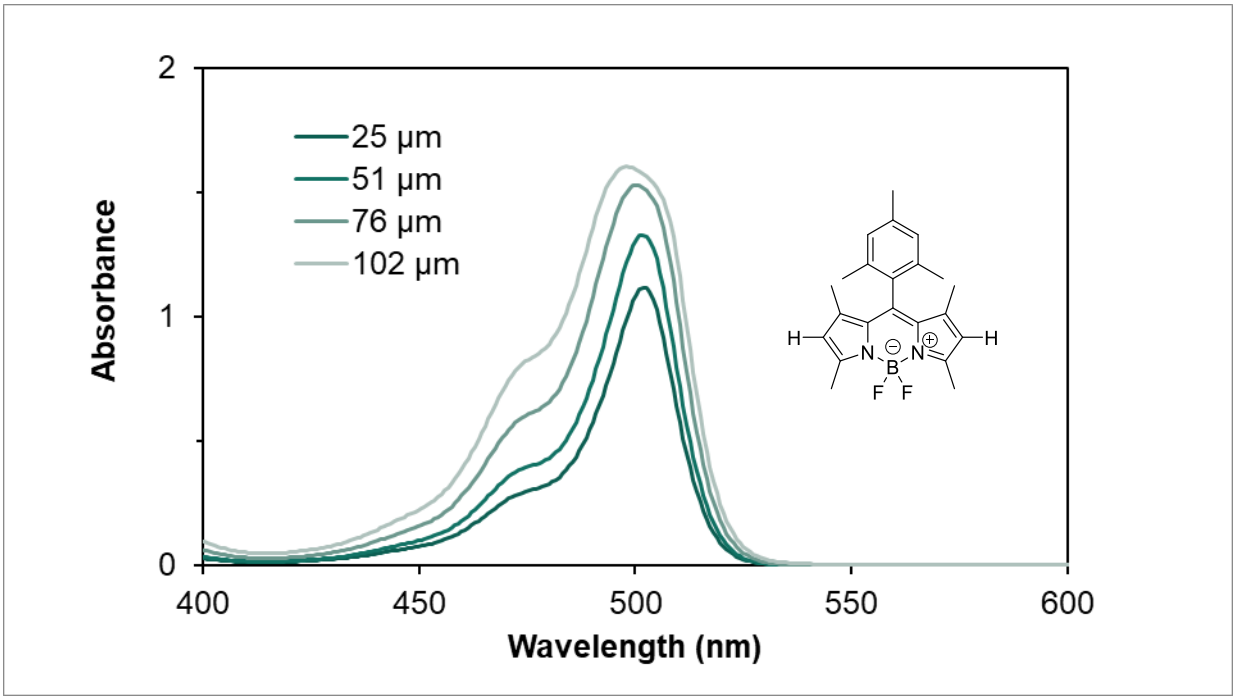


**Figure S3.** Absorption spectra for resin containing **Mes-H** BODIPY at different thickness

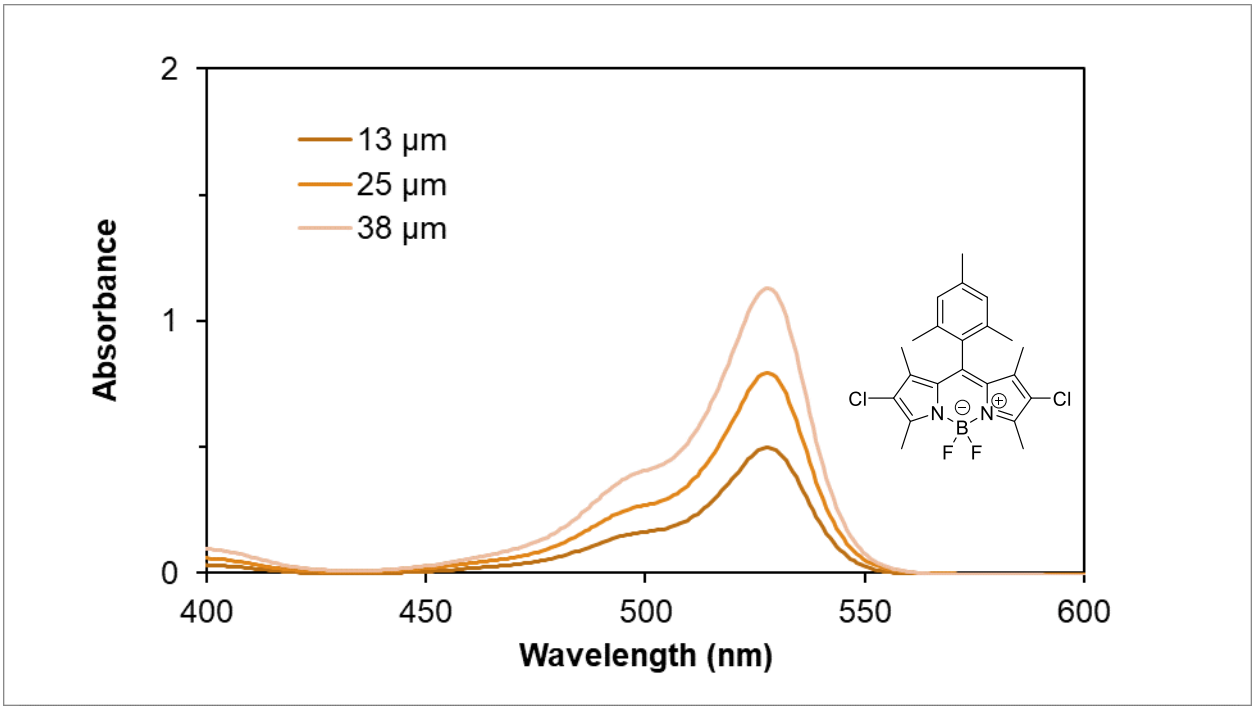


**Figure S4.** Absorption spectra for resin containing **Mes-Cl** BODIPY at different thickness

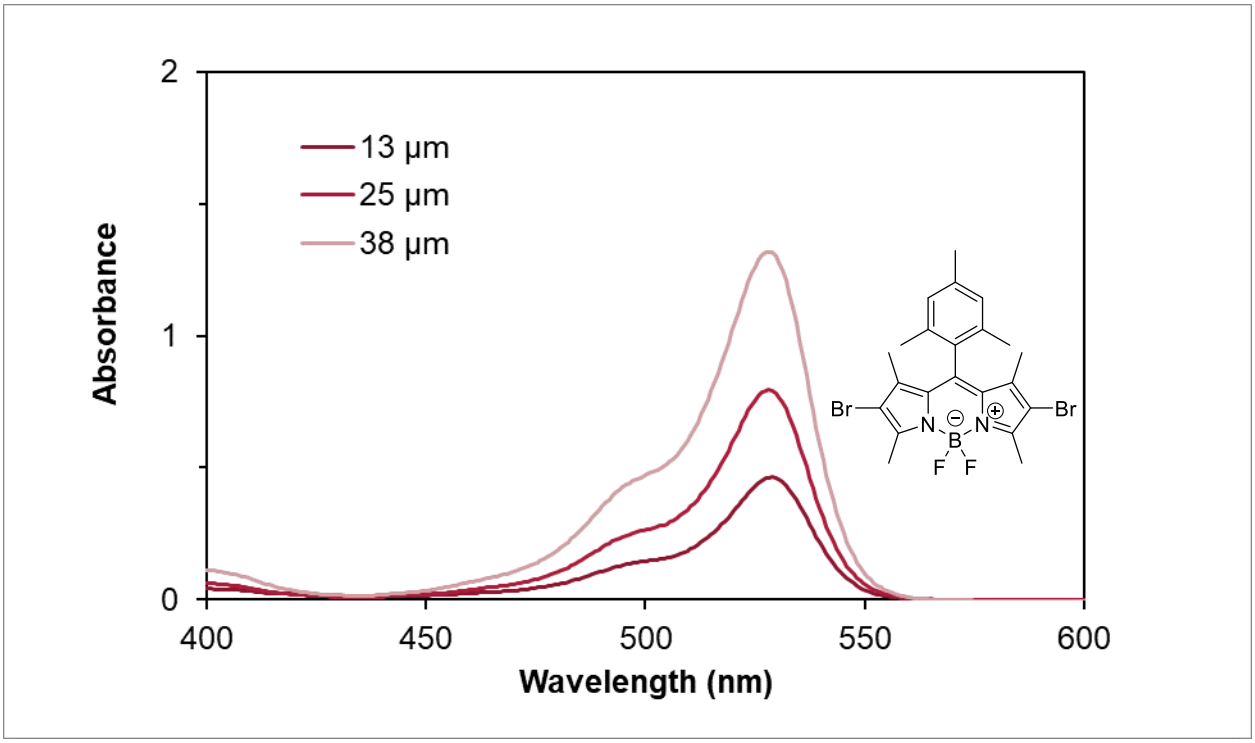


**Figure S5.** Absorption spectra for resin containing **Mes-Br** BODIPY at different thickness

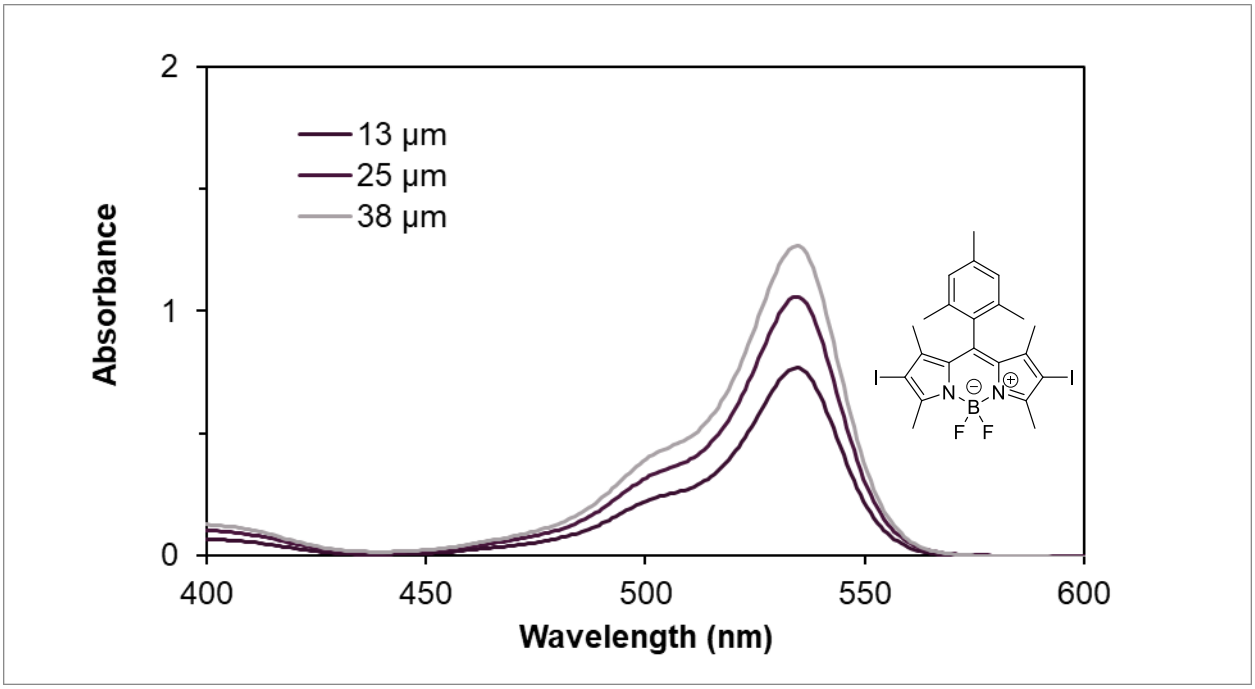


**Figure S6.** Absorption spectra for resin containing **Mes-I** BODIPY at different thickness

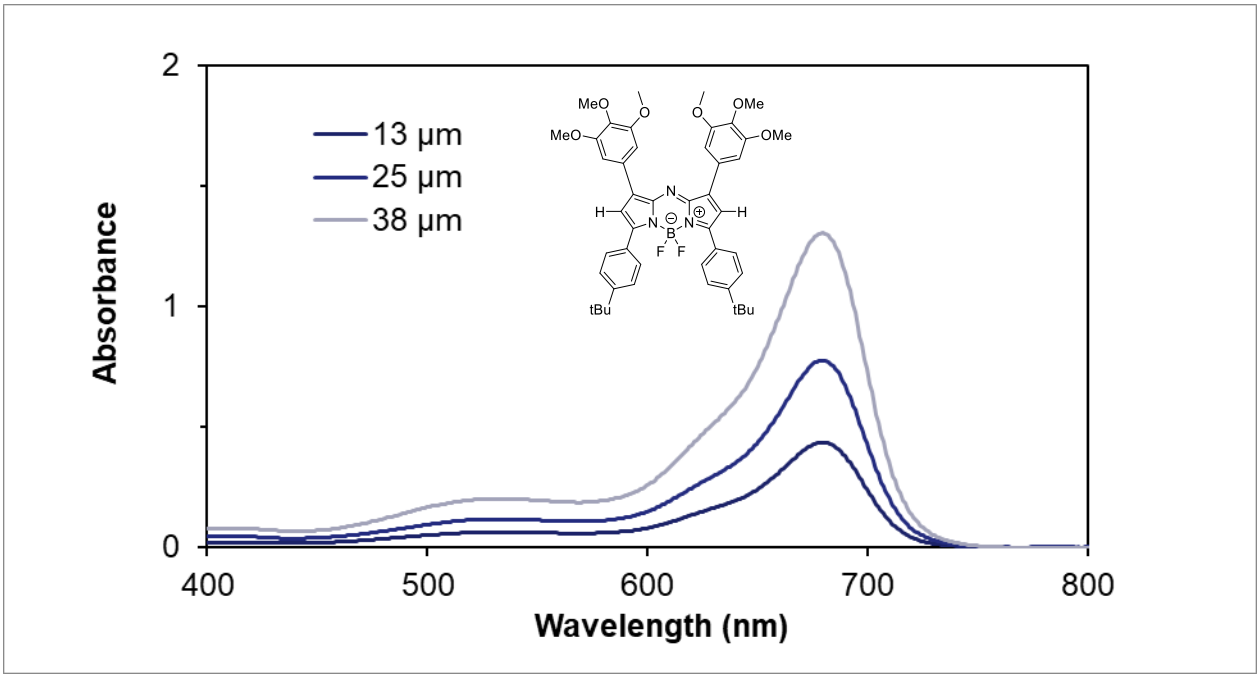


**Figure S7.** Absorption spectra for resin containing **aza-H** BODIPY at different thickness

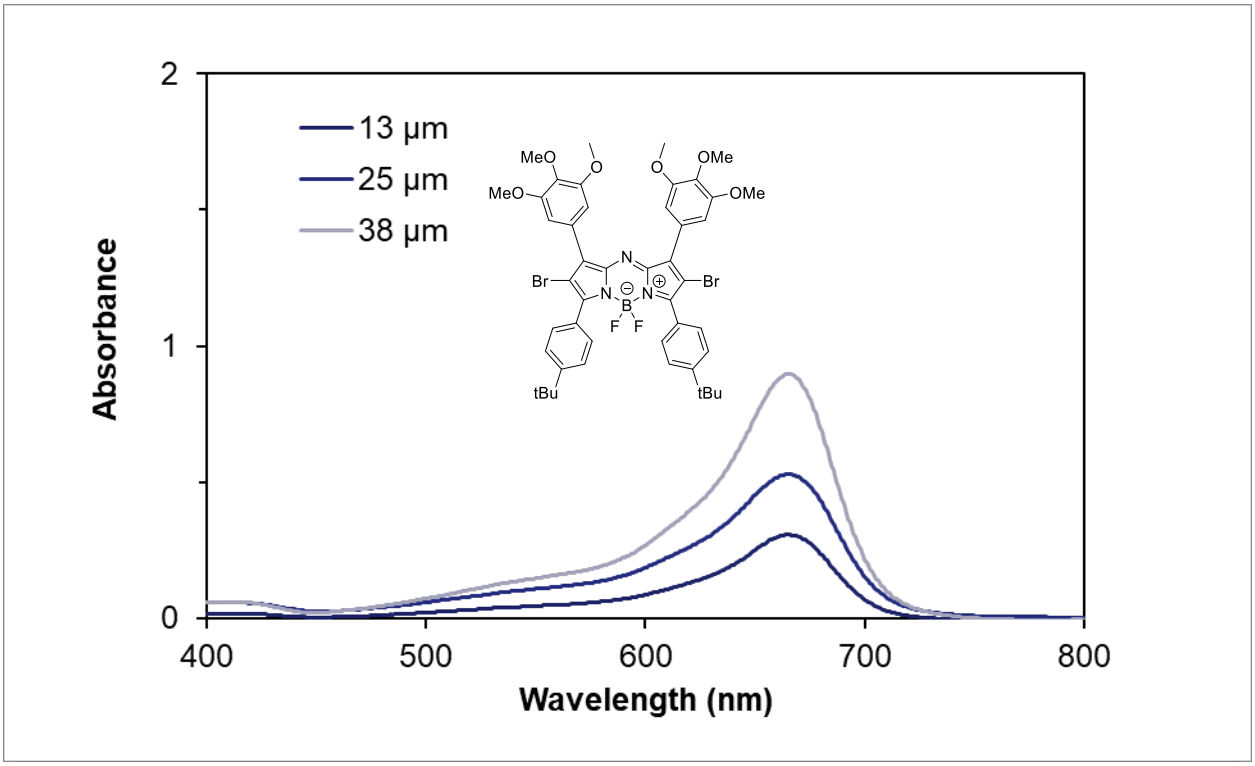


**Figure S8.** Absorption spectra for resin containing **aza-Br** BODIPY at different thickness

### *Normalizing Photons Absorbed*

The photon flux was calculated based on the following supplemental equations:

$$E = hc/\lambda \qquad \textit{(SE1)}$$

where $E$ = energy (mW), $h$ = Plank's constant (=6.626×10$^{-34}$J s), c = speed of light (3×10$^{8}$ m/s)

$$W = n \times (\frac{E}{s}) \qquad \textit{(SE2)}$$

where $W$ = watt , $n$ = number of photons, $E$ = energy of photons, and $s$ = seconds

$$-logT = A = \varepsilon cl \qquad \textit{(SE3)}$$

where $T$ = transmission, $A$ = absorption (AU), $\boldsymbol{\varepsilon}$ = extinction coefficient (M$^{-1}$ cm$^{-1}$), $c$ = concentration (M), and $l$ = path length (cm)

Equation ***SE1*** and ***SE2*** are used to convert the intensity output of the LED from (mW/cm$^2$ nm) into (# of photons/cm$^2$ s nm). T was calculated from equation ***SE3***, followed by the portion of photons absorbed as (1-T). Multiplying the light intensity by (1-T) provides the photon flux for each wavelength that's being absorbed by the sample. Finally, integrating each curve provided the total photon flux (or number of photons absorbed) for each sample (**Figure S9**). For ATR measurements a path length of 2.5 μm was used given an effective angle of 45°, a wavenumber of 808 cm$^{-1}$ (*vide infra*), a refractive index of 2.4 for the ATR (diamond), and a sample refractive index of 1.5 (estimate) (see calculator: https://www.piketech.com/pikecalc/).

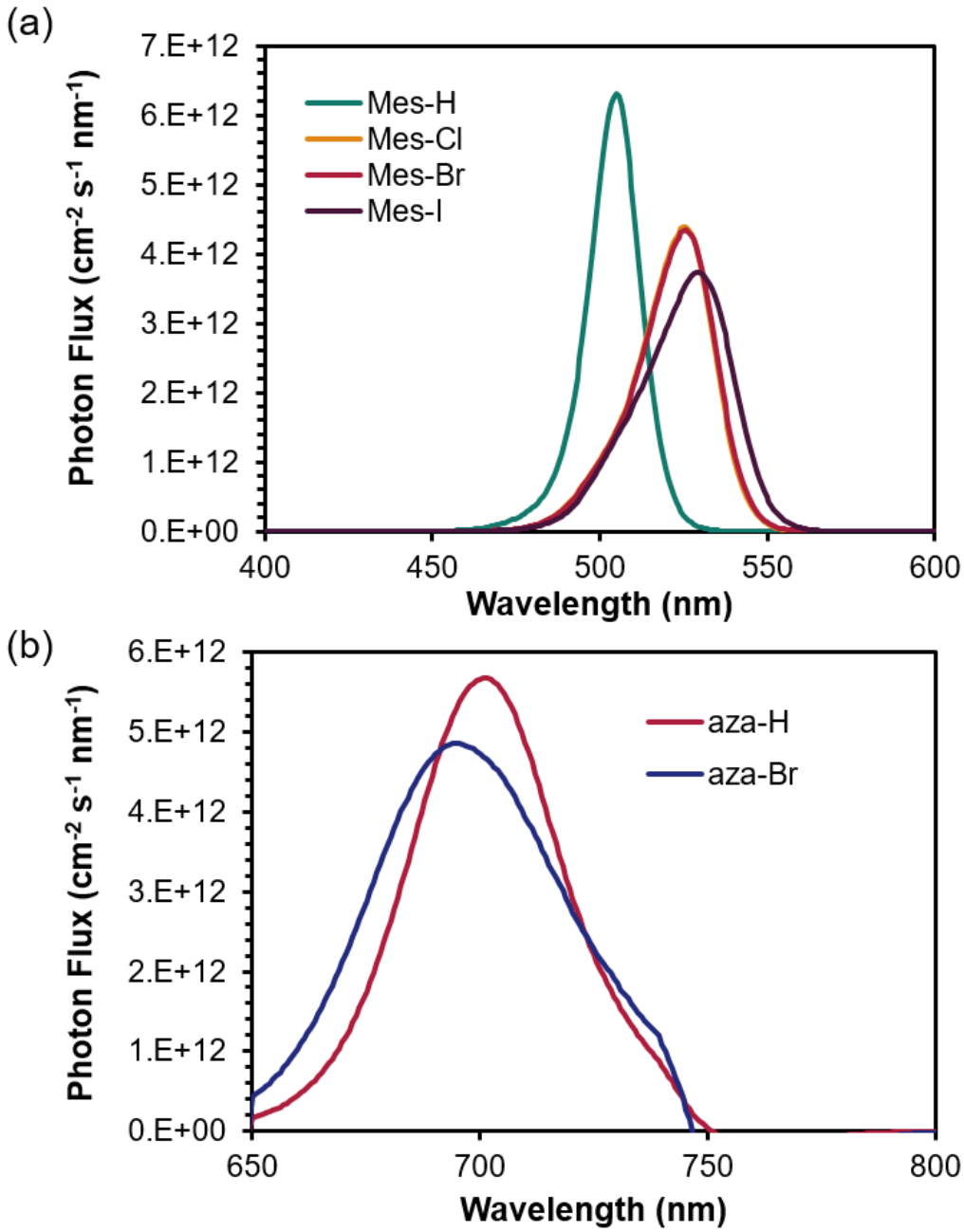


**Figure S9.** Normalized photons absorbed for (a) mestyl-BODIPY (~$9.7 \times 10^{13}$ $cm^{-2}$ $s^{-1}$) and (b) aza-BODIPY (~$2.6 \times 10^{14}$ $cm^{-2}$ $s^{-1}$) derivatives from a (a) green LED and (b) NIR LED.

### *Photopolymerization at Different LED Intensities*

The photopolymerizations were tested in triplicate at varying LED intensities with the 530, 656, and 740 nm LEDs utilizing the resin formulation: 0.1 mol% BODIPY, 0.1 mol% Borate V (donor), and 1.0 mol% iodonium salt (acceptor) on the photoATR-FTIR. The components were fully dissolved in the monomer and subsequently degassed with nitrogen or argon (~3 min). The tip of an Air-Tite Hypodermic Needle: size 22G (gauge) x 4 in. (length) was filled with the resin and dropped onto the center of the ATR crystal purged with nitrogen or argon for ~5 minutes prior to the measurement. Resolution was set at 2 $cm^{-1}$. Sample scanner velocity of 80 kHz was used and sample scan time was set at 50 scans. IR data was collected from 7000-400 $cm^{-1}$. Conversion data was determined by integrating the peak at 808 $cm^{-1}$ from 770-831 $cm^{-1}$ correlating to the C=C vinylic stretch on the acrylic monomers[9] (**Figure S10**). Polymerization Rates were calculated from the initial slopes of the data after the LED was turned on and polymerization was observed. LEDs were turned on after 10 seconds.

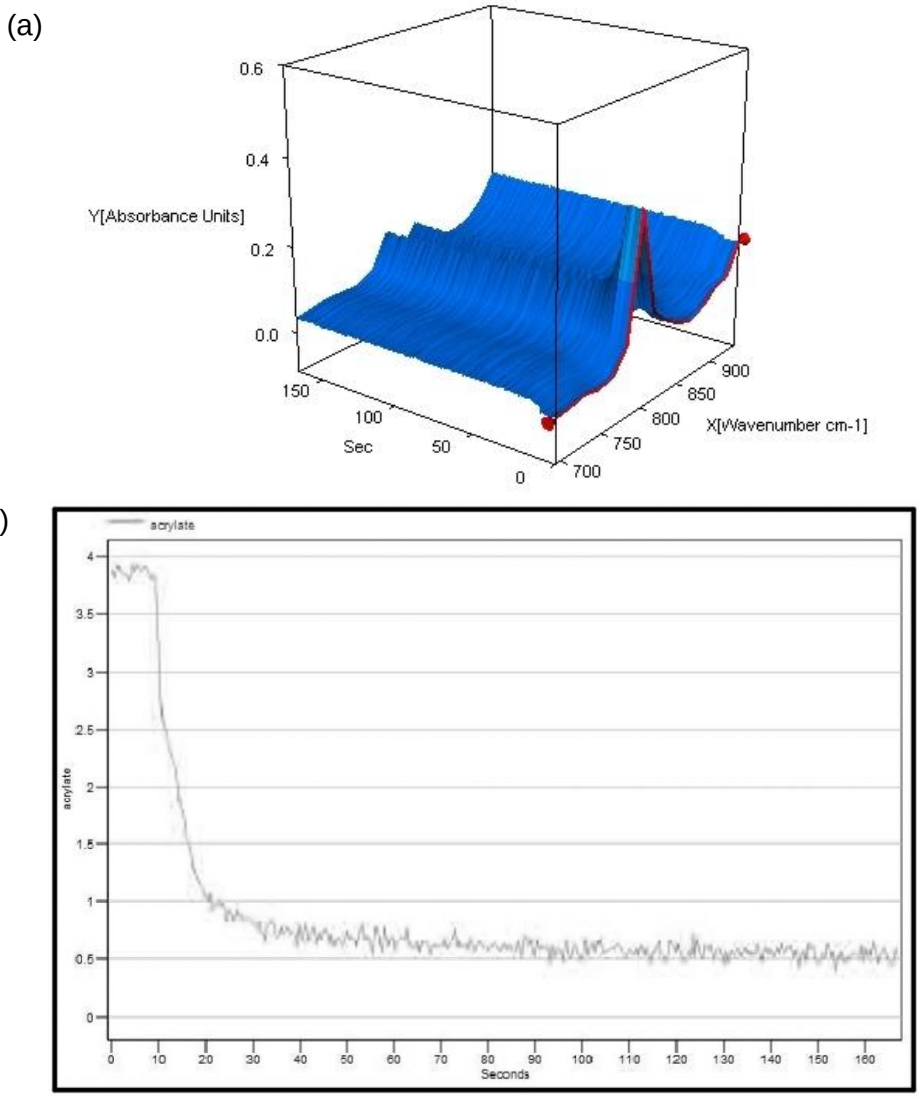


**Figure S10.** (a) Real-Time ATR-FTIR data of isobornyl acrylate photopolymerization using a 530 nm LED at 16 $mW/cm^2$ (resin formulation: 0.1 mol% **Mes-I**, 0.1 mol% Donor, 1.0 mol% Acceptor. (b). Absorbance vs. Time Plot of isobornyl acrylate photopolymerization

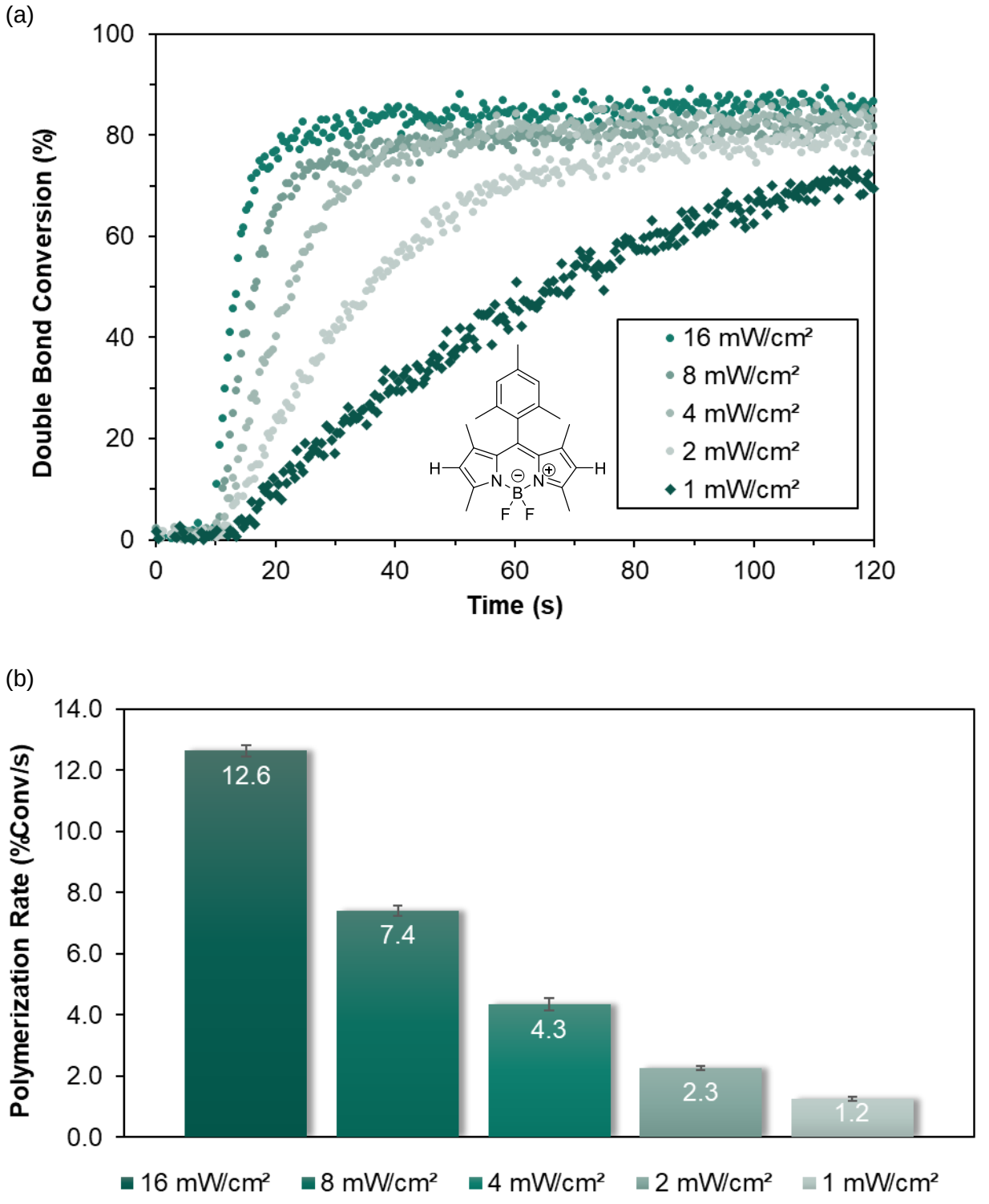


**Figure S11.** Photopolymerization with **Mes-H** and a 530 nm LED. **(a)** Double Bond Conversion vs Time ATR-FTIR data at varying intensities. **(b)** Polymerization Rate in %Conversion/second at the different LED intensities. Error bars represent ± 1 standard deviation.

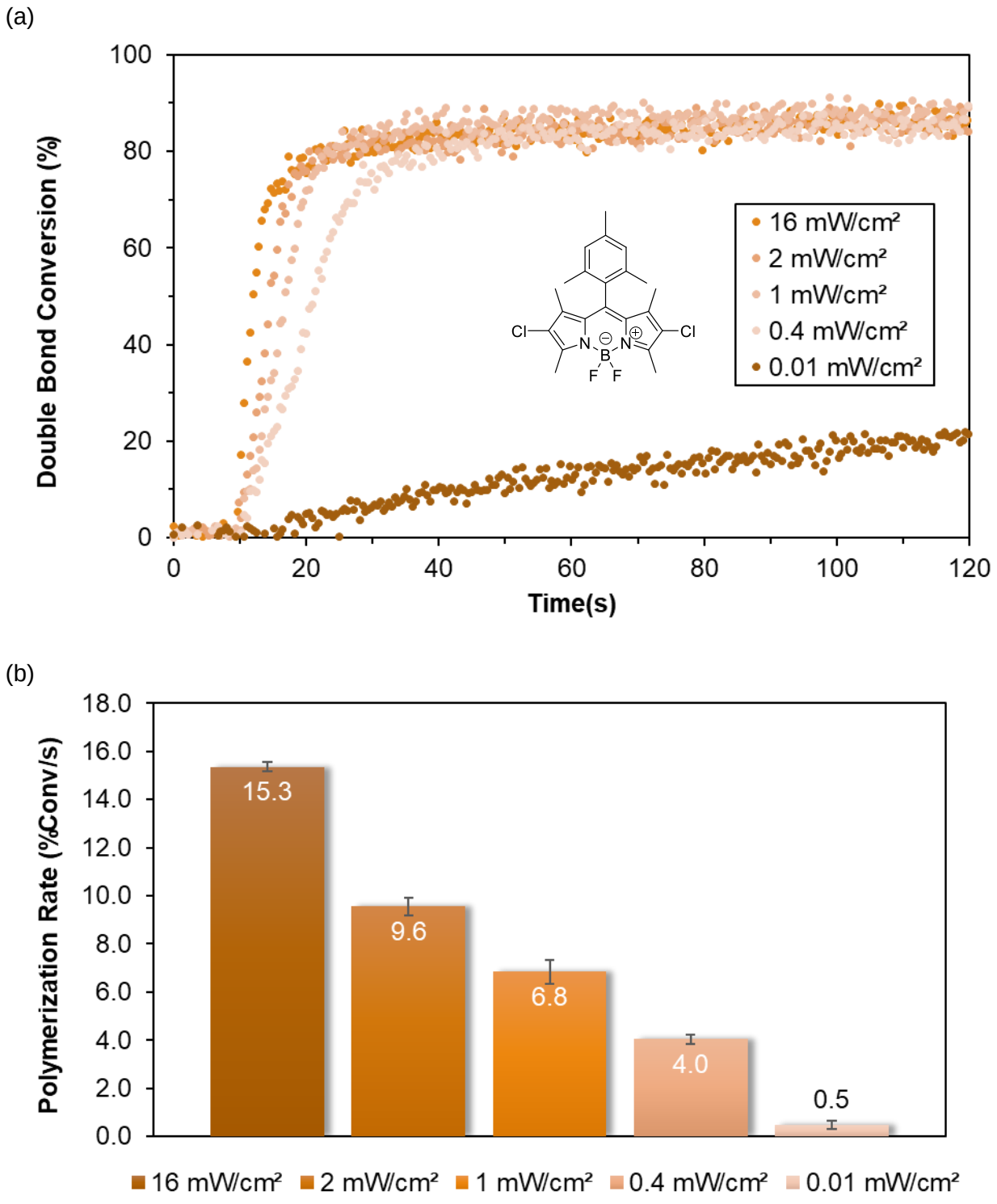


**Figure S12.** Photopolymerization with **Mes-Cl** and a 530 nm LED. **(a)** Double Bond Conversion vs Time ATR-FTIR data at varying intensities. **(b)** Polymerization Rate in %Conversion/second at the different LED intensities. Error bars represent ± 1 standard deviation.

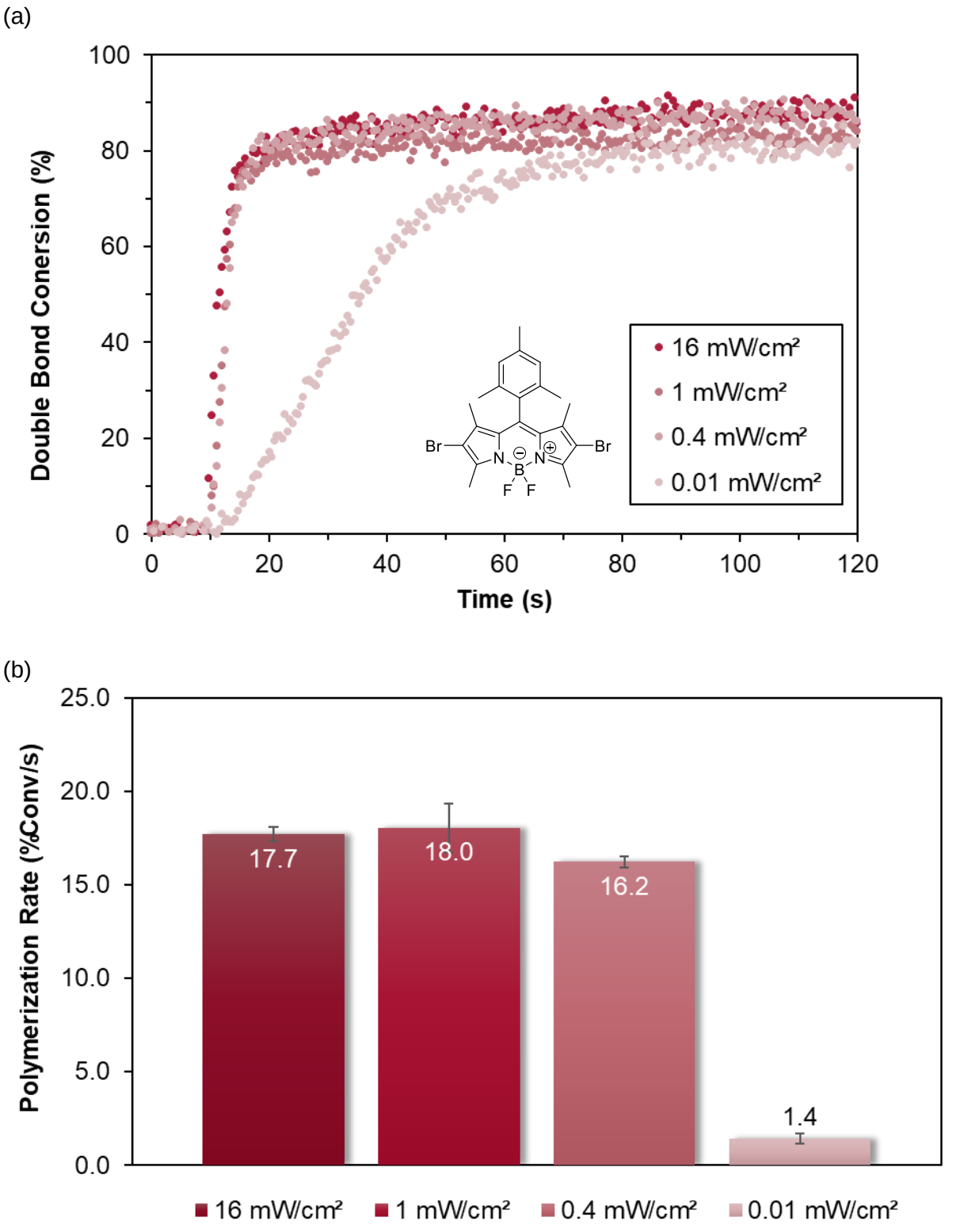


**Figure S13.** Photopolymerization with **Mes-Br** and a 530 nm LED. **(a)** Double Bond Conversion vs Time ATR-FTIR data at varying intensities. **(b)** Polymerization Rate in %Conversion/second at the different LED intensities. Error bars represent ± 1 standard deviation.

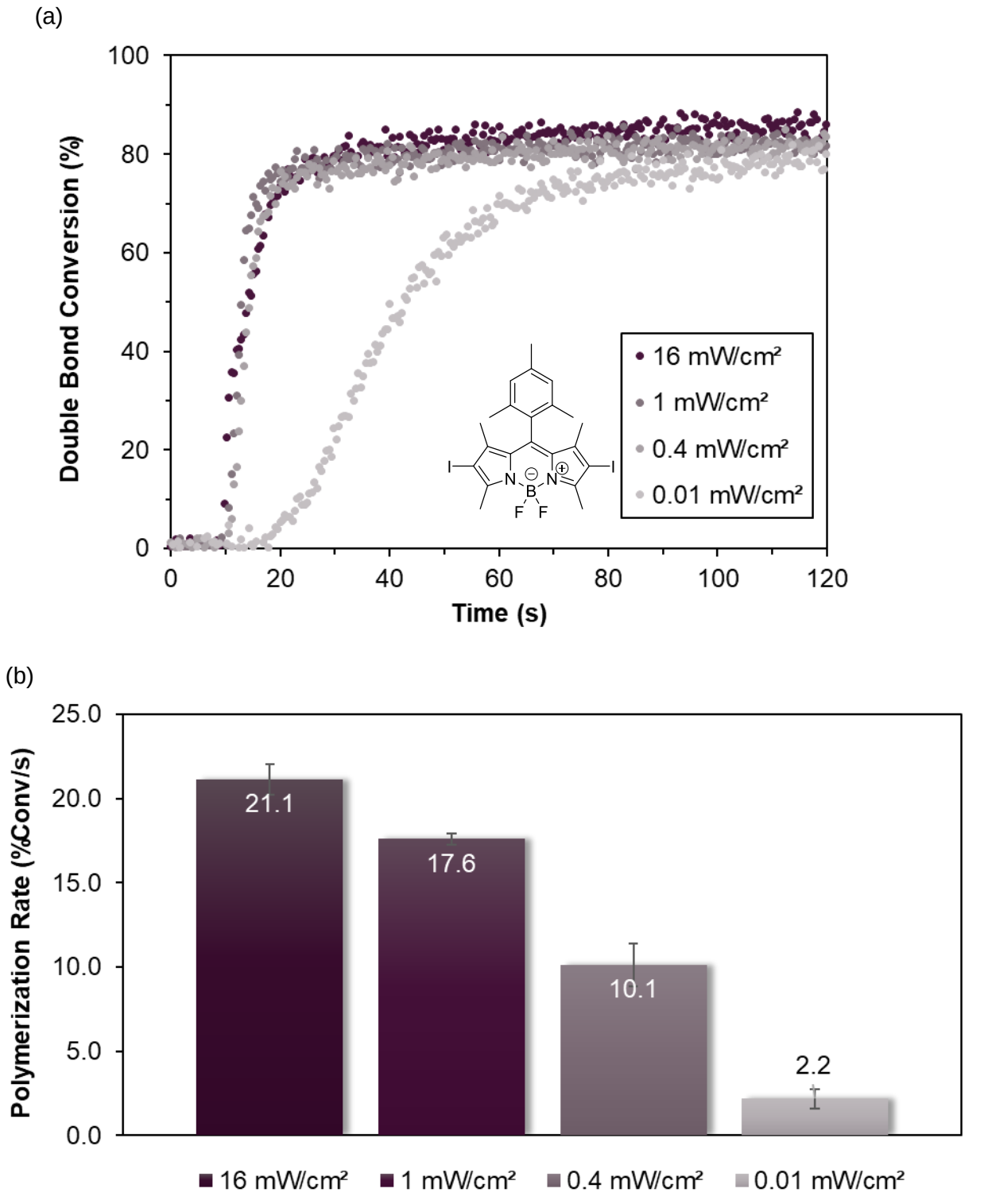


**Figure S14.** Photopolymerization with **Mes-I** and a 530 nm LED. **(a)** Double Bond Conversion vs Time ATR-FTIR data at varying intensities. **(b)** Polymerization Rate in %Conversion/second at the different LED intensities. Error bars represent ± 1 standard deviation.

(a)

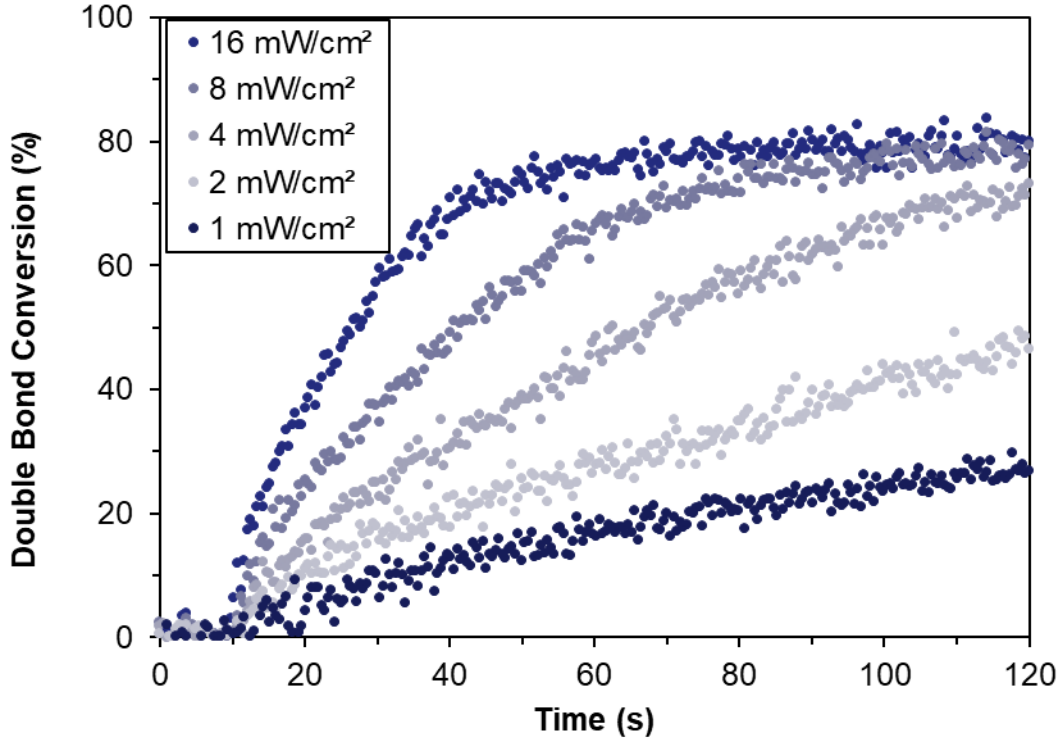


(b)

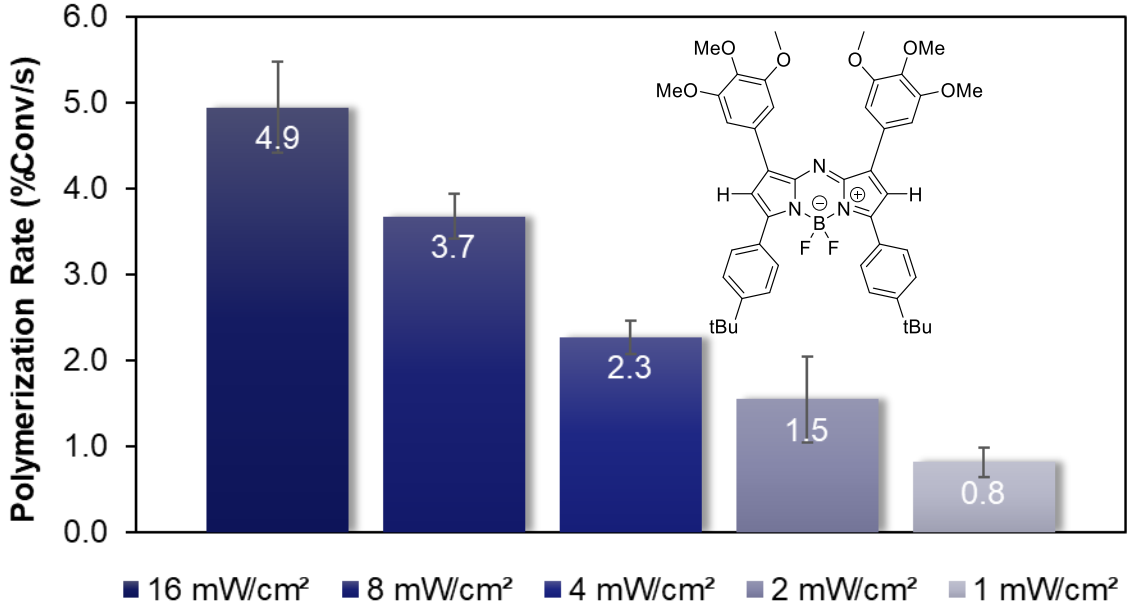


**Figure S15.** Photopolymerization with **aza-H** and a 656 nm LED. **(a)** Double Bond Conversion vs Time ATR-FTIR data at varying intensities. **(b)** Polymerization Rate in %Conversion/second at the different LED intensities. Error bars represent ± 1 standard deviation.

(a)

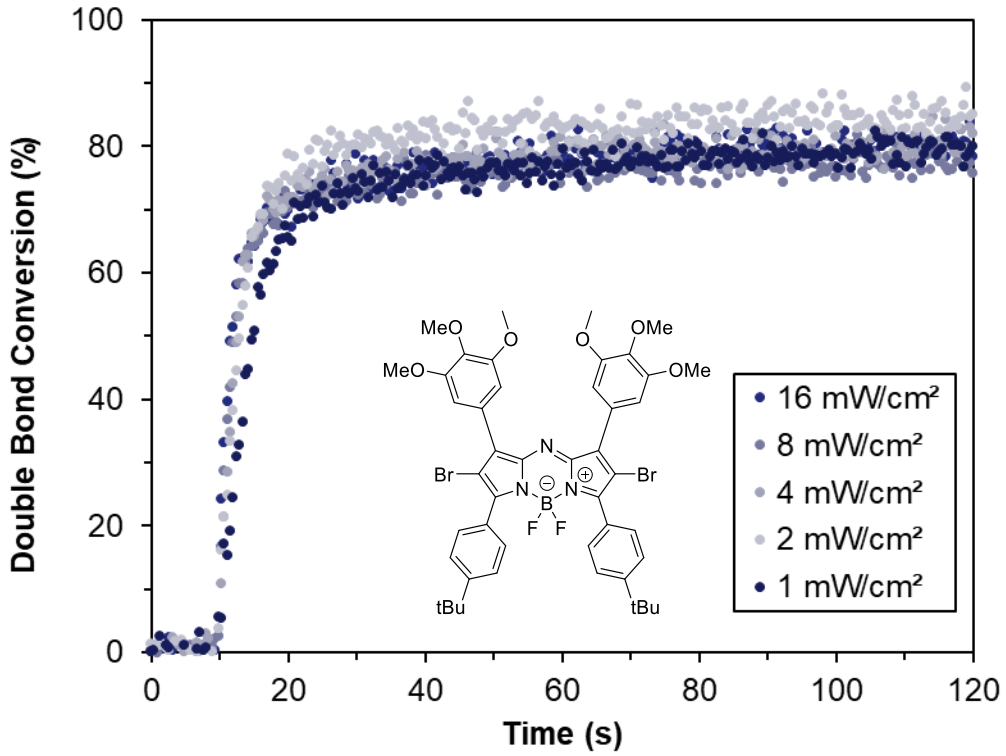


(b)

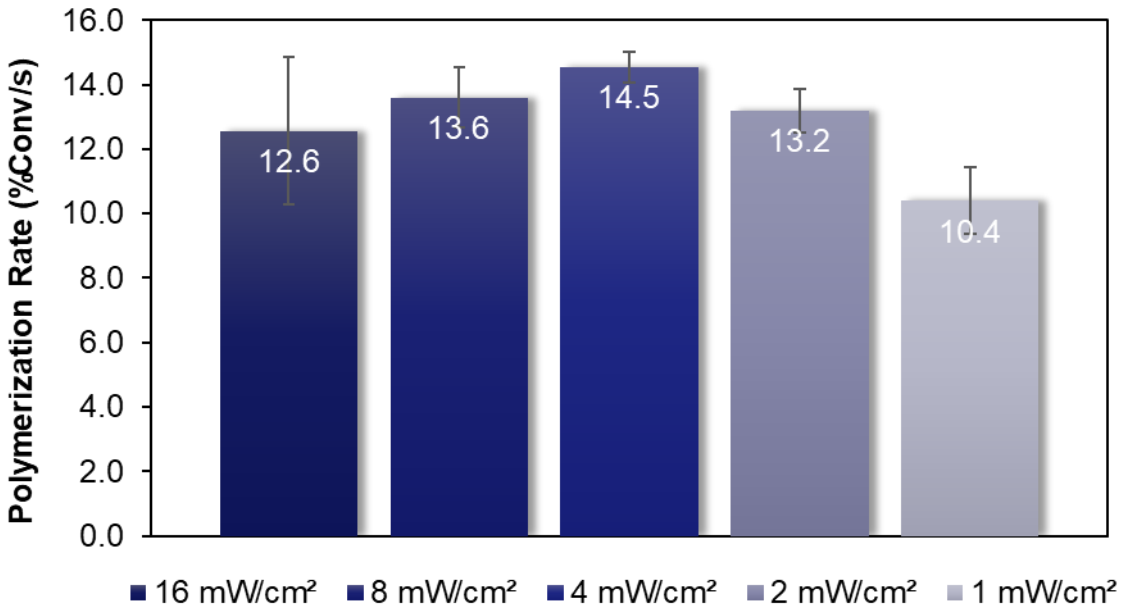


**Figure S16.** Photopolymerization with **aza-Br** and a 656 nm LED. **(a)** Double Bond Conversion vs Time ATR-FTIR data at varying intensities. **(b)** Polymerization Rate in %Conversion/second at the different LED intensities. Error bars represent ± 1 standard deviation.

(a)

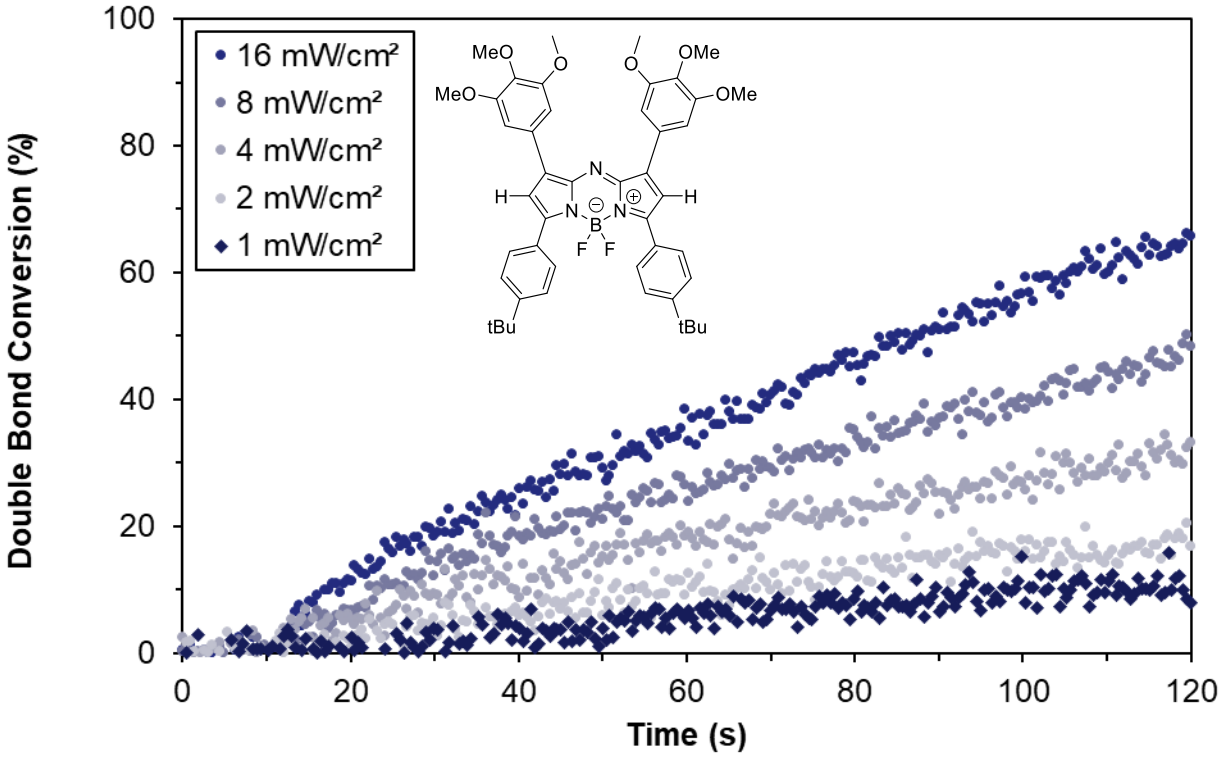


(b)

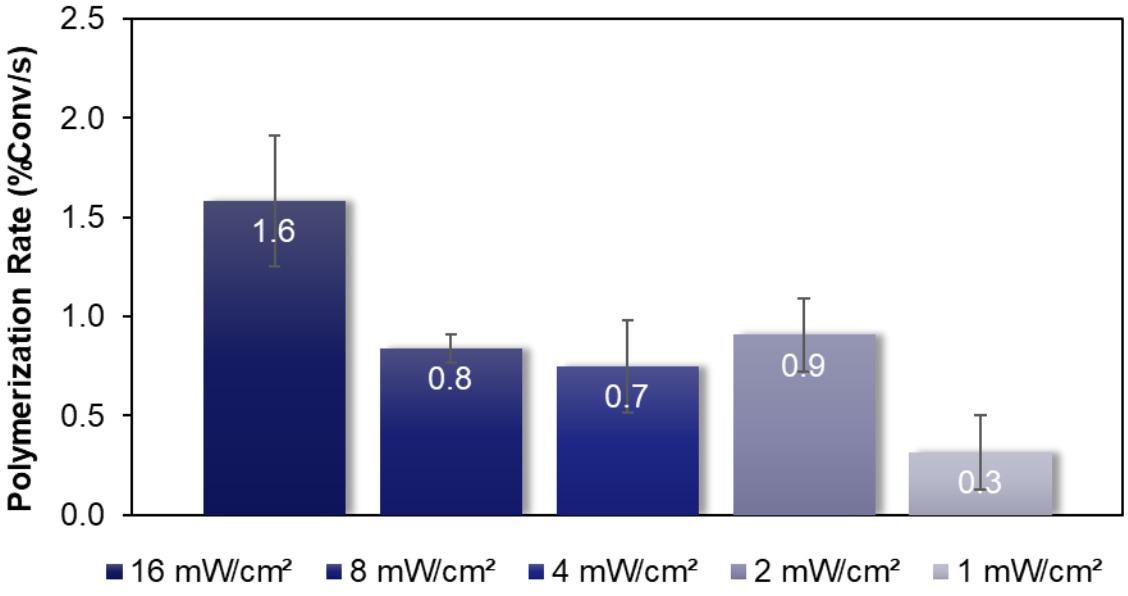


**Figure S17.** Photopolymerization with **aza-H** and a 740 nm LED. **(a)** Double Bond Conversion vs Time ATR-FTIR data at varying intensities. **(b)** Polymerization Rate in %Conversion/second at the different LED intensities. Error bars represent ± 1 standard deviation.

(a)

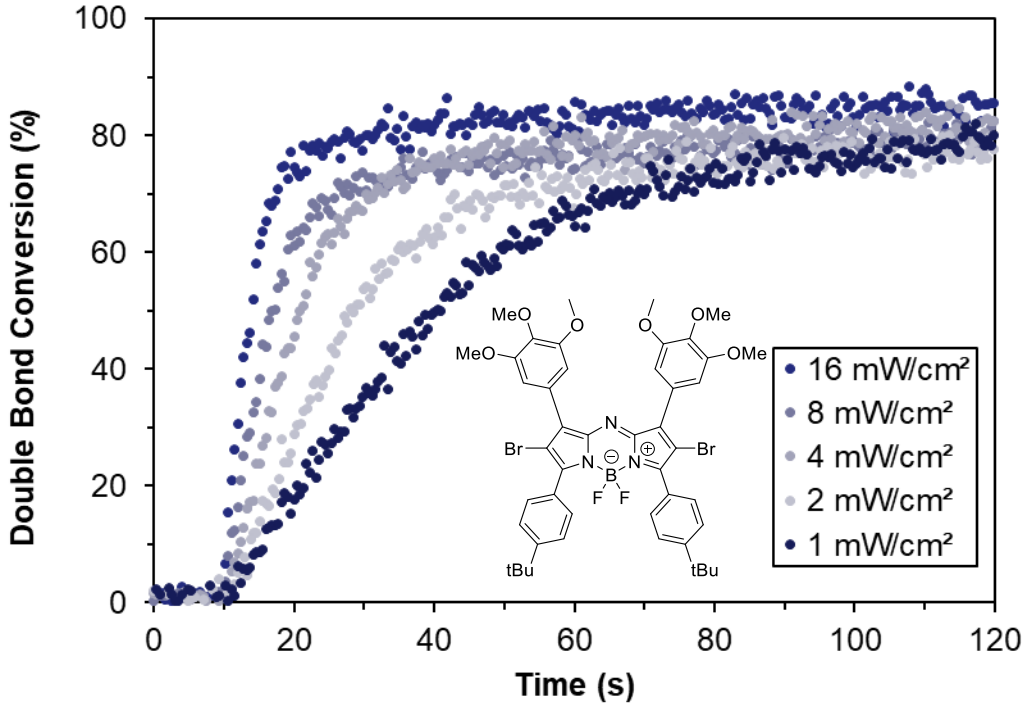


(b)

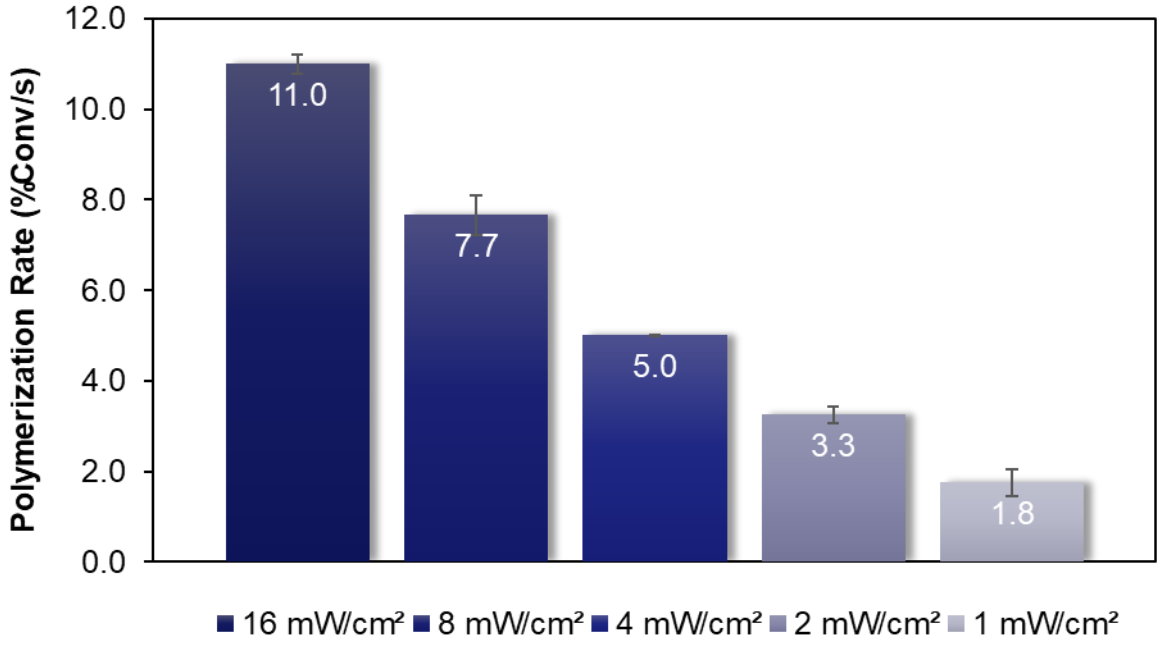


**Figure S18.** Photopolymerization with **aza-Br** and a 740 nm LED. **(a)** Double Bond Conversion vs Time ATR-FTIR data at varying intensities. **(b)** Polymerization Rate in %Conversion/second at the different LED intensities. Error bars represent ± 1 standard deviation.

***Photopolymerization Versatility***

BODIPY derivatives were employed as photosensitizers in the polymerization of resins with different monomer compositions

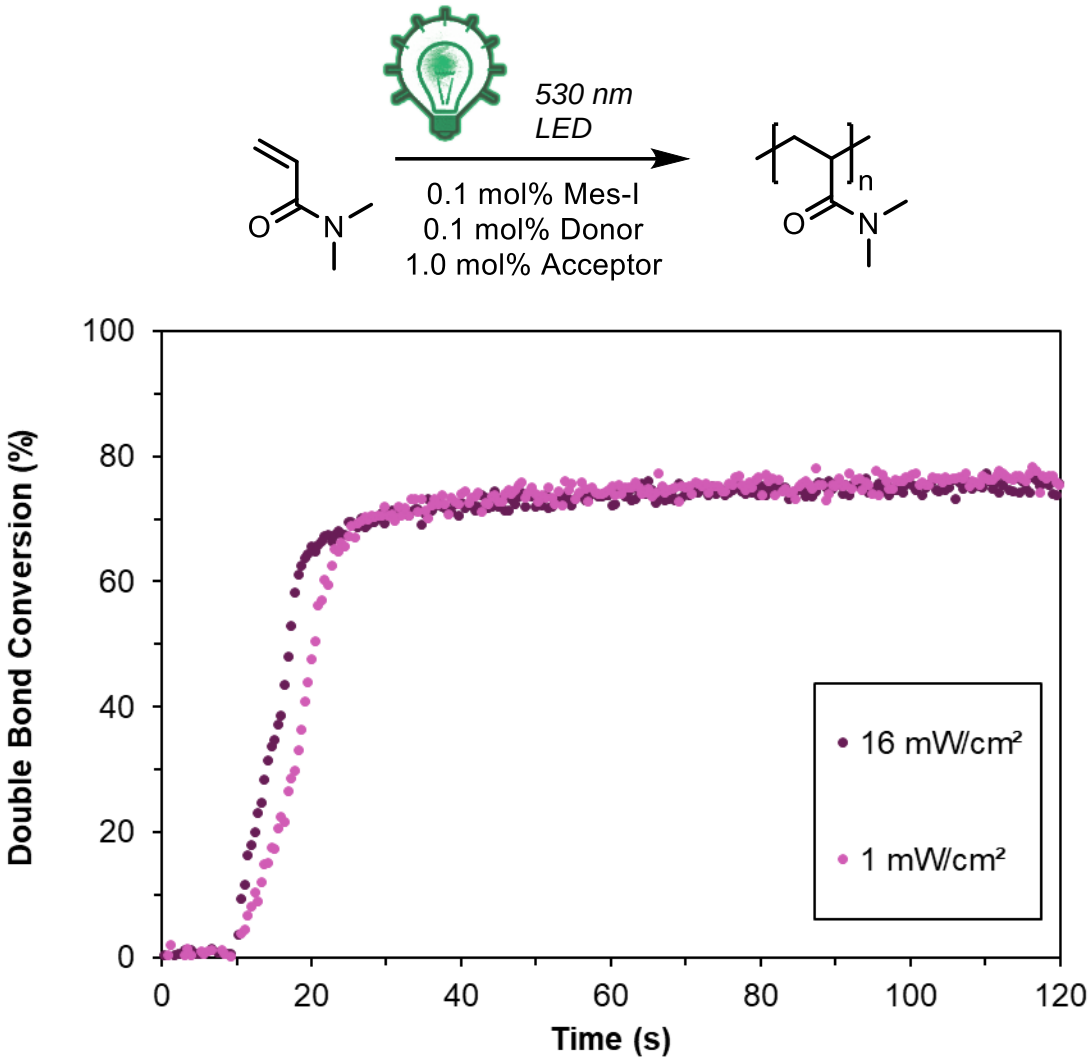


**Figure S19.** DMA photopolymerization with **Mes-I** BODIPY using resin formulation: 0.1 mol% BODIPY, 0.1 mol% Borate V (Donor), and 1.0 mol% H-Nu 254 (Acceptor). Irradiated with a 530 nm LED at 16 mW/cm$^2$ (Polymerization Rate: 5.7± 0.2 %Conv/s) and 1 mW/cm$^2$ (Polymerization Rate: 3.1 ± 0.4 %Conv/s).

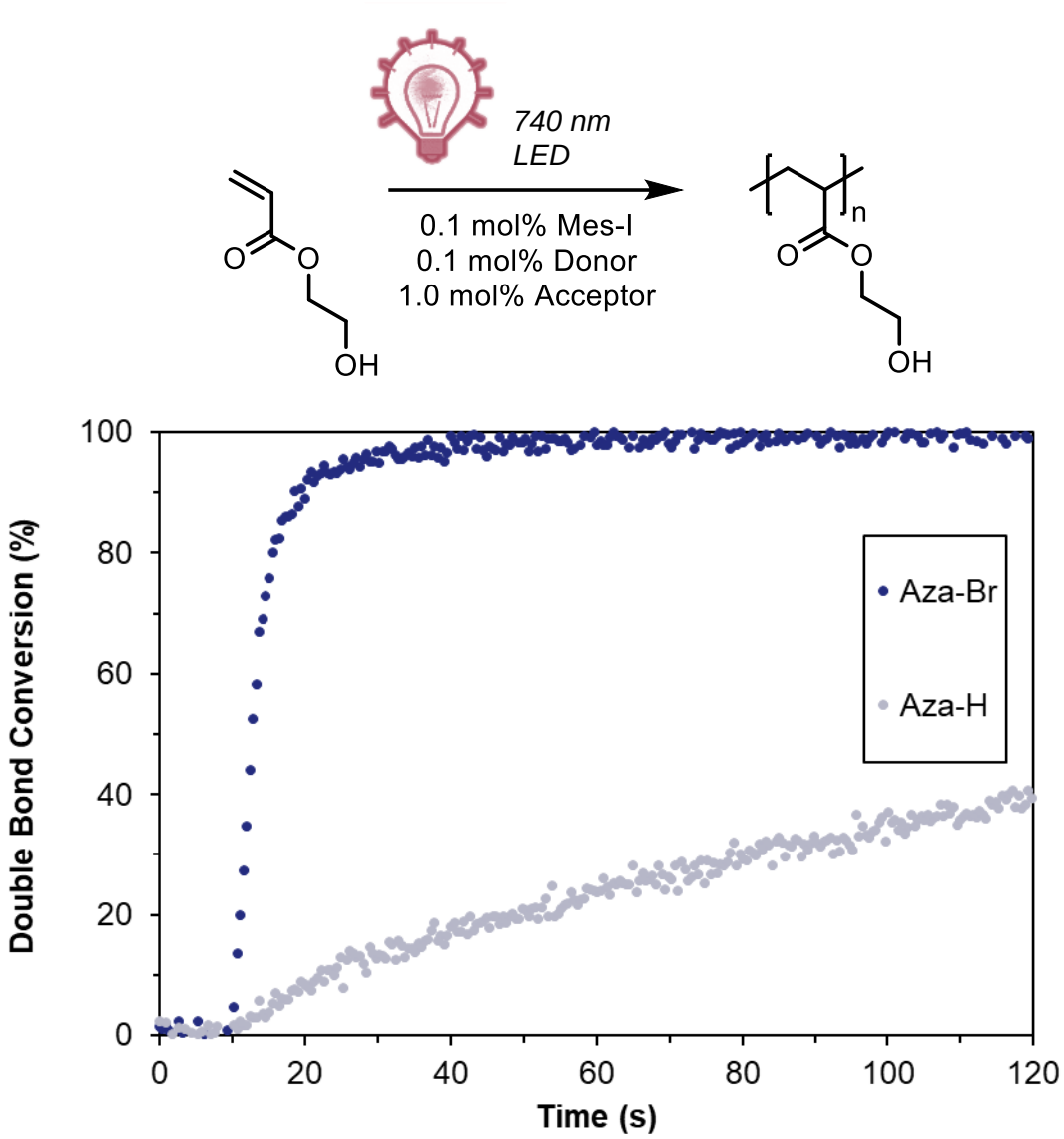


**Figure S20**. HEA photopolymerization with **aza-H** & **aza-Br** using resin formulation: 0.1 mol% BODIPY, 0.1 mol% Borate V (Donor) and 1.0 mol% H-Nu 254 (Acceptor). Irradiated with a 740nm LED at 16 mW/cm$^2$. (**aza-H** polymerization Rate: 1.2 ± 0.1 %Conv/s) (**aza-Br** polymerization Rate: 16.2 ± 1.1 %Conv/s)

***Emission Quantum Yield*** [10]

The emission quantum yields for all BODIPY derivatives were calculated based on the equation,

$$\Phi_{f,x} = \Phi_{f,R} \cdot \frac{A_R}{A_x} \cdot \frac{I_x}{I_R} \cdot \frac{n_x^2}{n_R^2} \qquad \textit{(SE4)}$$

where the index *R* denotes the reference dye and *x* denotes the sample, $\Phi_f$ is the emission quantum yield, *A* is the absorption, *I* is the integrated emission intensity, and *n* is the refractive index of the solvent being used.

For simplicity, absorption for all samples (in acetonitrile) including the reference dye, rhodamine 6G ($\Phi_f = 0.91$ in ethanol) were measured under dilute conditions (abs. = 0.1) to prevent aggregation. After recording all the emission spectrum for each sample and R6G, the area under the emission curve was integrated to calculate *I*. The refractive indices for acetonitrile and ethanol are 1.344 and 1.361, respectively. Following the equation, $\Phi_f$ was calculated for all samples.

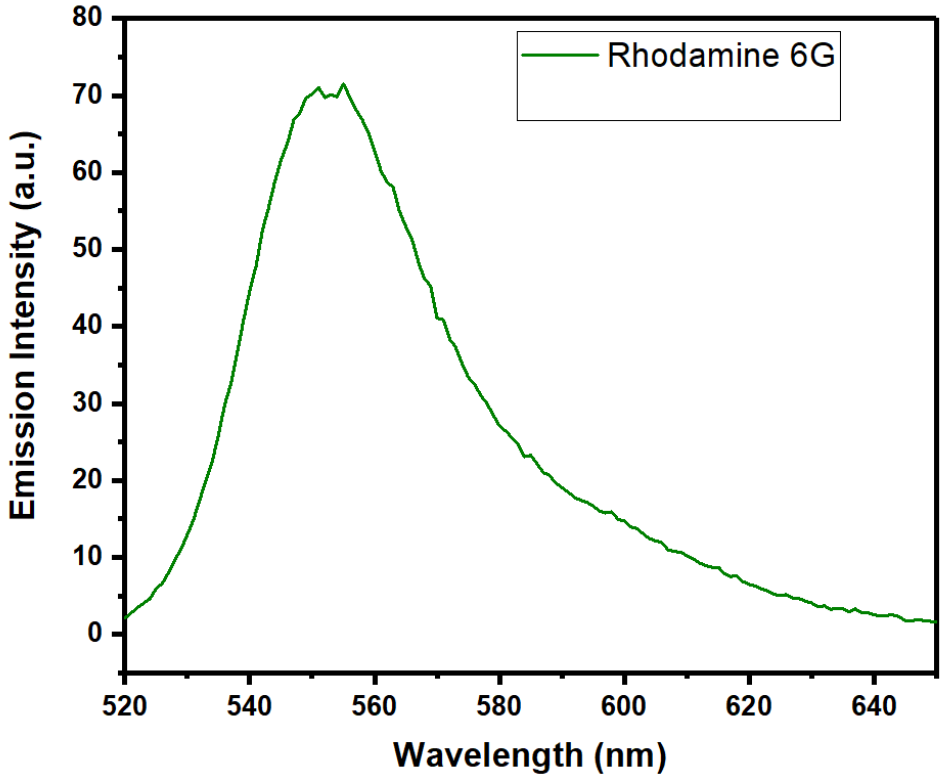


**Figure S21.** Emission spectrum of R6G in ethanol.

***Stern-Volmer Plot*** [11]

The Stern-Volmer experiments were conducted in acetonitrile solutions by gradually increasing the quencher (the iodonium salt or the borate salt) concentration in the presence of BODIPY derivatives (1 mM) and recording the fluorescence spectrum for each quencher concentration. The total emission intensity of each quencher concentration were fitted to the equation,

$$\frac{I_f^0}{I_f} = 1 + k_Q \tau_0 [Q] \qquad \textit{(SE5)}$$

where $I_f^0$ is the emission intensity without quenchers, $I_f$ is the emission intensity for the solution with quenchers, $k_Q$ is the rate constant of the quenching process, $\tau_0$ is the excited-state lifetime of the fluorophore without quenchers, and $[Q]$ is the quencher concentration.

***Cyclic Voltammetry Data***

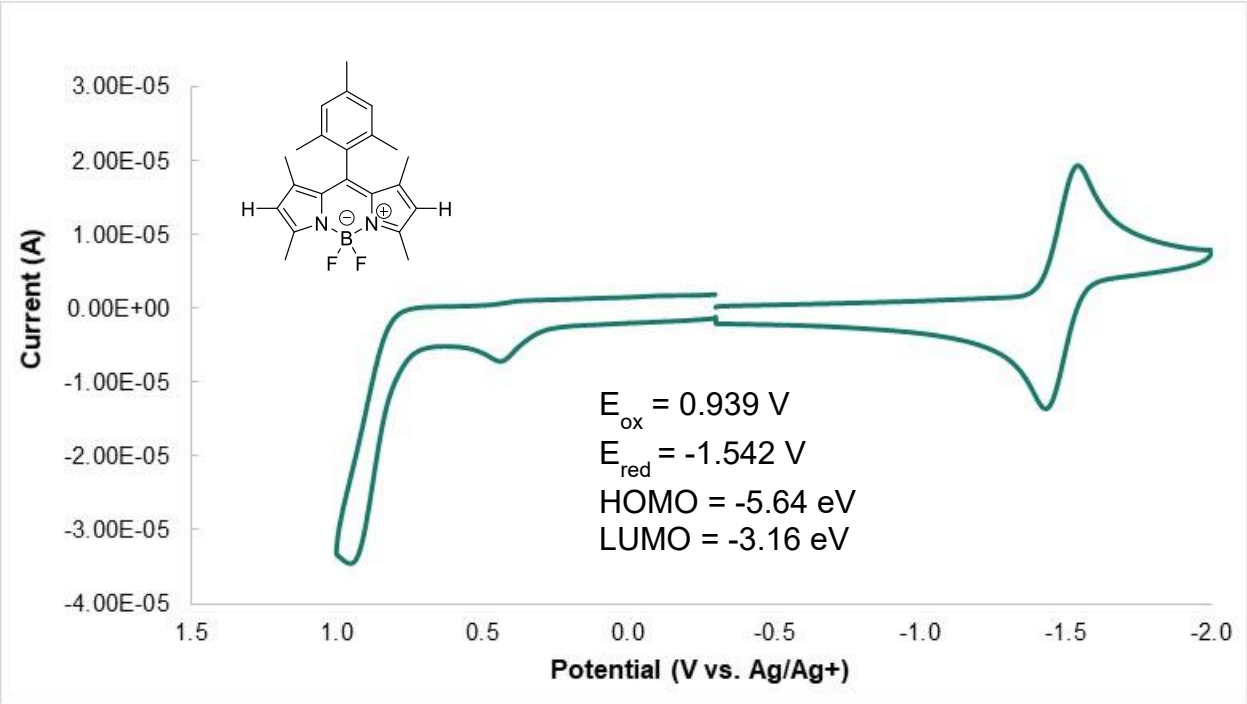


**Figure S22. Mes-H** BODIPY CV Trace. HOMO-LUMO energy levels calculated using the onset redox potentials

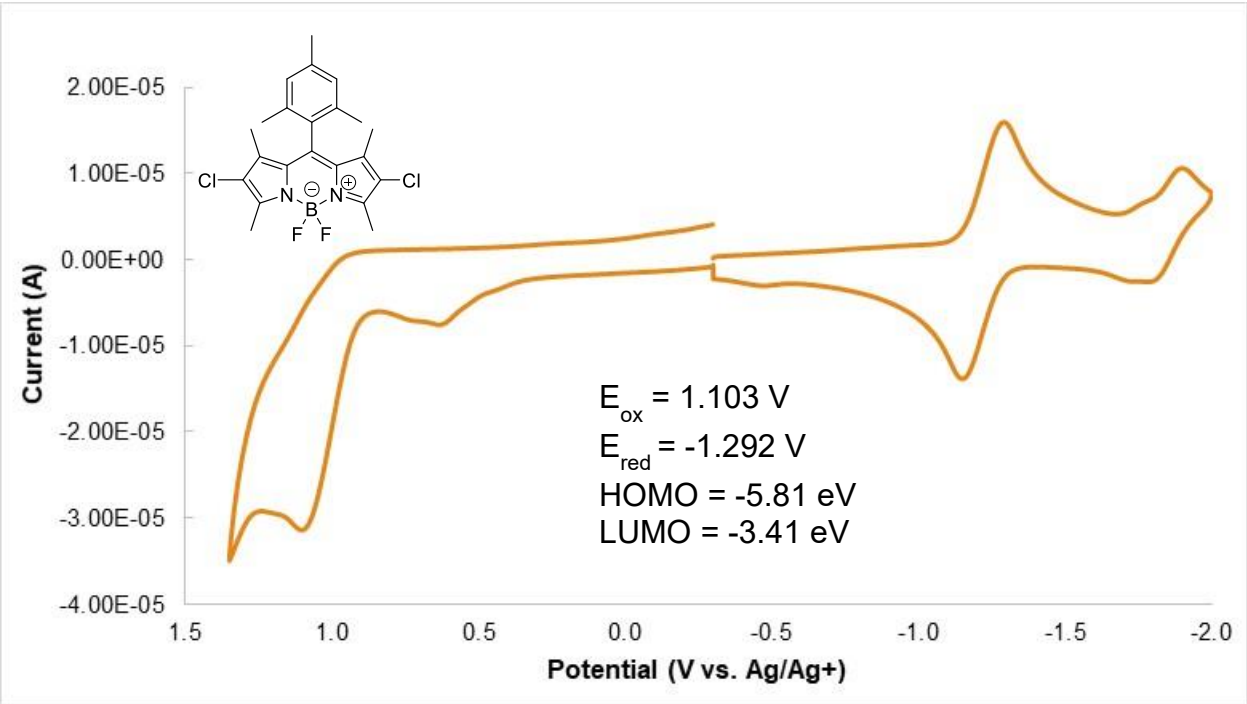


**Figure S23. Mes-Cl** BODIPY CV Trace. HOMO-LUMO energy levels calculated using the onset redox potentials

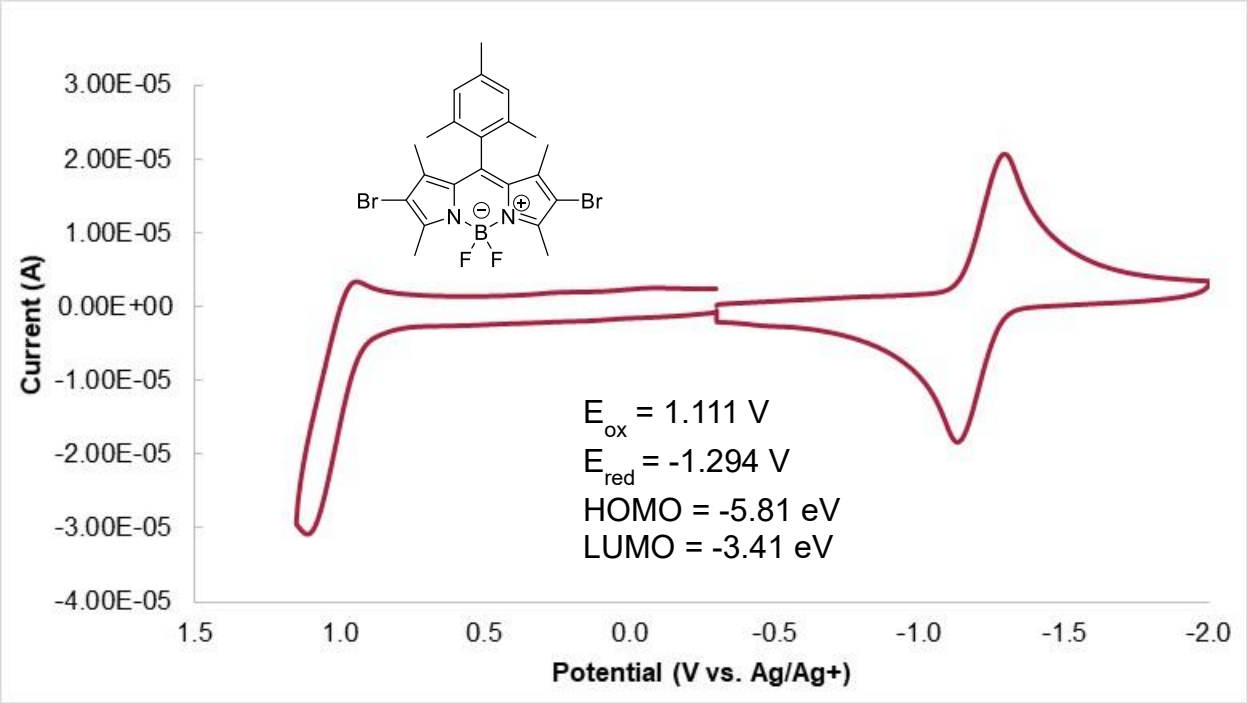


**Figure S24. Mes-Br** BODIPY CV Trace. HOMO-LUMO energy levels calculated using the onset redox potentials

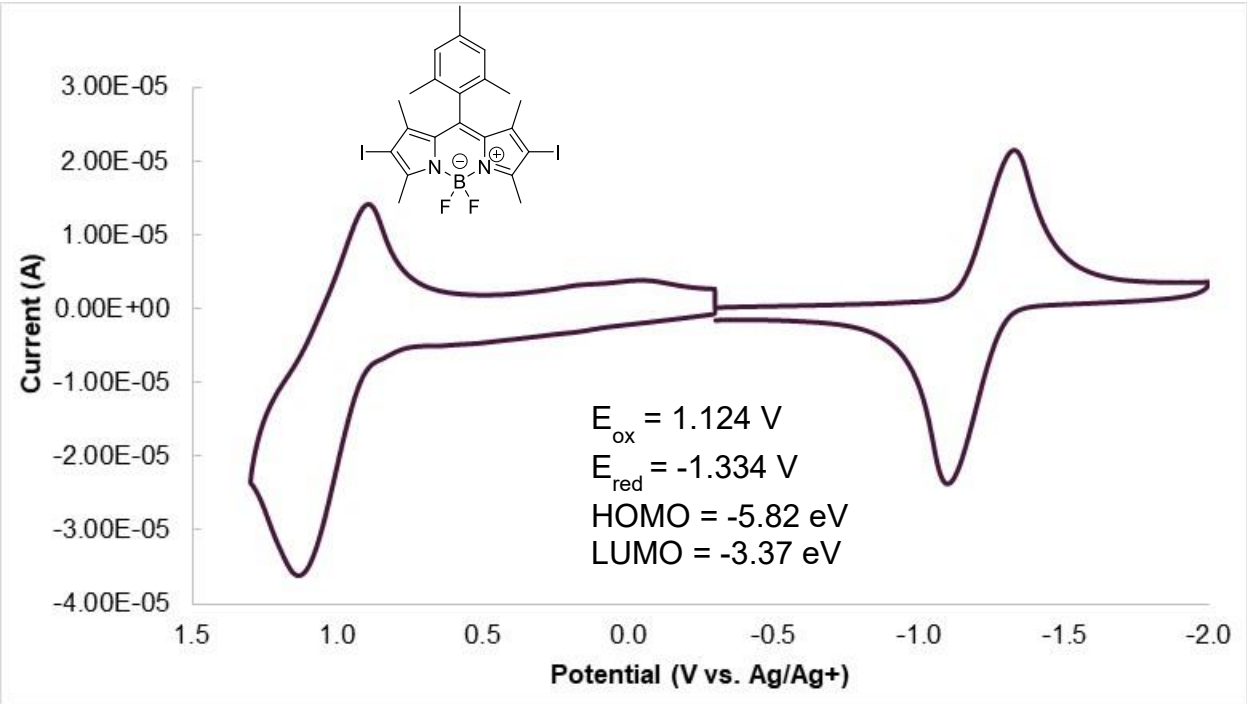


**Figure S25. Mes-I** BODIPY CV Trace. HOMO-LUMO energy levels calculated using the onset redox potentials

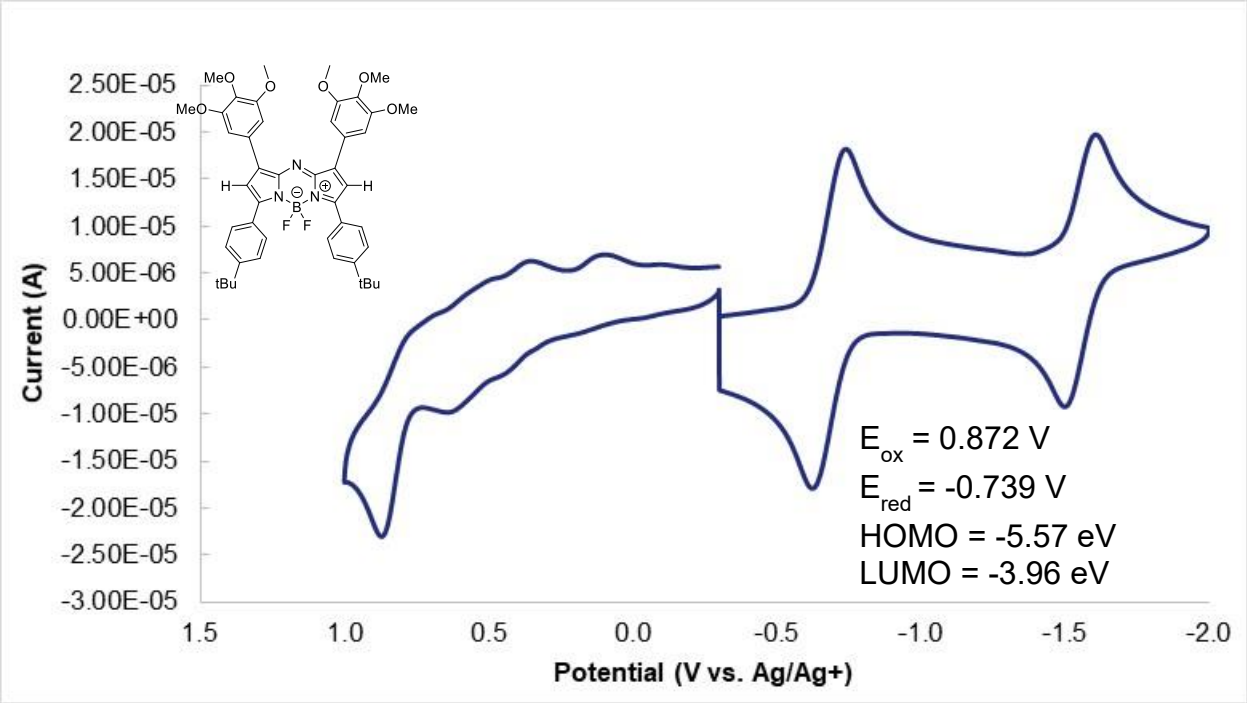


**Figure S26. aza-H** BODIPY CV Trace. HOMO-LUMO energy levels calculated using the onset redox potentials

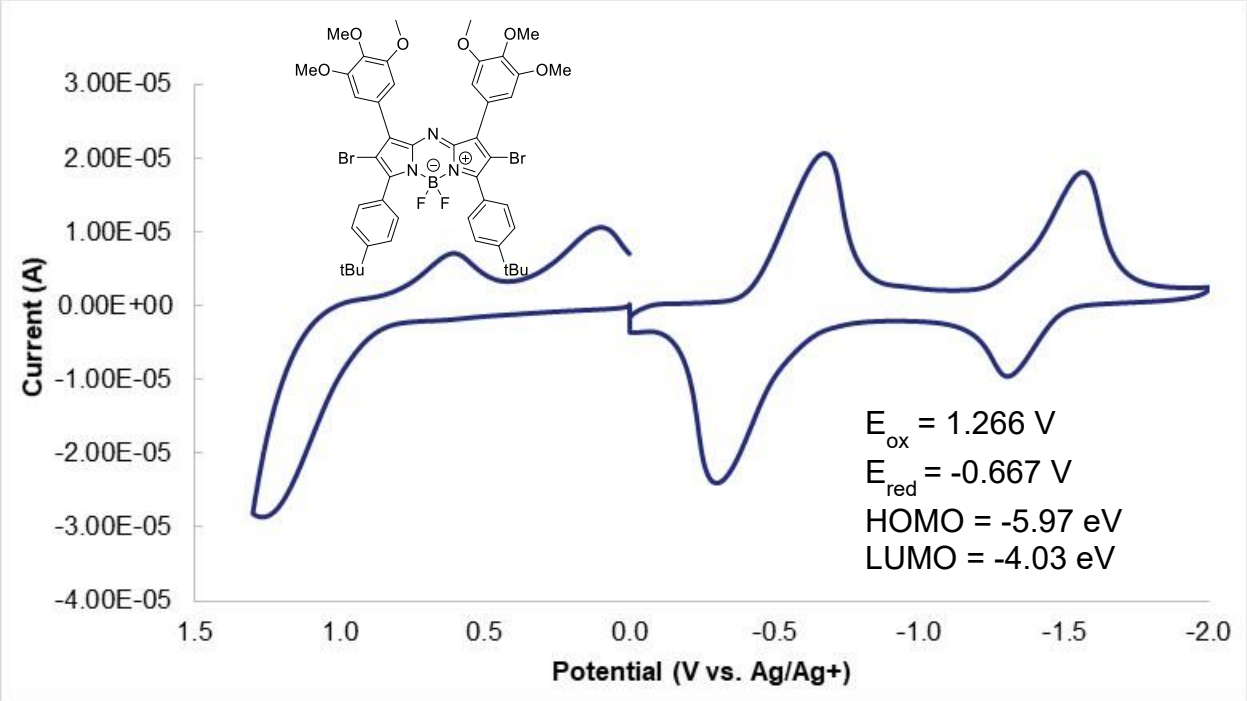


**Figure S27. aza-Br** BODIPY CV Trace. HOMO-LUMO energy levels calculated using the onset redox potentials

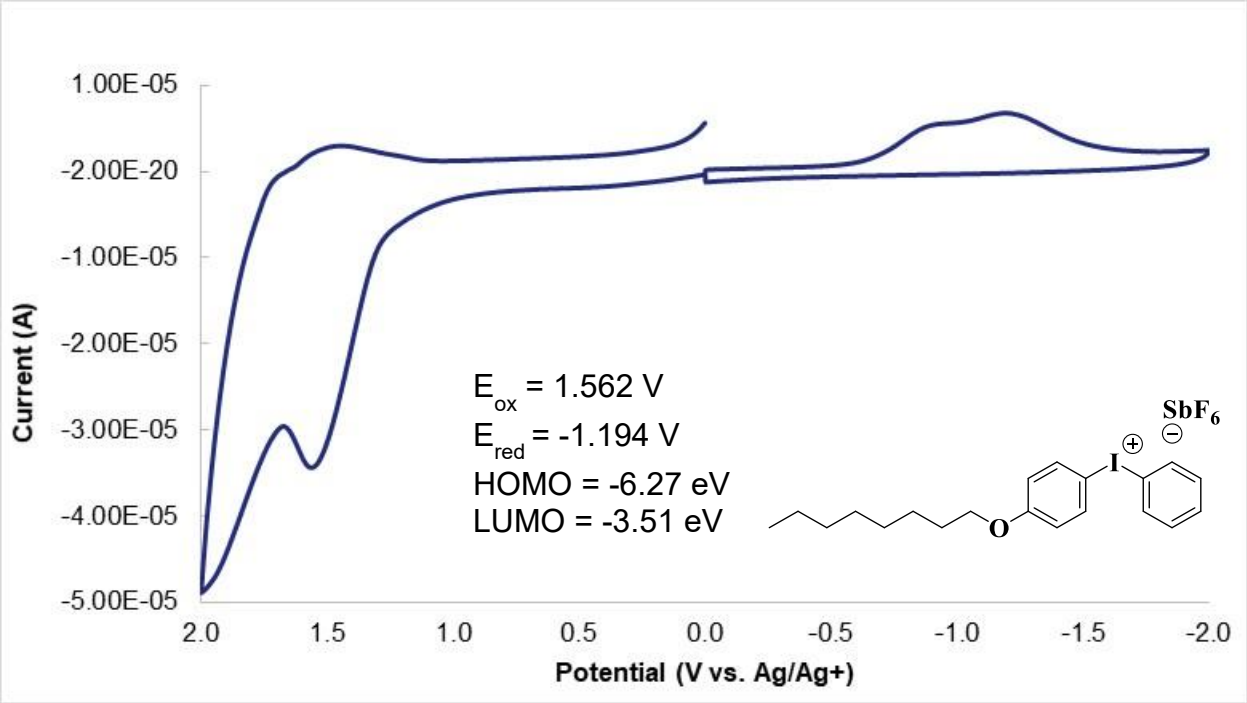


**Figure S28.** H-Nu 254 (Acceptor) CV Trace. HOMO-LUMO energy levels calculated using the onset redox potentials

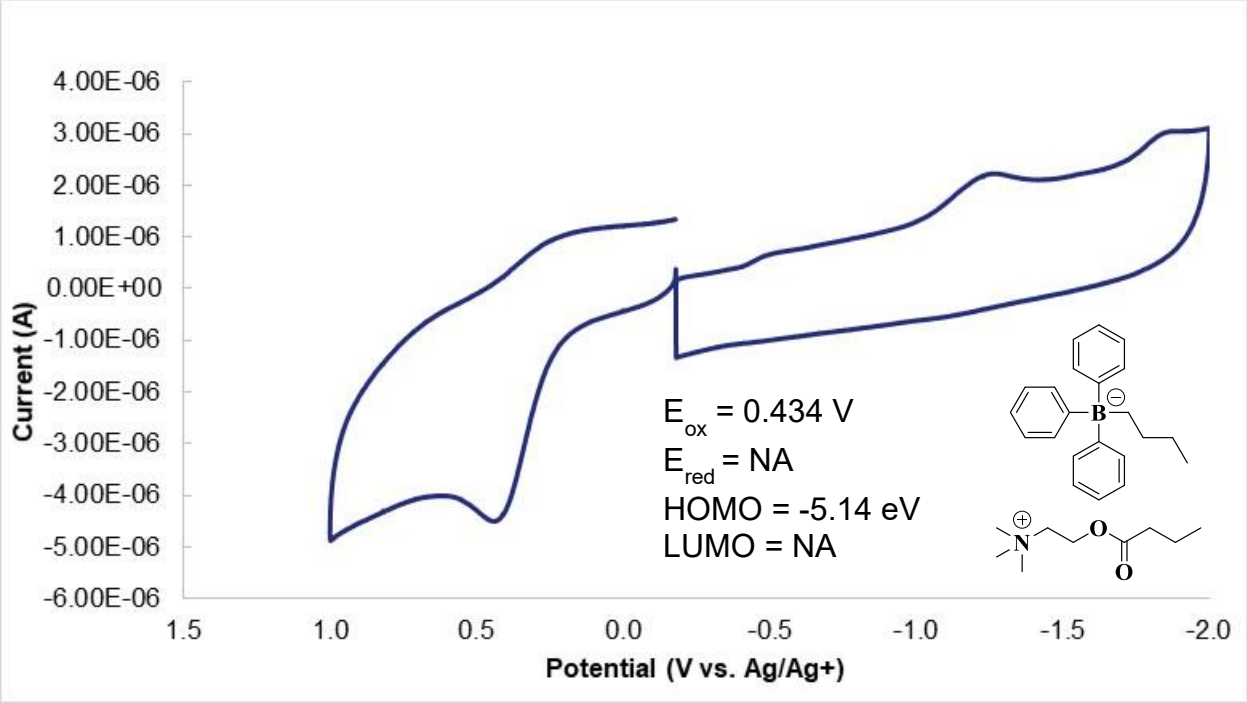


**Figure S29.** Borate V (Donor) CV Trace. HOMO-LUMO energy levels calculated using the onset redox potentials

***Computational Methods/Data***

**HOMO and LUMO Calculations**

The geometries for all molecules were optimized with the 6-31G* basis set and B3LYP functional in the gas phase. All converged geometries are listed below. All calculations on the **Mes-BODIPY** and **aza-BODIPY** molecules were done with these converged geometries. The def2-tzvp basis set and cam-b3lyp functional were used to compute the HOMO and LUMO levels. The energies were computed as follows:

$$E_{LUMO} = -(E_{Anion} - E_{Ground}) \quad \textit{(SE6)}$$

$$E_{HOMO} = E_{Cation} - E_{Ground} \quad \textit{(SE7)}$$

$E\_Ground$ is the energy of the neutral ground state, $E_{Anion}$ is the energy of the anion, and $E_{Cation}$ is the energy of the cation. Equation ***SE6*** yields the vertical electron affinity and Equation ***SE7*** yields the vertical ionization potential. For these calculations an implicit solvation model, SMD, was used with acetonitrile as the implicit solvent.[12] Linear response TDDFT was used to compute the singlet excited state energies, and the triplet excited states were modeled by setting the spin multiplicity to 3 to converge on the lowest triplet state.

For the two co-initiators, the donor **D,** and the acceptor **A**, the HOMO and LUMO levels were computed via a concerted electron transfer and bond cleavage mechanism. This mechanism was first used on diphenyliodinium.[13,14] It was shown that simultaneous addition of an electron and cleavage of the C-I bond was necessary to reproduce experimental results. Assuming only an electron transfer event yielded 5.88 and 2.25 eV for **D** HOMO and **A** LUMO, respectively. The diabatic electronic transfer event HOMO and LUMO values are off by over 1.0 eV. The equations used for the **A** LUMO (Equation ***SE8***) and the **D** HOMO (Equation ***SE9***) are

$$E_{Ar_2I^+ \,/\, Ar^{\cdot}+ArI} = E_{LUMO,Ad} - E_{BDE} \quad \textit{(SE8)}$$

$$E_{Ar_3RB^- \,/\, Ar^{\cdot}+Ar_2RB} = E_{HOMO,Ad} + E_{BDE} \quad \textit{(SE9)}$$

$E_{BDE}$ is the bond dissociation energy of the C-I or C-B bond. This was computed by optimizing the geometry of the dissociated fragments and computing their energy within the SMD implicit solvent model. The bond dissociation energy was then obtained by $E_{BDE} = E_{frag,1} + E_{frag,2} - E_{mol}$. For both **A** and **D** there are two unique bonds that can be cleaved. In the case of **A** one of the two aromatic rings has an ether while the other does not. In the case of **D** there are the aromatic rings (Ar) or the alkane chain (R) that are bonded to the Boron.

$E_{HOMO,Ad}$ and $E_{LUMO,Ad}$ are the adiabatic ionization potential and electron affinity, respectively. The adiabatic HOMO and LUMO use the optimized geometry of the iodine fragment or boron fragment after bond cleavage. For example, $E_{LUMO,Ad}$ for **A** is the adiabatic electron affinity of the $ArI^+$ fragment. These were computed in the SMD implicit solvation model. An adiabatic ionization potential/electron affinity is computed by taking the difference in energy between the minimized geometry of the ground state and the minimized geometry of the reduced/oxidized state. This is different from the commonly used diabatic ionization potential where only the minimized ground state geometry is used for both electronic states.

**Table S1. Breakdown of the energies involved in the concerted electron attachment/detachment and bond cleavage of the co-initiators.**

| HNU-254 | $E_{LUMO,Ad}$ (eV) | $E_{BDE}$ (eV) | $E_{Ar_2I^+ / Ar^{\cdot}+ArI}$ (eV) |
|---|---|---|---|
| **Ar$^{\cdot}$ + ArOI** | 5.89 | 1.94 | 3.95 |
| **ArO$^{\cdot}$ + ArI** | 6.53 | 2.62 | 3.91 |
| | | | |
| **Borate V** | $E_{HOMO,Ad}$ (eV) | $E_{BDE}$ (eV) | $E_{Ar_3RB^- / Ar^{\cdot}+Ar_2RB}$ (eV) |
| **Ar$^{\cdot}$ + Ar$_2$RB** | 2.07 | 3.36 | 5.43 |
| **R$^{\cdot}$ + Ar$_3$B** | 2.40 | 2.58 | 4.98 |

In **Table S1**, there are two values listed for the HOMO and LUMO energies of the initiators because there are two unique C-I or C-B bonds to cleave. In the case of the borate donor, the C-B bond with the aromatic ring vs alkane has significant differences. The $Ar_3B$ fragment has a larger ionization potential, but the R-B bond is significantly weaker than the Ar-B bond. Based on the bond dissociation energies, cleavage of an aromatic group requires more energy than the alkane chain, and thus a larger ionization potential. Interestingly, for the diphenyl iodonium acceptor (H-Nu 254) there are significant differences in the electron affinity and bond dissociation energy between the two aromatic groups, but they cancel with each other to yield almost identical electron affinities. In comparison, if we use equations ***SE6*** and ***SE7*** for the co-initiators we get 5.88 and 2.25 eV for the **D** HOMO and the **A** LUMO, respectively. This is in agreement with other work on similar co-initiators showing that the electron transfer process occurs with the bond cleavage and not independently of each other.

**Table S2. Computational and Experimental (right three columns) data for the photocatalysts.**

| | **Computational** | | | | **Experimental** | | |
|---|---|---|---|---|---|---|---|
| **BODIPY** | Singlet (eV) | Triplet (eV) | HOMO (eV) | LUMO (eV) | Singlet (eV) | HOMO (eV) | LUMO (eV) |
| **aza- H** | 2.16 | 0.87 | 5.47 | 3.85 | 1.85 | 5.57 | 3.96 |
| **aza-Br** | 2.20 | 0.93 | 5.73 | 4.06 | 1.89 | 5.97 | 4.03 |
| **Mes-H** | 2.98 | 1.60 | 5.42 | 3.06 | 2.49 | 5.64 | 3.16 |
| **Mes-Cl** | 2.86 | 1.58 | 5.59 | 3.25 | 2.37 | 5.81 | 3.41 |
| **Mes-Br** | 2.85 | 1.58 | 5.60 | 3.23 | 2.37 | 5.81 | 3.41 |
| **Mes-I** | 2.83 | 1.59 | 5.54 | 3.29 | 2.34 | 5.82 | 3.37 |
| **Donor** | | | 4.98 (5.43) | | | 5.14 | |
| **Acceptor** | | | | 3.95 (3.91) | | | 3.51 |

As can be seen in **Table S2**, the computational values for the HOMO and LUMO energies are within 0.2 eV of the experimental values. Surprisingly, it is very consistent across all values that we underestimate by ~0.2 eV, suggesting that for future screening a shift of 0.2 eV to the current computational protocol might yield more accurate results.

A rough depiction of the photo-induced electron transfer event that occurs in solution is given in **Figure S30**. Based on the computational results, electron transfer with **D** from the triplet excited state of **Mes-BODIPY** has a driving force of roughly -0.1 eV. In contrast, for the **aza-BODIPY** compounds that driving force is uphill by ~0.7 eV, indicating that the electron transfer to this co-

initiator might not be occurring for the **aza-BODIPY** compounds in the triplet excited state. The electron transfer event with **A** from the triplet excited state of **Mes-BODIPY** has a driving force of roughly ~1.0 eV. This is too uphill for the triplet state, but from the singlet excited state the electron transfer event is able to occur. For the **aza-BODIPY** compounds the driving force from the triplet excited state to the charge transfer state is 0.05 eV.

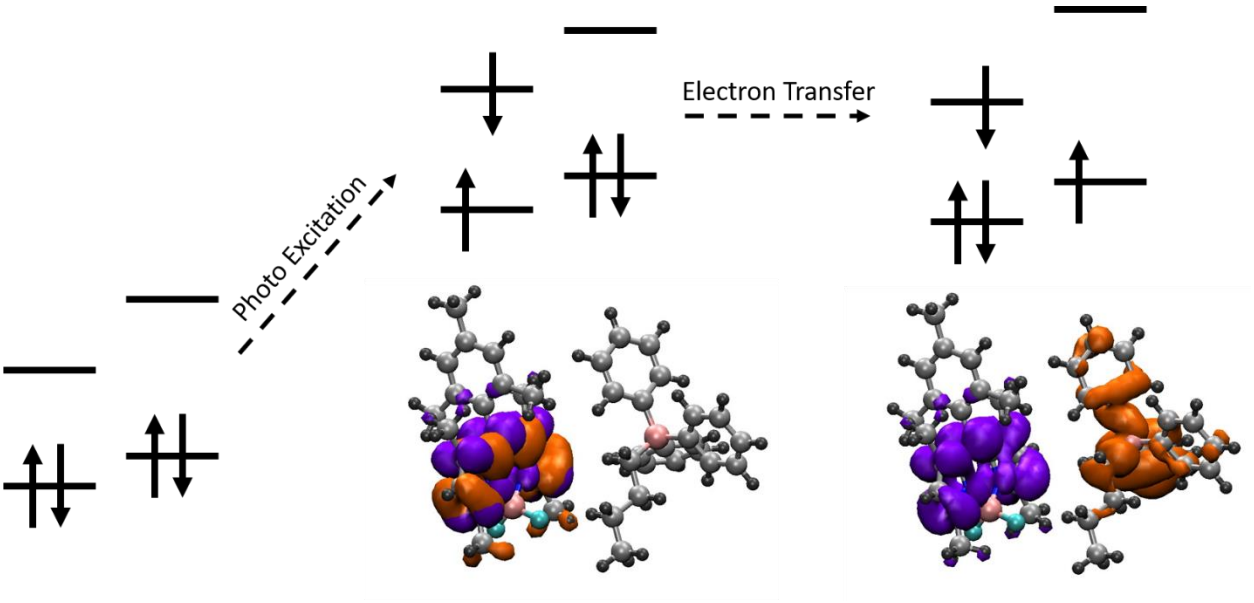


**Figure S30.** Rough schematic of the photo-induced electron transfer even that occurs in solution. The orbitals shown are from electron attachment/detachment plots showing where an electron came from (purple) and where it went to (orange). The first plot is the localized singlet excited state and the second is the charge transfer state between the dye and co-initiator.

## Geometries

### aza-H

| | | | |
|---|---|---|---|
| C | 0.331524742 | -1.060580441 | -0.226577487 |
| N | -1.045208222 | -1.186769531 | -0.195620509 |
| B | -1.983254786 | 0.053856663 | -0.347984765 |
| N | -1.075693788 | 1.308581308 | -0.134117025 |
| N | 0.969597829 | 0.085043219 | -0.144293662 |
| C | 0.303494998 | 1.210166651 | -0.052794788 |
| C | -1.402557226 | 2.609899636 | 0.027749974 |
| C | 0.857615041 | 2.511983453 | 0.172325124 |
| C | -0.224989254 | 3.364291391 | 0.220016844 |
| H | -0.200042129 | 4.430779051 | 0.376888153 |
| C | 0.925378989 | -2.358863543 | -0.188053113 |
| C | -1.333815309 | -2.502960976 | -0.092174693 |
| C | -0.130678165 | -3.240174767 | -0.068563546 |
| F | -2.996658402 | 0.026131354 | 0.579615026 |
| F | -2.483104788 | 0.065920304 | -1.653384831 |
| C | 2.261862066 | 2.853533618 | 0.343758513 |
| C | 2.713018252 | 4.124797272 | 0.010347402 |
| H | 2.049471687 | 4.861241724 | -0.42514086 |
| C | 4.044599353 | 4.478622843 | 0.184599079 |
| C | 4.952315015 | 3.561913905 | 0.724605728 |
| C | 4.488702799 | 2.281449123 | 1.078349174 |
| C | 3.167323514 | 1.928637777 | 0.8731672 |
| H | 2.813851049 | 0.943539869 | 1.134046307 |
| C | 2.343471024 | -2.67274689 | -0.283681268 |
| C | 3.202619407 | -1.882944807 | -1.042083494 |
| H | 2.840608061 | -1.005411666 | -1.560082607 |
| C | 4.536920776 | -2.237506199 | -1.186053262 |
| C | 5.041483766 | -3.374804732 | -0.557885899 |
| C | 4.181975963 | -4.159225797 | 0.229738782 |
| C | 2.846407881 | -3.812273232 | 0.355124088 |
| H | 2.181807684 | -4.406056238 | 0.967911341 |
| C | -2.741197506 | 3.183332342 | 0.010519547 |
| C | -2.994172729 | 4.321393968 | 0.787041581 |
| H | -2.214654637 | 4.716357865 | 1.428170064 |
| C | -4.233333381 | 4.926141396 | 0.780402212 |
| H | -4.388954857 | 5.793416622 | 1.412476496 |
| C | -5.280433999 | 4.443068672 | -0.009122008 |
| C | -5.017299481 | 3.319088244 | -0.786817814 |
| H | -5.787268162 | 2.905564369 | -1.425652997 |
| C | -3.780911602 | 2.695043084 | -0.778857761 |
| H | -3.620372966 | 1.833580575 | -1.411348174 |
| C | -2.659810941 | -3.103063677 | -0.030574334 |
| C | -3.772194039 | -2.601390163 | -0.711917428 |
| H | -3.677137782 | -1.714781596 | -1.322673012 |
| C | -4.989732641 | -3.246581959 | -0.634119132 |
| H | -5.82559374 | -2.827290807 | -1.183211525 |
| C | -5.170820222 | -4.406767556 | 0.121983718 |
| C | -4.057528466 | -4.902615504 | 0.795480175 |
| H | -4.140148345 | -5.794274374 | 1.403234505 |
| C | -2.828857966 | -4.270583493 | 0.716509334 |
| H | -1.98985502 | -4.673513215 | 1.272324928 |
| C | -6.633352219 | 5.143668613 | 0.007746777 |
| C | -6.542231307 | -5.067311153 | 0.190465644 |
| C | -6.995503934 | -5.451268312 | -1.222389869 |
| C | -7.54747553 | -4.080152904 | 0.79634016 |
| C | -6.535006485 | -6.329519339 | 1.049480946 |
| C | -6.457506119 | 6.592567732 | -0.461660668 |
| C | -7.18662775 | 5.139704495 | 1.4377382 |
| C | -7.64860687 | 4.462391176 | -0.904463371 |
| O | 6.219417557 | 3.964243792 | 1.005007329 |
| O | 4.372479268 | 5.756132214 | -0.132036101 |
| O | 5.401275417 | 1.46185198 | 1.65134849 |
| O | 5.324132901 | -1.502208165 | -2.018820197 |
| O | 6.357188553 | -3.692158856 | -0.68164681 |
| O | 4.752588277 | -5.233266401 | 0.819300153 |
| C | 4.942853565 | 0.243307791 | 2.197434756 |
| H | 4.538900497 | -0.422996261 | 1.428667689 |
| H | 5.812447069 | -0.224949147 | 2.65564942 |
| H | 4.178338662 | 0.418674551 | 2.960840704 |
| C | 7.273055319 | 3.283744429 | 0.342322138 |
| H | 8.191317147 | 3.801036093 | 0.619551347 |
| H | 7.333826617 | 2.240024187 | 0.652740166 |
| H | 7.145112989 | 3.33520489 | -0.744735863 |
| C | 5.549574157 | 5.998875537 | -0.879570582 |
| H | 5.408594138 | 6.969145806 | -1.356827907 |
| H | 6.434360673 | 6.030374824 | -0.242916146 |
| H | 5.684161486 | 5.239903418 | -1.657376037 |
| C | 6.338079346 | -0.735930333 | -1.389543776 |
| H | 6.89721385 | -0.252019963 | -2.190135755 |
| H | 5.898334448 | 0.032956578 | -0.745522922 |
| H | 7.0112307 | -1.368427849 | -0.806087363 |
| C | 6.626195236 | -4.764928165 | -1.572163626 |
| H | 6.284078282 | -4.521432999 | -2.582794736 |
| H | 7.707507874 | -4.898448597 | -1.577788763 |
| H | 6.148564108 | -5.687098949 | -1.231341312 |
| C | 3.936118903 | -6.059148126 | 1.613919684 |
| H | 3.516326505 | -5.510793472 | 2.463945747 |
| H | 3.119634048 | -6.497609923 | 1.030050539 |
| H | 4.580244225 | -6.85468093 | 1.984785083 |
| H | -0.07531013 | -4.317358087 | -0.057734504 |
| H | -7.062060619 | -4.580746746 | -1.87729678 |
| H | -7.982765976 | -5.919828239 | -1.184378644 |
| H | -6.298489149 | -6.159699608 | -1.67677784 |
| H | -7.628121677 | -3.168100793 | 0.201764114 |
| H | -7.251743054 | -3.793721152 | 1.808492432 |
| H | -8.539806313 | -4.537279724 | 0.845974012 |
| H | -5.850395532 | -7.085351958 | 0.656120086 |
| H | -7.536547172 | -6.766673224 | 1.063137975 |
| H | -6.067208643 | 6.627951906 | -1.481644607 |
| H | -6.516718965 | 5.653483798 | 2.129948793 |
| H | -7.324475371 | 4.118574707 | 1.80140817 |
| H | -8.154675933 | 5.647493334 | 1.469884672 |
| H | -7.324299002 | 4.470760911 | -1.94790439 |
| H | -8.602573799 | 4.992513451 | -0.850977081 |
| H | -7.828951549 | 3.425877922 | -0.608778224 |

### aza-Br

| | | | |
|---|---|---|---|
| C | 0.35930138 | -1.184277942 | -0.206614973 |
| N | -1.021662082 | -1.222881999 | -0.265292713 |
| B | -1.893340304 | 0.062636854 | -0.467725639 |
| N | -0.918055418 | 1.259652067 | -0.201884683 |
| N | 1.059809567 | -0.073301988 | -0.191942368 |
| C | 0.455962861 | 1.092191725 | -0.197180548 |
| C | -1.187430862 | 2.562118826 | -0.002711929 |
| C | 1.087696086 | 2.361442508 | -0.029240767 |
| C | 0.047837161 | 3.257528827 | 0.11808554 |
| Br | 0.218467413 | 5.113573853 | 0.246828678 |
| C | 0.868120403 | -2.512566263 | -0.037966413 |
| C | -1.417282087 | -2.500010417 | -0.128260094 |

| | | | |
|---|---|---|---|
| C | -0.265122976 | -3.310386243 | 0.023529915 |
| F | -2.947608328 | 0.080736256 | 0.404675143 |
| F | -2.305095613 | 0.116615871 | -1.79701635 |
| C | 2.525204076 | 2.613462181 | -0.038064671 |
| C | 3.112062369 | 3.357901945 | 0.971317621 |
| H | 2.529808726 | 3.736407654 | 1.800996053 |
| C | 4.47758761 | 3.624378224 | 0.959904827 |
| C | 5.269713491 | 3.164172765 | -0.094333369 |
| C | 4.667080683 | 2.408876838 | -1.119300958 |
| C | 3.311814356 | 2.12688119 | -1.084726932 |
| H | 2.850658996 | 1.539192597 | -1.86543879 |
| C | 2.274041274 | -2.876007143 | 0.069435997 |
| C | 3.244234678 | -2.172996479 | -0.637505914 |
| H | 2.972050895 | -1.349933648 | -1.282051725 |
| C | 4.583116811 | -2.516107034 | -0.528733894 |
| C | 4.979220476 | -3.576524183 | 0.285866403 |
| C | 4.005687916 | -4.266843055 | 1.025456025 |
| C | 2.669999415 | -3.920331902 | 0.912042458 |
| H | 1.926677401 | -4.441612664 | 1.495319771 |
| C | -2.526984487 | 3.135127138 | 0.0605468 |
| C | -2.846670873 | 4.040802949 | 1.070683585 |
| H | -2.103748683 | 4.300107119 | 1.814319574 |
| C | -4.115556316 | 4.587913977 | 1.158294867 |
| H | -4.326862741 | 5.273713878 | 1.967982221 |
| C | -5.107699408 | 4.268746206 | 0.235484531 |
| C | -4.771319918 | 3.373170367 | -0.781400461 |
| H | -5.512326139 | 3.102505385 | -1.524788147 |
| C | -3.515709281 | 2.808723137 | -0.870984657 |
| H | -3.294124944 | 2.113535512 | -1.669318349 |
| C | -2.809277081 | -2.940259197 | -0.153923109 |
| C | -3.679273982 | -2.559696574 | -1.176482708 |
| H | -3.324238778 | -1.924000796 | -1.976789738 |
| C | -4.99110413 | -2.988295878 | -1.172676665 |
| H | -5.634119788 | -2.673543771 | -1.986694955 |
| C | -5.503413243 | -3.792314131 | -0.152995466 |
| C | -4.625667708 | -4.16740661 | 0.86039598 |
| H | -4.969457247 | -4.784277482 | 1.681207814 |
| C | -3.301541932 | -3.760722956 | 0.85754693 |
| H | -2.651548443 | -4.062304481 | 1.670066469 |
| C | -6.518001077 | 4.841901624 | 0.308233226 |
| C | -6.969936318 | -4.205961687 | -0.176525814 |
| C | -7.253638921 | -5.010879042 | -1.449514004 |
| C | -7.844852838 | -2.94544695 | -0.170510518 |
| C | -7.351274764 | -5.061139855 | 1.027626997 |
| C | -6.852215627 | 5.557254435 | -1.005374886 |
| C | -7.51299602 | 3.696011167 | 0.52592016 |
| C | -6.681162867 | 5.841364579 | 1.450393022 |
| O | 6.618258926 | 3.345321495 | -0.063915837 |
| O | 4.954759929 | 4.277265822 | 2.04630813 |
| O | 5.504736936 | 1.976297128 | -2.087954231 |
| O | 5.492082865 | -1.830378262 | -1.275843373 |
| O | 6.295300163 | -3.893863032 | 0.393153962 |
| O | 4.467622494 | -5.255244745 | 1.823495239 |
| C | 4.966886053 | 1.192823012 | -3.130766676 |
| H | 4.189678271 | 1.736195361 | -3.678166666 |
| H | 5.795944835 | 0.98006321 | -3.80378932 |
| H | 4.565279876 | 0.248479987 | -2.752536277 |
| C | 7.170285729 | 4.165793116 | -1.081822843 |
| H | 8.243119029 | 4.204769573 | -0.894686485 |
| H | 6.987343251 | 3.750203041 | -2.073324899 |
| H | 6.757807849 | 5.179377083 | -1.029459201 |
| C | 5.937999086 | 5.283321756 | 1.896899171 |
| H | 5.893332041 | 5.879128764 | 2.808797027 |
| H | 6.936911049 | 4.861749361 | 1.782759646 |
| H | 5.712854198 | 5.930386457 | 1.042632041 |
| C | 6.415007469 | -1.043099425 | -0.530957876 |
| H | 7.01440826 | -0.499647908 | -1.259785698 |
| H | 5.88322136 | -0.323259915 | 0.098713783 |
| H | 7.059819153 | -1.670442229 | 0.086942983 |
| C | 6.678006703 | -5.090578652 | -0.268202906 |
| H | 6.477357651 | -5.017761821 | -1.341689118 |
| H | 7.749753877 | -5.201780334 | -0.106955297 |
| H | 6.156168205 | -5.955569673 | 0.148124037 |
| C | 3.528355941 | -5.969491031 | 2.59190943 |
| H | 3.015768032 | -5.314650559 | 3.304402112 |
| H | 2.784280039 | -6.464548009 | 1.959031323 |
| H | 4.094537374 | -6.721028392 | 3.139570209 |
| Br | -0.335040219 | -5.178746142 | 0.08067893 |
| H | -7.025069983 | -4.437047258 | -2.349478518 |
| H | -8.309833569 | -5.291432991 | -1.488191178 |
| H | -6.656087951 | -5.92540979 | -1.472836251 |
| H | -7.651800414 | -2.314354185 | -1.040505027 |
| H | -7.661408323 | -2.344958717 | 0.723874348 |
| H | -8.903449495 | -3.22042758 | -0.18577389 |
| H | -6.788372629 | -5.997603419 | 1.052261699 |
| H | -8.412393555 | -5.315605621 | 0.972570513 |
| H | -7.185508716 | -4.533530339 | 1.969998645 |
| H | -6.809242137 | 4.879813372 | -1.860338556 |
| H | -6.157269114 | 6.379517516 | -1.193077957 |
| H | -7.863809557 | 5.969801163 | -0.958289961 |
| H | -7.475222354 | 2.968632445 | -0.28765443 |
| H | -8.532167546 | 4.088991802 | 0.579498194 |
| H | -7.302331785 | 3.165587836 | 1.457686305 |
| H | -6.004752221 | 6.693719381 | 1.346135112 |
| H | -6.505004731 | 5.379512339 | 2.425097682 |
| H | -7.702774187 | 6.229296267 | 1.45106323 |

## Mes-H

| | | | |
|---|---|---|---|
| C | -0.514014782 | -1.218359069 | 0.002721759 |
| N | -1.901649352 | -1.255535427 | -0.012899633 |
| B | -2.838512818 | -0.020756871 | -0.030212684 |
| N | -1.918268878 | 1.226515228 | -0.029506715 |
| C | 0.167172346 | -0.000101422 | -0.001469343 |
| C | -0.530241019 | 1.208646144 | -0.01856598 |
| C | -2.332219894 | 2.497458701 | -0.041427075 |
| C | -0.073812495 | 2.558580878 | -0.025287676 |
| C | -1.212811217 | 3.342819313 | -0.039035595 |
| H | -1.248597165 | 4.422472532 | -0.046132317 |
| C | -0.039158417 | -2.561773306 | 0.01919342 |
| C | -2.298106774 | -2.532066177 | -0.008422003 |
| C | -1.167214007 | -3.36175872 | 0.011483369 |
| F | -3.646003665 | -0.018861493 | 1.101082182 |
| F | -3.623938306 | -0.033410906 | -1.176816966 |
| H | -1.187786885 | -4.441813544 | 0.019102155 |
| C | 1.652710359 | 0.01063215 | 0.011595917 |
| C | 2.356982042 | 0.035970472 | -1.198635082 |
| C | 3.744792598 | 0.047395544 | -1.164304964 |
| H | 4.291505133 | 0.067026668 | -2.10304466 |
| C | 4.450464834 | 0.036669936 | 0.034165622 |
| C | 3.726948935 | 0.012345213 | 1.218094401 |
| H | 4.258548673 | 0.00346076 | 2.165135531 |
| C | 2.335838199 | -0.002454079 | 1.230481045 |

| | | | |
|---|---|---|---|
| C | 1.634450753 | 0.053863283 | -2.512784022 |
| H | 1.000746332 | 0.94044568 | -2.607316917 |
| H | 2.339427617 | 0.048236569 | -3.34475802 |
| H | 0.97298414 | -0.810533064 | -2.618345534 |
| C | 1.5948693 | -0.032820246 | 2.534015655 |
| H | 0.927579343 | 0.827632182 | 2.636106485 |
| H | 0.964846858 | -0.923349426 | 2.614063305 |
| H | 2.288080402 | -0.028771507 | 3.375883906 |
| C | 5.949567481 | 0.051056074 | 0.040778372 |
| H | 6.355161661 | -0.819889341 | -0.481284537 |
| H | 6.338218823 | 0.939135745 | -0.464996466 |
| H | 6.340929753 | 0.045248149 | 1.058806059 |
| C | 1.318095685 | 3.087525851 | -0.025895348 |
| H | 1.899466162 | 2.727562822 | 0.825334851 |
| H | 1.868588343 | 2.793403897 | -0.922903368 |
| H | 1.295765624 | 4.177746592 | 0.012859041 |
| C | 1.359524093 | -3.072034716 | 0.046233934 |
| H | 1.351781349 | -4.16263624 | 0.013028092 |
| H | 1.950233828 | -2.70980908 | -0.797711269 |
| H | 1.891555654 | -2.765864937 | 0.950306572 |
| C | -3.762662515 | 2.885263548 | -0.053783377 |
| H | -4.279399428 | 2.487932666 | 0.822951805 |
| H | -3.856319829 | 3.970587635 | -0.062652897 |
| H | -4.268068493 | 2.474719057 | -0.931050152 |
| C | -3.723057088 | -2.939545069 | -0.023349576 |
| H | -4.250857917 | -2.535145021 | 0.843466824 |
| H | -4.228147616 | -2.55005074 | -0.910319825 |
| H | -3.802005456 | -4.026052784 | -0.015205018 |

## Mes-Br

| | | | |
|---|---|---|---|
| C | -0.20418 | -1.21444 | 0.00027 |
| N | -1.59066 | -1.24220 | 0.00071 |
| C | 0.48619 | -0.00010 | 0.00002 |
| C | -0.20424 | 1.21436 | 0.00025 |
| N | -1.59068 | 1.24209 | 0.00067 |
| B | -2.52283 | -0.00004 | 0.00164 |
| C | 0.27334 | 2.55611 | -0.00026 |
| C | -2.00719 | 2.51071 | 0.00035 |
| C | -0.86932 | 3.33856 | -0.00021 |
| C | 0.27334 | -2.55624 | -0.00024 |
| C | -0.86920 | -3.33850 | -0.00019 |
| C | -2.00707 | -2.51079 | 0.00039 |
| C | 1.67017 | 3.06151 | -0.00070 |
| H | 1.66577 | 4.15165 | 0.00238 |
| H | 2.22481 | 2.72300 | -0.87832 |
| H | 2.22735 | 2.71788 | 0.87327 |
| C | 1.67016 | -3.06160 | -0.00068 |
| H | 1.66580 | -4.15171 | 0.00233 |
| H | 2.22731 | -2.71805 | 0.87329 |
| H | 2.22484 | -2.72306 | -0.87821 |
| C | 1.97171 | 0.00002 | -0.00115 |
| C | 2.66648 | 0.00011 | 1.21523 |
| C | 4.05455 | 0.00024 | 1.19078 |
| C | 4.76947 | 0.00022 | -0.00254 |
| C | 4.05465 | 0.00029 | -1.19227 |
| C | 2.66346 | 0.00017 | -1.21566 |
| C | 1.93528 | 0.00021 | 2.52457 |
| H | 2.63588 | 0.00029 | 3.36005 |
| H | 1.28845 | -0.87606 | 2.62341 |
| H | 1.28846 | 0.87655 | 2.62323 |
| C | 1.93339 | 0.00033 | -2.52564 |
| H | 2.63467 | 0.00048 | -3.36055 |
| H | 1.28667 | 0.87667 | -2.62504 |
| H | 1.28670 | -0.87598 | -2.62532 |
| C | 6.26803 | -0.00056 | 0.00431 |
| H | 6.65918 | -0.88521 | 0.51404 |
| H | 6.66029 | 0.87379 | 0.53055 |
| H | 6.67054 | 0.00848 | -1.00938 |
| H | 4.59386 | 0.00041 | 2.13399 |
| H | 4.59318 | 0.00049 | -2.13552 |
| F | -3.31175 | -0.00002 | 1.14217 |
| F | -3.31416 | -0.00013 | -1.13713 |
| Br | -0.93106 | -5.20689 | -0.00090 |
| Br | -0.93114 | 5.20700 | -0.00090 |
| C | -3.43339 | 2.90150 | 0.00040 |
| H | -3.52702 | 3.98596 | 0.00388 |
| H | -3.94122 | 2.49130 | 0.87607 |
| H | -3.93951 | 2.49740 | -0.87916 |
| C | -3.43320 | -2.90161 | 0.00029 |
| H | -3.52686 | -3.98601 | 0.00531 |
| H | -3.93886 | -2.49889 | -0.88013 |
| H | -3.94154 | -2.49007 | 0.87498 |

## Mes-Cl

| | | | |
|---|---|---|---|
| C | 1.23847969 | 0.21046298 | 0.01156558 |
| N | 1.40920422 | 1.58667024 | 0.00812525 |
| B | 0.27015721 | 2.64099374 | -0.01548310 |
| N | -1.06091159 | 1.84123296 | -0.01731212 |
| C | -0.04059945 | -0.35111150 | -0.00436641 |
| C | -1.17742023 | 0.45910884 | -0.01863321 |
| C | -2.27923369 | 2.38722205 | -0.02263215 |
| C | -2.56140629 | 0.12450779 | -0.02938914 |
| C | -3.22031266 | 1.34179589 | -0.02873118 |
| Cl | -4.91560391 | 1.57509470 | -0.03434441 |
| C | 2.52353636 | -0.40229469 | 0.03505356 |
| C | 2.71362310 | 1.86996797 | 0.02493942 |
| C | 3.41934006 | 0.65347041 | 0.04130204 |
| F | 0.36373902 | 3.41231580 | -1.16480984 |
| F | 0.33848735 | 3.44228589 | 1.11370435 |
| Cl | 5.12645523 | 0.53383448 | 0.06663912 |
| C | -0.19350859 | -1.82836577 | -0.00311093 |
| C | -0.32575164 | -2.51011497 | 1.21262446 |
| C | -0.46463427 | -3.89170035 | 1.19054118 |
| H | -0.57005648 | -4.42152174 | 2.13293687 |
| C | -0.47529040 | -4.61097593 | 0.00101022 |
| C | -0.34951144 | -3.90765526 | -1.18925865 |
| H | -0.36528033 | -4.44974904 | -2.13034533 |
| C | -0.20499169 | -2.52476922 | -1.21522410 |
| C | -0.31397531 | -1.77574463 | 2.52021645 |
| H | -1.14770553 | -1.07162184 | 2.59506634 |
| H | -0.38405298 | -2.47202640 | 3.35644520 |
| H | 0.60037853 | -1.18823777 | 2.64133386 |
| C | -0.07024148 | -1.80567053 | -2.52440310 |
| H | -0.86711881 | -1.06925199 | -2.66163559 |
| H | 0.87386293 | -1.25662152 | -2.58221212 |
| H | -0.10840636 | -2.50671025 | -3.35863054 |
| C | -0.59967894 | -6.10437839 | 0.01043142 |
| H | 0.34981057 | -6.57221530 | 0.28826135 |
| H | -1.34723937 | -6.43674811 | 0.73406637 |
| H | -0.88125055 | -6.48769611 | -0.97146026 |

| | | | |
|---|---|---|---|
| C | -3.22275553 | -1.20553546 | -0.03607293 |
| H | -4.29340595 | -1.07935486 | -0.19882618 |
| H | -2.82549585 | -1.85923944 | -0.81319165 |
| H | -3.08825575 | -1.72914270 | 0.91428335 |
| C | 2.89363368 | -1.84138911 | 0.04748296 |
| H | 3.97164857 | -1.94030491 | 0.17725330 |
| H | 2.39416892 | -2.38541632 | 0.85101839 |
| H | 2.61802917 | -2.33713198 | -0.88689140 |
| C | -2.52937221 | 3.84433459 | -0.01550749 |
| H | -1.94083703 | 4.33707600 | -0.79120878 |
| H | -3.58766181 | 4.04525833 | -0.17454225 |
| H | -2.22548251 | 4.27766375 | 0.94114291 |
| C | 3.25576201 | 3.24563458 | 0.02626135 |
| H | 2.91456723 | 3.79112114 | -0.85636643 |
| H | 2.89672224 | 3.79648161 | 0.89843546 |
| H | 4.34401283 | 3.22073635 | 0.03744831 |

## Mes-I

C -0.3415600000 0.0006400000 -0.0002300000
C 0.3451200000 -1.2100400000 0.0006300000
C 0.3495100000 1.2088200000 -0.0005400000
N 1.7274600000 -1.2380500000 0.0016600000
N 1.7319400000 1.2317700000 -0.0000200000
B 2.6612400000 -0.0048700000 0.0034800000
C -0.1336000000 -2.5465100000 -0.0005900000
C 1.0046600000 -3.3270000000 -0.0006900000
C 2.1402200000 -2.5029100000 0.0006900000
C -0.1243000000 2.5470700000 -0.0013400000
C 2.1493500000 2.4950700000 -0.0004600000
C 1.0168100000 3.3233500000 -0.0012400000
F 3.4477200000 -0.0075100000 -1.1258400000
F 3.4408700000 -0.0050200000 1.1379000000
C -1.5189800000 3.0547700000 -0.0022900000
H -2.0703000000 2.7161500000 -0.8783200000
H -1.5122800000 4.1421000000 0.0004100000
H -2.0732700000 2.7117200000 0.8700900000
C 3.5759400000 2.8775100000 -0.0001000000
H 4.0738800000 2.4675100000 -0.8776300000
H 4.0747900000 2.4621700000 0.8743500000
H 3.6772600000 3.9584000000 0.0030000000
C -1.5301400000 -3.0491000000 -0.0015100000
H -2.0801900000 -2.7086300000 -0.8776100000
H -2.0831600000 -2.7038700000 0.8708200000
H -1.5274100000 -4.1364500000 0.0013300000
C 3.5653800000 -2.8906500000 -0.0006000000
H 3.6628000000 -3.9714800000 0.0300200000
H 4.0732900000 -2.4535100000 0.8576800000
H 4.0571700000 -2.5068400000 -0.8934800000
C -1.8220200000 0.0033400000 -0.0015500000
C -2.5118700000 0.0048000000 1.2125800000
C -3.8966400000 0.0074600000 1.1891700000
C -4.6088900000 0.0085700000 -0.0028100000
C -3.8970700000 0.0071900000 -1.1910800000
C -2.5089400000 0.0045600000 -1.2135300000
C -6.1058100000 0.0102000000 0.0054500000
H -6.4934500000 0.8811700000 0.5340900000
H -6.4951800000 -0.8745200000 0.5096100000
H -6.5069900000 0.0244300000 -1.0056200000
C -1.7720200000 0.0036600000 2.5146300000
H -1.1244800000 0.8769400000 2.6032500000
H -1.1295200000 -0.8732200000 2.6045200000
H -2.4640800000 0.0062400000 3.3536300000
C -1.7703500000 0.0030900000 -2.5163400000
H -1.1237400000 0.8769000000 -2.6064600000
H -2.4631900000 0.0044300000 -3.3547000000
H -1.1272500000 -0.8733300000 -2.6064200000
H -4.4353600000 0.0088000000 2.1295100000
H -4.4347500000 0.0082900000 -2.1315500000
I 1.0791500000 5.0386000000 -0.0021800000
I 1.0607000000 -5.0424600000 -0.0023800000

## Borate (donor)

| | | | |
|---|---|---|---|
| B | 0.097693053 | 0.046959314 | 0.233138715 |
| H | 2.400933447 | -0.027040905 | -1.356922754 |
| C | 2.685678771 | 0.177889541 | -0.328221504 |
| C | 1.677540033 | 0.258599418 | 0.642760119 |
| C | 2.116887779 | 0.526499048 | 1.943161213 |
| H | 1.386829067 | 0.595559114 | 2.744009911 |
| C | 3.460566409 | 0.705261798 | 2.259683703 |
| H | 3.750334102 | 0.913027784 | 3.28658682 |
| C | 4.428739267 | 0.618659452 | 1.272070073 |
| H | 5.478738565 | 0.758114079 | 1.511111919 |
| C | 4.029106991 | 0.34994255 | -0.031987361 |
| H | 4.771749518 | 0.278676799 | -0.822329972 |
| H | -0.514028119 | 2.777080474 | 0.494851558 |
| C | -0.486758143 | 2.512466215 | -0.558488892 |
| C | -0.698238481 | 3.515242875 | -1.494234602 |
| H | -0.895225933 | 4.531519139 | -1.162884535 |
| C | -0.655609809 | 3.225459912 | -2.851732066 |
| H | -0.820920397 | 4.004218223 | -3.590090347 |
| C | -0.393356774 | 1.921445892 | -3.244012222 |
| H | -0.350110052 | 1.671542219 | -4.300944471 |
| C | -0.186422728 | 0.93000253 | -2.291721524 |
| H | 0.011236611 | -0.081921329 | -2.633070183 |
| C | -0.227103593 | 1.181703048 | -0.914592271 |
| H | -1.93584007 | -1.05631625 | -1.407737597 |
| C | -1.246871159 | -1.835891075 | -1.09607183 |
| C | -0.133183892 | -1.480927455 | -0.31991818 |
| C | 0.708884986 | -2.541905564 | 0.037717297 |
| H | 1.589646185 | -2.327386786 | 0.636010311 |
| C | 0.466848312 | -3.855688448 | -0.345433953 |
| H | 1.15370519 | -4.641797378 | -0.042736079 |
| C | -0.644371936 | -4.166966751 | -1.115935051 |
| H | -0.837159562 | -5.1907899 | -1.422308201 |
| C | -1.503768138 | -3.142829241 | -1.489693574 |
| H | -2.380457633 | -3.363563334 | -2.093066309 |
| C | -0.861918246 | 0.259991892 | 1.559927806 |
| C | -2.367153356 | 0.155203342 | 1.361057448 |
| C | -3.181559644 | 0.450548662 | 2.614545281 |
| C | -4.682311869 | 0.316523368 | 2.405733453 |
| H | -0.649031835 | 1.243529173 | 2.007824834 |
| H | -0.56940513 | -0.471528305 | 2.328796961 |
| H | -2.625386603 | -0.850285674 | 1.007125989 |
| H | -2.685134699 | 0.841948453 | 0.564583703 |
| H | -2.946870243 | 1.463432774 | 2.96516486 |
| H | -2.860701891 | -0.225944573 | 3.416925786 |
| H | -5.031964182 | 1.005294376 | 1.630201762 |
| H | -5.248289537 | 0.526722359 | 3.319042351 |
| H | -4.940030122 | -0.695913778 | 2.078979009 |

## Borate donor $Ar_2RB$ fragment

| | | | |
|---|---|---|---|
| B | -0.74185737 | 0.02561770 | -0.15856039 |
| H | -1.69510054 | 2.61638522 | -0.12325854 |
| C | -1.10121650 | 2.43102071 | -1.00957130 |
| C | -0.93021908 | 3.45448838 | -1.92313503 |
| H | -1.39225651 | 4.41819542 | -1.75187647 |
| C | -0.15362822 | 3.24783072 | -3.05214921 |
| H | -0.00489002 | 4.05064081 | -3.76296391 |
| C | 0.43696522 | 2.01349160 | -3.26472923 |
| H | 1.05278851 | 1.85130287 | -4.14007623 |
| C | 0.23473055 | 0.98585514 | -2.35999696 |
| H | 0.69862829 | 0.02531764 | -2.54226281 |
| C | -0.53748924 | 1.16549302 | -1.20725841 |
| H | -1.52964539 | -1.20364195 | -2.52270876 |
| C | -1.10842965 | -1.91948948 | -1.82847262 |
| C | -0.64461859 | -1.47752658 | -0.58475299 |
| C | -0.12150453 | -2.44583049 | 0.27847305 |
| H | 0.24526622 | -2.15004109 | 1.25315594 |
| C | -0.04017532 | -3.77785226 | -0.08618539 |
| H | 0.38658802 | -4.50106323 | 0.59687999 |
| C | -0.51613242 | -4.18690561 | -1.32099966 |
| H | -0.46497936 | -5.23014951 | -1.60516859 |
| C | -1.06049130 | -3.25502551 | -2.18882936 |
| H | -1.44208201 | -3.56926496 | -3.15185306 |
| C | -1.09850858 | 0.37397302 | 1.33624806 |
| C | -2.59267673 | 0.15833736 | 1.63206506 |
| C | -2.96822469 | 0.43956918 | 3.08038274 |
| C | -4.44932443 | 0.23860125 | 3.36162446 |
| H | -0.82949287 | 1.40141247 | 1.59214747 |
| H | -0.52957294 | -0.26936487 | 2.01542418 |
| H | -2.87043685 | -0.86997217 | 1.38310272 |
| H | -3.19642476 | 0.79722010 | 0.97891550 |
| H | -2.68279970 | 1.46473703 | 3.33416789 |
| H | -2.37720141 | -0.20972464 | 3.73282184 |
| H | -5.06056747 | 0.89742893 | 2.74139379 |
| H | -4.69076678 | 0.44808664 | 4.40443139 |
| H | -4.75542299 | -0.78797447 | 3.15053009 |

## Borate donor Ar fragment

| | | | |
|---|---|---|---|
| H | 2.37470700 | -0.03560779 | -1.37786960 |
| C | 2.68522200 | 0.17172528 | -0.36223035 |
| C | 1.79565374 | 0.27235792 | 0.67009038 |
| C | 2.10462401 | 0.53018835 | 1.97555585 |
| H | 1.35036064 | 0.59727428 | 2.74861894 |
| C | 3.45470794 | 0.70537318 | 2.27048557 |
| H | 3.75767217 | 0.91262288 | 3.28922190 |
| C | 4.40536907 | 0.61535346 | 1.26557085 |
| H | 5.45161461 | 0.75306309 | 1.50371050 |
| C | 4.02863182 | 0.35062877 | -0.04249790 |
| H | 4.77854097 | 0.28220926 | -0.82073399 |

## Borate donor $Ar_3B$ fragment

| | | | |
|---|---|---|---|
| B | 0.77493457 | -0.06715661 | -0.58002560 |
| H | 2.92141517 | 1.61735054 | -1.05401438 |
| C | 3.02350715 | 1.11136638 | -0.10253120 |
| C | 2.02915014 | 0.21623832 | 0.30744561 |
| C | 2.20620042 | -0.41206169 | 1.54520109 |
| H | 1.45786480 | -1.11055274 | 1.89729917 |
| C | 3.30846335 | -0.15011502 | 2.33943315 |
| H | 3.41150631 | -0.63753196 | 3.30041125 |
| C | 4.28401352 | 0.72947799 | 1.89984918 |
| H | 5.15335798 | 0.92716480 | 2.51404011 |
| C | 4.14354396 | 1.35539623 | 0.67215746 |
| H | 4.90528212 | 2.04037872 | 0.32249145 |
| H | 0.63773889 | 2.66039368 | -0.10893354 |
| C | 0.19895248 | 2.40526133 | -1.06500925 |
| C | -0.34180960 | 3.41060463 | -1.84686324 |
| H | -0.32817869 | 4.43491412 | -1.49701030 |
| C | -0.89171856 | 3.10662526 | -3.08130511 |

| | | | |
|---|---|---|---|
| H | -1.30356030 | 3.89288493 | -3.70098697 |
| C | -0.91173454 | 1.79295865 | -3.52023091 |
| H | -1.33562140 | 1.55025264 | -4.48615072 |
| C | -0.39840575 | 0.78900884 | -2.71820287 |
| H | -0.43310975 | -0.23460903 | -3.06885138 |
| C | 0.17838556 | 1.06735404 | -1.47422316 |
| H | -1.88957919 | -0.76778537 | -0.85529393 |
| C | -1.26546004 | -1.64365579 | -0.73241624 |
| C | 0.11577023 | -1.48394891 | -0.57610644 |
| C | 0.87947148 | -2.64594545 | -0.41976980 |
| H | 1.95154758 | -2.56238919 | -0.29559160 |
| C | 0.29892691 | -3.90191302 | -0.43581750 |
| H | 0.91605464 | -4.78490741 | -0.33001506 |
| C | -1.07314684 | -4.02791637 | -0.57834526 |
| H | -1.53105912 | -5.00884704 | -0.57970933 |
| C | -1.85692067 | -2.89446643 | -0.71858383 |
| H | -2.93009092 | -2.98698408 | -0.82537266 |

### Borate donor R fragment

| | | | |
|---|---|---|---|
| C | -0.91458078 | 0.29536599 | 1.73703316 |
| C | -2.36551754 | 0.16615303 | 1.46257378 |
| C | -3.25169612 | 0.45171380 | 2.68700201 |
| C | -4.73371760 | 0.31479980 | 2.37534087 |
| H | -0.42952901 | 1.26162812 | 1.71283523 |
| H | -0.33674072 | -0.54554254 | 2.09463808 |
| H | -2.59237229 | -0.84225967 | 1.10469424 |
| H | -2.65824830 | 0.85541778 | 0.66422736 |
| H | -3.03852785 | 1.45903531 | 3.05261017 |
| H | -2.97509833 | -0.23194711 | 3.49318594 |
| H | -5.03662693 | 1.01116647 | 1.59092534 |
| H | -5.34604739 | 0.51738417 | 3.25470806 |
| H | -4.97105450 | -0.69339309 | 2.03013499 |

### Borate donor $Ar_2RB^{-1}$ fragment

| | | | |
|---|---|---|---|
| B | -0.74572265 | -0.01091703 | -0.25840328 |
| H | -1.69124312 | 2.59140886 | -0.10850613 |
| C | -1.12005325 | 2.43901177 | -1.01683342 |
| C | -0.97320310 | 3.50736803 | -1.87890918 |
| H | -1.42525592 | 4.46179884 | -1.62861871 |
| C | -0.25440535 | 3.37252256 | -3.06161939 |
| H | -0.13463219 | 4.20825499 | -3.74021938 |
| C | 0.31537330 | 2.13436987 | -3.34270666 |
| H | 0.90151001 | 2.00549019 | -4.24711800 |
| C | 0.15807685 | 1.06799325 | -2.48043582 |
| H | 0.65141861 | 0.13668459 | -2.72505609 |
| C | -0.57797177 | 1.15472224 | -1.27289733 |
| H | -0.88080370 | -1.30282913 | -2.77571322 |
| C | -0.72276187 | -2.00385078 | -1.96740533 |
| C | -0.63539817 | -1.50903826 | -0.63986906 |
| C | -0.50879734 | -2.52431966 | 0.34411430 |
| H | -0.45097926 | -2.23664887 | 1.38686943 |
| C | -0.43787033 | -3.86871542 | 0.03938235 |
| H | -0.33037021 | -4.59198171 | 0.84162673 |
| C | -0.50462449 | -4.30600494 | -1.27930170 |
| H | -0.45087877 | -5.36019607 | -1.52210036 |
| C | -0.65717271 | -3.34620505 | -2.27692940 |
| H | -0.73775923 | -3.65704716 | -3.31376911 |
| C | -1.09764389 | 0.36161412 | 1.27083630 |
| C | -2.56610333 | 0.16166398 | 1.65836198 |
| C | -2.88346121 | 0.46423414 | 3.11874888 |
| C | -4.35002073 | 0.26535092 | 3.47493169 |
| H | -0.82265153 | 1.39965169 | 1.48948648 |
| H | -0.48806524 | -0.24046547 | 1.95703547 |
| H | -2.86038386 | -0.86969197 | 1.43722812 |
| H | -3.19764111 | 0.79061762 | 1.02034927 |
| H | -2.58880631 | 1.49442564 | 3.34500121 |
| H | -2.26197159 | -0.17305142 | 3.75658414 |
| H | -4.98930565 | 0.91454212 | 2.87193507 |
| H | -4.55013695 | 0.48474776 | 4.52659174 |
| H | -4.66145335 | -0.76433187 | 3.28428364 |

### Borate donor $Ar_3B^{-1}$ fragment

| | | | |
|---|---|---|---|
| B | 0.77286918 | -0.06609833 | -0.57580267 |
| H | 2.87480455 | 1.74276617 | -0.94964543 |
| C | 2.99977454 | 1.18562139 | -0.02925398 |
| C | 2.03065250 | 0.21767881 | 0.31211154 |
| C | 2.28650843 | -0.47172829 | 1.51698060 |
| H | 1.57542729 | -1.21807467 | 1.84945484 |
| C | 3.39523348 | -0.22117196 | 2.30328484 |
| H | 3.53364356 | -0.77677091 | 3.22496895 |
| C | 4.32670438 | 0.73940081 | 1.92970409 |
| H | 5.19743599 | 0.93692215 | 2.54331227 |
| C | 4.11289178 | 1.44008233 | 0.74927230 |
| H | 4.82901930 | 2.18995776 | 0.42970173 |
| H | 0.76255240 | 2.70972790 | -0.21040084 |
| C | 0.27037677 | 2.43739552 | -1.13584927 |
| C | -0.25427861 | 3.44321751 | -1.92559578 |
| H | -0.15782932 | 4.47651672 | -1.60916666 |
| C | -0.90955355 | 3.14300303 | -3.11312410 |
| H | -1.31958467 | 3.92912832 | -3.73549073 |
| C | -1.02427276 | 1.80870387 | -3.48231679 |
| H | -1.52409746 | 1.54608881 | -4.40874160 |
| C | -0.49964275 | 0.80913267 | -2.68463915 |
| H | -0.59661568 | -0.21870291 | -3.01201436 |
| C | 0.17496514 | 1.07060514 | -1.47330570 |
| H | -1.88486622 | -0.81984375 | -1.01152130 |
| C | -1.26130368 | -1.68589121 | -0.82642487 |
| C | 0.11272390 | -1.48652264 | -0.57372913 |
| C | 0.84303872 | -2.66814902 | -0.32473912 |
| H | 1.90724281 | -2.59069724 | -0.13978605 |
| C | 0.26323106 | -3.92295014 | -0.32925218 |
| H | 0.87819005 | -4.79684339 | -0.14120871 |
| C | -1.09425047 | -4.07549808 | -0.58160624 |
| H | -1.55166490 | -5.05750309 | -0.58536728 |
| C | -1.84985341 | -2.93647485 | -0.83007154 |
| H | -2.91378048 | -3.02618346 | -1.02276945 |

### Diphenyl iodonium acceptor

| | | | |
|---|---|---|---|
| H | -4.08026116 | -2.42709696 | -1.30423506 |
| C | -4.38903304 | -1.59293444 | -1.92226579 |
| C | -5.74646784 | -1.23623742 | -1.93556131 |
| C | -6.17314265 | -0.16206800 | -2.72572342 |
| H | -7.21390733 | 0.12955106 | -2.75004296 |
| C | -5.26035221 | 0.53445003 | -3.49678263 |
| H | -5.59791123 | 1.35749948 | -4.11451932 |
| C | -3.92752913 | 0.15614183 | -3.46459372 |
| C | -3.47519837 | -0.90606286 | -2.68520463 |
| H | -2.43299298 | -1.20015190 | -2.67637378 |
| C | -1.86791077 | 2.72479906 | -3.49778430 |
| C | -0.72517310 | 2.50688904 | -2.74649686 |

| | | | |
|---|---|---|---|
| H | -0.20945697 | 1.55520865 | -2.75760588 |
| C | -0.25238765 | 3.55596103 | -1.97171275 |
| H | 0.64163879 | 3.41582684 | -1.37587084 |
| C | -0.91713417 | 4.77389815 | -1.96450455 |
| H | -0.54028819 | 5.58791741 | -1.35664540 |
| C | -2.05765175 | 4.96169910 | -2.73287257 |
| H | -2.57067657 | 5.91596825 | -2.72792581 |
| C | -2.54968690 | 3.92994750 | -3.51921024 |
| H | -3.43440929 | 4.07360653 | -4.12637788 |
| I | -2.57774559 | 1.14583457 | -4.69390724 |
| O | -6.54187082 | -1.97546333 | -1.17816523 |
| C | -7.95006447 | -1.71693837 | -1.14858532 |
| C | -8.59421226 | -2.76551275 | -0.27821633 |
| C | -10.09470681 | -2.55782909 | -0.13605023 |
| C | -10.74868104 | -3.65217646 | 0.69373742 |
| C | -12.24392879 | -3.46477220 | 0.89130624 |
| H | -8.34470575 | -1.75944561 | -2.17031434 |
| H | -8.12024562 | -0.70996468 | -0.74967039 |
| H | -8.11824343 | -2.74864982 | 0.70744145 |
| H | -8.39301093 | -3.75143955 | -0.70926625 |
| H | -10.56180499 | -2.52563912 | -1.12834058 |
| H | -10.29084085 | -1.58272758 | 0.32639733 |
| H | -10.25659120 | -3.70212065 | 1.67276304 |
| H | -10.56494119 | -4.62189805 | 0.21514351 |
| H | -12.43026303 | -2.50638303 | 1.39186590 |
| H | -12.73697478 | -3.39577877 | -0.08649711 |
| C | -12.87950504 | -4.58677045 | 1.69689526 |
| C | -14.37476344 | -4.41388892 | 1.91060909 |
| C | -14.99053149 | -5.53831506 | 2.72510410 |
| H | -12.38044199 | -4.66179057 | 2.67147753 |
| H | -12.69522114 | -5.54301842 | 1.19115495 |
| H | -14.87289027 | -4.34809900 | 0.93618153 |
| H | -14.55980096 | -3.45530714 | 2.40897813 |
| H | -14.84099928 | -6.50600320 | 2.23831854 |
| H | -16.06530623 | -5.39669999 | 2.85597362 |
| H | -14.53996609 | -5.59680518 | 3.71987510 |

## Diphenyl iodonium acceptor ArO fragment

| | | | |
|---|---|---|---|
| H | 4.25892466 | -2.26570170 | 0.08048574 |
| C | 4.56332593 | -1.22764839 | 0.05705625 |
| C | 3.57433945 | -0.24642470 | 0.00544025 |
| C | 3.92079767 | 1.09864369 | -0.02364191 |
| H | 3.16473780 | 1.86854144 | -0.06316546 |
| C | 5.26774993 | 1.46525748 | -0.00289285 |
| H | 5.54677489 | 2.51073728 | -0.02670977 |
| C | 6.19234604 | 0.46670185 | 0.04702104 |
| C | 5.90136561 | -0.87207804 | 0.07889044 |
| H | 6.67168975 | -1.63106617 | 0.11978644 |
| O | 2.29734370 | -0.70485809 | -0.01458548 |
| C | 1.23086545 | 0.22517847 | -0.02845407 |
| C | -0.06495126 | -0.55075671 | -0.05525833 |
| C | -1.28875335 | 0.35117327 | 0.00221316 |
| C | -2.59777436 | -0.42177764 | -0.07077216 |
| C | -3.83230386 | 0.46034028 | 0.03931939 |
| H | 1.31052787 | 0.87207534 | -0.90925198 |
| H | 1.28266739 | 0.86211037 | 0.86204497 |
| H | -0.07206760 | -1.24476431 | 0.78878143 |
| H | -0.08928316 | -1.16047714 | -0.96176634 |
| H | -1.25322151 | 1.07609030 | -0.81782679 |
| H | -1.26715881 | 0.93690227 | 0.92686189 |
| H | -2.61754696 | -1.17244249 | 0.72612314 |
| H | -2.63396264 | -0.97999066 | -1.01169176 |
| H | -3.80206647 | 1.00735564 | 0.98734908 |
| H | -3.80784087 | 1.22047370 | -0.74879838 |
| C | -5.13826174 | -0.31509344 | -0.05140610 |
| C | -6.37669856 | 0.55992390 | 0.07561734 |
| C | -7.67473064 | -0.22729515 | -0.01802969 |
| H | -5.15782296 | -1.08329799 | 0.72910798 |
| H | -5.17405831 | -0.85341723 | -1.00435585 |
| H | -6.35661106 | 1.32764763 | -0.70383259 |
| H | -6.34210101 | 1.09597196 | 1.02862703 |
| H | -7.74872264 | -0.75139421 | -0.97293745 |
| H | -8.54546369 | 0.42318381 | 0.07147917 |
| H | -7.73737852 | -0.97655666 | 0.77360689 |

## Diphenyl iodonium acceptor ArOI fragment

| | | | |
|---|---|---|---|
| H | -1.51029916 | -2.65887663 | 0.04388551 |
| C | -1.85266525 | -1.63585629 | -0.03240821 |
| C | -0.90634907 | -0.61474740 | -0.04167935 |
| C | -1.32723829 | 0.70388464 | -0.14055461 |
| H | -0.61817570 | 1.51720715 | -0.14994805 |
| C | -2.68228734 | 0.99231897 | -0.23002477 |
| H | -2.99912495 | 2.02248962 | -0.30727015 |
| C | -3.61408510 | -0.02458714 | -0.22137999 |
| C | -3.19657435 | -1.34461525 | -0.12151960 |
| H | -3.91950816 | -2.14784883 | -0.11430825 |
| O | 0.38644980 | -1.00083218 | 0.04771687 |
| C | 1.40314296 | -0.01367365 | 0.01443449 |
| C | 2.73993053 | -0.71058993 | 0.10571569 |
| C | 3.90631036 | 0.26302719 | 0.02127911 |
| C | 5.26224982 | -0.42175431 | 0.11482632 |
| C | 6.43535212 | 0.53957107 | -0.00408955 |
| H | 1.27247302 | 0.68188045 | 0.85038581 |
| H | 1.33047972 | 0.55924171 | -0.91643749 |
| H | 2.80518324 | -1.44487296 | -0.70086782 |
| H | 2.78349253 | -1.26968834 | 1.04339393 |
| H | 3.82363046 | 1.00756331 | 0.81981742 |
| H | 3.84924900 | 0.81906035 | -0.92004141 |
| H | 5.33558490 | -1.18102676 | -0.67050065 |
| H | 5.33005197 | -0.96177099 | 1.06451742 |
| H | 6.36389596 | 1.07987230 | -0.95377056 |
| H | 6.36405392 | 1.29917475 | 0.78153924 |
| C | 7.79119552 | -0.14552228 | 0.08203475 |
| C | 8.96636599 | 0.81155028 | -0.05304409 |
| C | 10.31589076 | 0.11416600 | 0.02428516 |
| H | 7.85851255 | -0.91118085 | -0.69821645 |
| H | 7.86851506 | -0.67917489 | 1.03511391 |
| H | 8.90344034 | 1.57324156 | 0.72999201 |
| H | 8.88508735 | 1.34772073 | -1.00316092 |
| H | 10.43340392 | -0.41011672 | 0.97475366 |
| H | 11.13901184 | 0.82364126 | -0.06698072 |
| H | 10.42318529 | -0.62341693 | -0.77337254 |
| I | -5.65316057 | 0.42029852 | -0.36519866 |

## Diphenyl iodonium acceptor ArI fragment

| | | | |
|---|---|---|---|
| I | -1.54744803 | -0.00764247 | -0.00568268 |
| C | 0.54543909 | -0.00301250 | -0.00223030 |
| C | 1.22640793 | 1.20272781 | -0.00072089 |

| | | | |
|---|---|---|---|
| H | 0.68439369 | 2.13801946 | -0.00205211 |
| C | 2.61163954 | 1.19994812 | 0.00268682 |
| H | 3.14490881 | 2.14147742 | 0.00397726 |
| C | 3.30950947 | 0.00426628 | 0.00454599 |
| H | 4.39124200 | 0.00716304 | 0.00741264 |
| C | 2.61790981 | -1.19504377 | 0.00281141 |
| H | 3.15622510 | -2.13369452 | 0.00422846 |
| C | 1.23262785 | -1.20517299 | -0.00057605 |
| H | 0.69566776 | -2.14338968 | -0.00182864 |

**Diphenyl iodonium acceptor**
**Ar fragment**

| | | | |
|---|---|---|---|
| C | 0.00418794 | -1.38266127 | 0.00279541 |
| C | -1.21506211 | -0.76648879 | 0.00214859 |
| H | -2.14470584 | -1.32053036 | 0.00257747 |
| C | -1.20649691 | 0.62584949 | 0.00145270 |
| H | -2.14429537 | 1.16714145 | 0.00121353 |
| C | -0.00391997 | 1.31598157 | 0.00098877 |
| H | -0.00713521 | 2.39771805 | 0.00011625 |
| C | 1.20278025 | 0.63302773 | 0.00142562 |
| H | 2.13727591 | 1.18000742 | 0.00107682 |
| C | 1.21973552 | -0.75922858 | 0.00250609 |
| H | 2.15272718 | -1.30760018 | 0.00304190 |

**Diphenyl iodonium acceptor**
**$ArOI^{+1}$ fragment**

| | | | |
|---|---|---|---|
| H | -1.38022165 | -2.70970061 | -0.19120946 |
| C | -1.79282878 | -1.71689160 | -0.07636631 |
| C | -0.88596913 | -0.61892172 | -0.02789321 |
| C | -1.37948122 | 0.70517671 | 0.11212242 |
| H | -0.69959603 | 1.54276044 | 0.13637234 |
| C | -2.72001231 | 0.90753179 | 0.21680461 |
| H | -3.10668515 | 1.91062884 | 0.32746133 |
| C | -3.61790283 | -0.18613771 | 0.18481680 |
| C | -3.12762229 | -1.50222560 | 0.02837953 |
| H | -3.81811711 | -2.33250468 | -0.00299183 |
| O | 0.36786473 | -0.92683817 | -0.11592440 |
| C | 1.43226293 | 0.07149598 | -0.06498986 |
| C | 2.74946029 | -0.65683164 | -0.07318012 |
| C | 3.92110840 | 0.31847678 | -0.04816930 |
| C | 5.26794345 | -0.39041246 | -0.00545294 |
| C | 6.45062982 | 0.56636259 | -0.03989539 |
| H | 1.29862907 | 0.65591972 | 0.84608516 |
| H | 1.31557180 | 0.71760692 | -0.93642513 |
| H | 2.80490978 | -1.28557487 | -0.96395442 |
| H | 2.79434893 | -1.32016142 | 0.79314806 |
| H | 3.83388315 | 0.97841161 | 0.82054124 |
| H | 3.87933237 | 0.96321302 | -0.93147861 |
| H | 5.33831535 | -1.08274287 | -0.84996150 |
| H | 5.32312916 | -1.00487773 | 0.89828330 |
| H | 6.40539486 | 1.16289760 | -0.95668827 |
| H | 6.36943121 | 1.27636054 | 0.78946807 |
| C | 7.79586388 | -0.14112443 | 0.03378904 |
| C | 8.98441576 | 0.80574391 | -0.04693006 |
| C | 10.32213966 | 0.08729043 | 0.03751348 |
| H | 7.86403937 | -0.87415343 | -0.77683577 |
| H | 7.85377175 | -0.71387878 | 0.96504157 |
| H | 8.91407762 | 1.54374382 | 0.75763947 |
| H | 8.93042744 | 1.37056164 | -0.98211726 |
| H | 10.41699447 | -0.45923169 | 0.97766348 |
| H | 11.15497891 | 0.78772134 | -0.02351730 |
| H | 10.43410268 | -0.63268520 | -0.77520621 |
| I | -5.61023867 | 0.13784806 | 0.38103874 |

**Diphenyl iodonium acceptor**
**$ArI^{+1}$ fragment**

| | | | |
|---|---|---|---|
| I | -1.46664807 | -0.00059082 | -0.00075150 |
| C | 0.54605030 | -0.00023476 | -0.00038710 |
| C | 1.24139840 | 1.23359349 | -0.00022475 |
| H | 0.69216750 | 2.16472572 | -0.00038585 |
| C | 2.60745254 | 1.22237129 | 0.00014934 |
| H | 3.15974244 | 2.15170791 | 0.00029621 |
| C | 3.29475712 | 0.00033356 | 0.00034914 |
| H | 4.37714466 | 0.00055282 | 0.00066190 |
| C | 2.60794522 | -1.22198696 | 0.00014893 |
| H | 3.16062258 | -2.15109322 | 0.00029559 |
| C | 1.24189401 | -1.23377422 | -0.00022527 |
| H | 0.69305485 | -2.16513904 | -0.00038704 |

### *Transient Absorption Data*

### TA spectra of Mes-BODIPY Derivatives

TA spectra of **Mes-H**, **Mes-Cl**, **Mes-Br**, and **Mes-I** are plotted in **Figure S31**. Spectra of **Mes-I** are reproduced from **Figure 4a** of the main text. Examining spectra of **Mes-H**, upon photoexcitation a photobleach of **Mes-H**'s ground state absorption appears at ~490 nm that adds to a negative band at 540 nm attributed to stimulated emission, signaling promotion of a population of **Mes-H** molecules to their lowest excited spin-singlet state ($S_1$). The decay rate of the ground state bleach and stimulated emission are identical, indicating excited **Mes-H** molecules return directly from the $S_1$ state to the ground state ($S_0$). Unfortunately, due to poor spectral overlap of **Mes-H**'s absorption spectrum with the Nd:YAG laser used to record nanosecond decay kinetics, we were unable to accurately measure the lifetime of **Mes-H**. However, based on our femtosecond TA data, we estimate this value to fall in the range of a few nanoseconds, consistent of reports of structurally-related BODIPY dyes.[15,16]

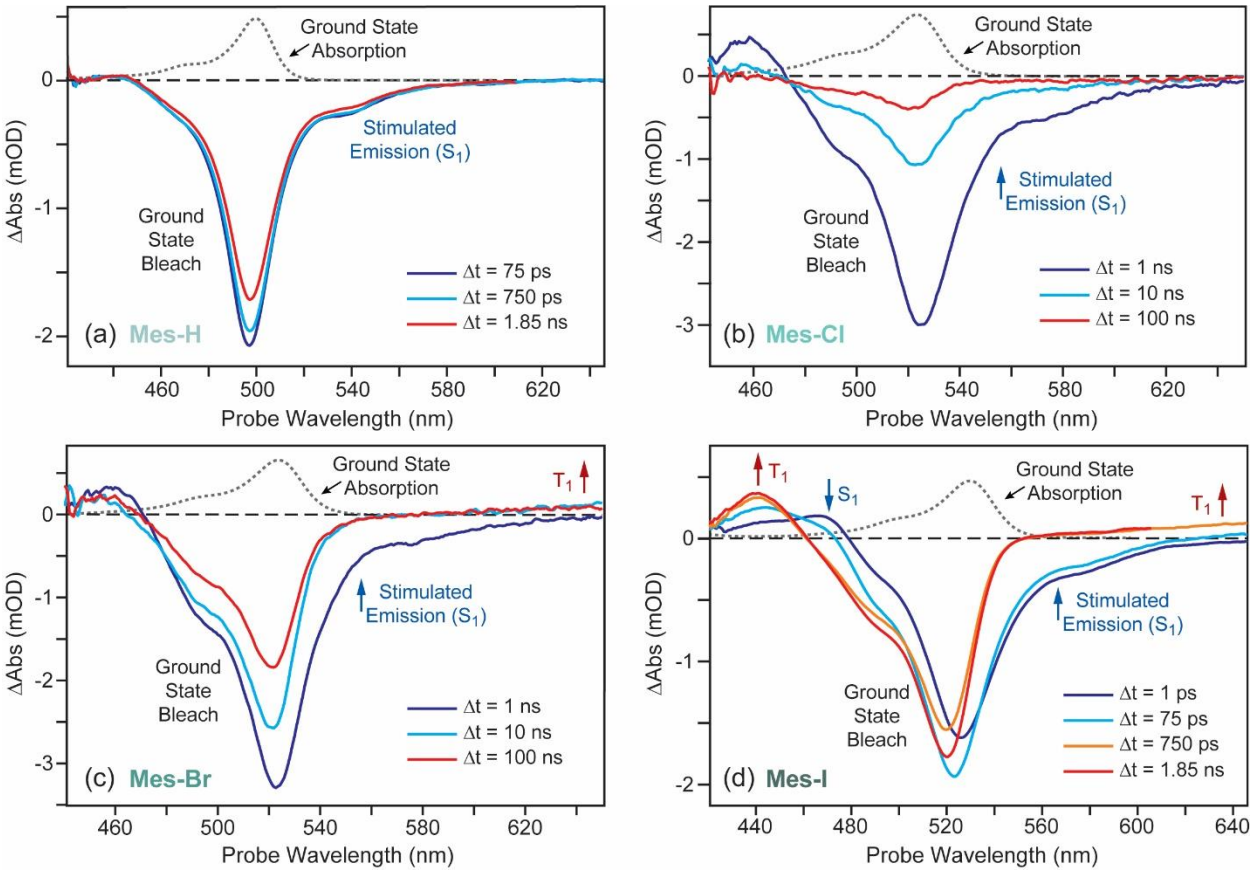


**Figure S31:** TA spectra of **Mes-H** (a), **Mes-Cl** (b), **Mes-Br** (c), and **Mes-I** (d) in acetonitrile. Excitation pulses centered at 525 nm derived from the output of a NOPA were used to collect spectra of **Mes-H** and **Mes-I** while spectra of **Mes-Cl** and **Mes-Br** were taken following excitation at 532 nm using the output of a frequency-doubled Nd:YAG laser. The polarization of the pump and probe pulses were set perpendicular to one another.

In contrast, **Mes-I** exhibits relaxation kinetics distinct from that of **Mes-H**. Rather than decaying to the ground state, **Mes-I** evolves from the $S_1$ state to its lowest excited spin-triplet state ($T_1$), as signaled by a loss of stimulated emission and growth of induced absorption bands at 440 nm and 700 nm associated with the BODIPY $T_1$ state.[15–18] We attribute formation of **Mes-I**'s $T_1$ state to

intersystem crossing enhanced by its pendant iodine atoms. Spectral evolution consistent with $T_1$ state formation is apparent for **Mes-Br** albeit on a slower timescale. For **Mes-Cl**, intersystem crossing is even slower and competes with direct relaxation of $S_1$ to the ground state ($S_0$), as signaled by loss of ground state bleach amplitude as $T_1$ excited state absorption bands appear.

**Global Target Analysis**

To quantify rate constants for intersystem crossing and yields for triplet formation, a global target analysis method outlined in prior work[19,20] was applied to TA spectra of Mes-BODIPY derivatives. Briefly, TA data sets, $\Delta Abs(t, \lambda_{probe})$, were decomposed into a linear combination of species-associated decay spectra (SADS), $\{\sigma_n(\lambda_{probe})\}$, with time-dependent weights, $\{c_n(t)\}$, whose values are the solutions to a set of sequential first-order rate equations:

$$\Delta Abs(t, \lambda_{probe}) = \sum_n c_n(t)\sigma_n(\lambda_{probe}) \qquad \textit{(SE10)}$$

$$\frac{dc_1(t)}{dt} = I_0 - k_1 c_1(t) \qquad \textit{(SE11)}$$

$$\frac{dc_n(t)}{dt} = k_{n-1}c_{n-1}(t) - k_n c_n(t), \;\; n > 1 \qquad \textit{(SE12)}$$

Here, the set of SADS, $\{\sigma_n(\lambda_{probe})\}$, represent spectroscopically distinct configurations of the system that include singlet and triplet excited states of the BODIPY molecules we examine. $I_0$ describes the photoexcited population prepared by the excitation pulse while the set of rate constants, $\{k_n(t)\}$, describe the exchange of this population between the configurations associated with each $\sigma_n(\lambda_{probe})$.

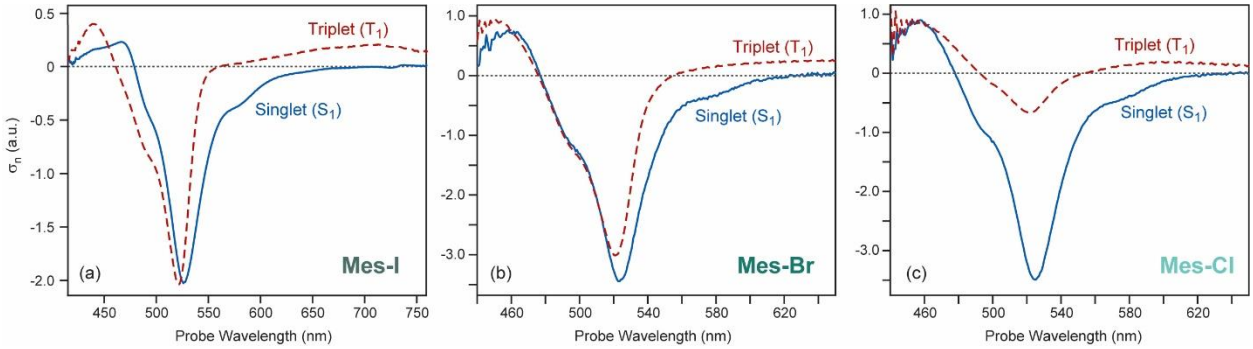


**Figure S32:** Species associated decay spectra, $\sigma_n(\lambda_{probe})$, assigned to the lowest excited singlet ($S_1$) and triplet ($T_1$) states of **Mes-I** (a), **Mes-Br** (b), and **Mes-Cl** (c) extracted from global target analysis of TA spectra.

Figure **S32** displays SADS we assign to the $S_1$ and $T_1$ states of **Mes-I**, **Mes-Br**, and **Mes-Cl**. Comparing these spectra, we note that they contain similar distinguishing characteristics. Specifically, stimulated emission to the red of the ground state bleach of each molecule signifies the $S_1$ state while this feature is replaced by an induced absorption band following intersystem crossing to form the Mes-BODIPY $T_1$ state. $T_1$ state formation is also signaled by changes in the amplitude of higher-energy induced absorption bands, which can most clearly be identified for **Mes-I** via a loss of induced absorption amplitude at 475 nm and gain at 440 nm.

By fitting the loss and gain of these features, we extract time constants for **Mes-I**, **Mes-Br**, and **Mes-Cl** for the growth of their respective $T_1$ states. Importantly, these time constants ($\tau$) represent the sum of all rates that lead to the decay of excited population from the $S_1$ state to the ground state ($k_{S1}$) and formation of the $T_1$ state via intersystem crossing ($k_{ISC}$):

$$\frac{1}{\tau} = k_{S1} + k_{ISC} \qquad \textit{(SE13)}$$

For **Mes-Br** and **Mes-Cl** in particular, we can see these two processes are likely competitive as significant ground state bleach relaxation occurs as features associated with their $T_1$ states appear. While it is possible the loss of ground state bleach amplitude could result from overlapping absorption between the $T_1$ state and ground state absorption spectrum of **Mes-Br** and **Mes-Cl**, the lack of ground state bleach decay in **Mes-I** as intersystem crossing occurs coupled with prior work showing a lack of overlap between ground state and $T_1$ absorption bands[15,16] instead supports the hypothesis that intersystem crossing in **Mes-Br** and **Mes-Cl** experiences significant competition with the return of photoexcited $S_1$ state population to the ground state.

Assuming the value of $k_{S1}$ is similar for all three halogenated Mes-BODIPY derivatives and all loss of ground state bleach amplitude results from $S_1$ to $S_0$ decay , we extract intersystem crossing rates of $5.1 \times 10^9$ $s^{-1}$, $0.34 \times 10^9$ $s^{-1}$ and $0.13 \times 10^9$ $s^{-1}$ for **Mes-I**, **Mes-Br**, and **Mes-Cl** as well as triplet yields of 89%, 35%, and 17% (see **Table 1**, main text). We note this assumption likely overestimates the $S_1$ state rate of decay (and hence underestimates the $T_1$ yield) as it neglects any overlapping contributions to the ground state bleach from stimulated emission from the $S_1$ state. Nevertheless, even within the limitations of this assumption, we observe a clear increase in the rate of $T_1$ state production upon Mes-BODIPY halogenation. This increased production correlates well with photopolymerization rate gains we report in the main text, indicating that extending the photoexcited lifetime of Mes-BODIPY dyes via intersystem crossing forms an effective strategy for achieving rapid photopolymerization needed for 3D printing.

### Transient Absorption Spectra of aza-BODIPY Derivatives

**Figure S33** highlights TA spectra of **aza-H** and **aza-Br** recorded following 645 nm photoexcitation. Following a small growth of induced absorption amplitude at 725 nm over a 730 fs time scale, which we attribute to relaxation dynamics of **aza-H** molecules along the $S_1$ potential energy surface, we find TA spectra of **aza-H** decay uniformly with a time constant of 165 ps. Similar to **Mes-H**, the lack of spectral evolution of **aza-H** suggests that the majority of its excited population decays directly from its $S_1$ state to the ground state. It is notable that the lifetime of **aza-H** is at least an order of magnitude shorter than that of **Mes-H**. This short lifetime likely underlies **aza-H**'s poor performance as a photocatalyst relative to **Mes-H** and all other halogenated BODIPY's investigated here.

Upon first investigation, TA spectra of **aza-Br** appear similar to spectra of **aza-H** as we observe a rapid, sub-nanosecond decay of the **aza-Br** ground state bleach, suggesting return of photoexcited population to the ground state. However, following this rapid decay, we find the ground state bleach amplitude stabilizes and maintains its value over nanosecond time delays (**Figure S33c**). Concomitant with this stabilization, changes in induced absorption bands become apparent. Notably a band centered at <440 nm decreases in amplitude, revealing a new band peaked at 475 nm and the induced absorption band centered near 725 nm reduces its amplitude relative to the **aza-Br** ground state bleach, driving the signal null caused by interference between these features to shift to longer wavelength (**Figure S33d**). Taken together, this spectral evolution suggests a portion of the excited **aza-Br** population forms a long-lived excited state. As bromination is expected to enhance intersystem crossing, we assign this long-lived state to the **aza-Br** $T_1$ state. This assignment is supported by prior work on aza-substituted BODIPY dyes, which has noted their $T_1$ states to show induced absorption features near 475 nm,[21] similar to our observations here.

While we are confident in assigning this long-lived state to the **aza-Br** $T_1$ state, less clear is the yield for its formation. $T_1$ induced absorption features emerge simultaneous with a ~90% loss in the amplitude of the **aza-Br** ground state bleach. One possible interpretation of this result is that the ground state bleach happens to spectrally overlap with the $T_1$ absorption spectrum, causing

$T_1$ growth to partially cancel the amplitude of the ground state bleach. An alternative interpretation is that intersystem crossing competes with the direct relaxation of population in the $S_1$ state to the ground state ($S_0$). In this latter case, the 90% loss of ground state bleach amplitude would represent the relative rates for intersystem crossing ($k_{ISC}$) and $S_1$ to $S_0$ decay ($k_{S1}$).

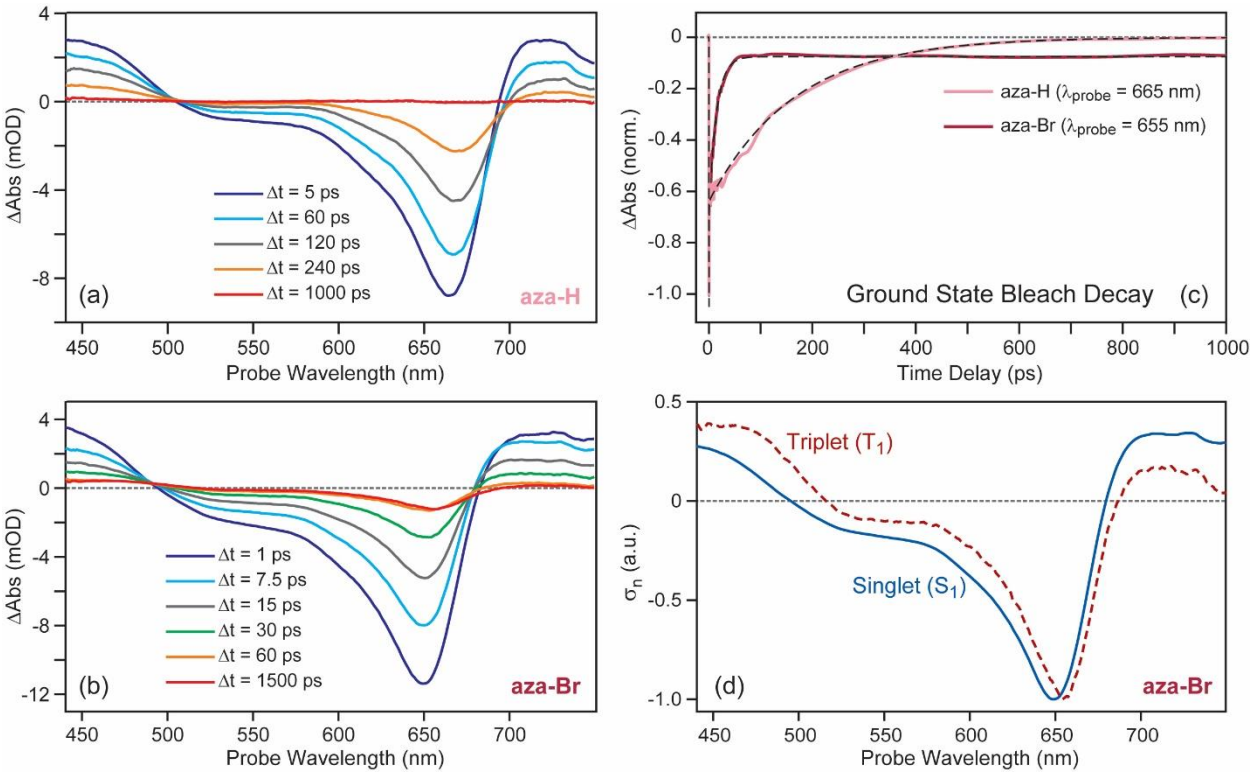


**Figure S33:** TA spectra of **aza-H** (a) and **aza-Br** (b) in acetonitrile recorded following photoexcitation at 645 nm. The relative polarization of the pump and probe pulses was set at the magic angle (54.7º) to suppress signal contributions from molecular reorientation. (c) Ground state bleach relaxation kinetics recorded at a probe wavelength of 665 nm for **aza-H** and 655 nm for **aza-Br**. A persistent non-zero amplitude is seen for **aza-Br**, signaling $T_1$ state formation. (d) SADS, $\sigma_n(\lambda_{probe})$, assigned to the lowest excited singlet ($S_1$) and triplet ($T_1$) states of **aza-Br** using global target analysis.

Examining our TA spectra for **Mes-I** (**Figure S31d**), we find it undergoes rapid intersystem crossing with minimal corresponding changes in the amplitude of its ground state bleach. This suggests induced absorption features of the **Mes-I** $T_1$ state exhibit minimal spectral overlap with the **Mes-I** ground state. Work on related halogenated BODIPY derivatives[21] suggests this conclusion should likewise hold true for **aza-Br**. Thus, we assign the dynamics of **aza-Br** to competition between $S_1$ relaxation and ISC. Assuming the ground state bleach decay arises solely from $S_1$ to $S_0$ relaxation allows us to decompose our measured time scale for the appearance of the $T_1$ state ($\tau$ = 14.4 ps) into corresponding time scales for $S_1$ to $S_0$ relaxation ($1/k_{S1}$ = 15.8 ps) and intersystem crossing ($1/k_{ISC}$ = 164 ps), from which we can further estimate a $T_1$ formation yield of 8.8%.

Interestingly, we find deactivation of the $S_1$ state in **aza-Br** is highly accelerated relative to other BODIPY compounds, which typically exhibit single excited state lifetimes in the nanosecond regime.[15,16] The origin of this phenomenon is beyond the scope of the present study and left to future work. Nonetheless, even with this shortened $S_1$ lifetime, halogenation accelerates intersystem crossing to a great enough extent that sufficient **aza-Br** transitions to its $T_1$ state from which redox processes can be initiated, making **aza-Br** into an effective NIR photocatalyst.

## CHARACTERIZATION

### *$^1$H NMR Spectra*

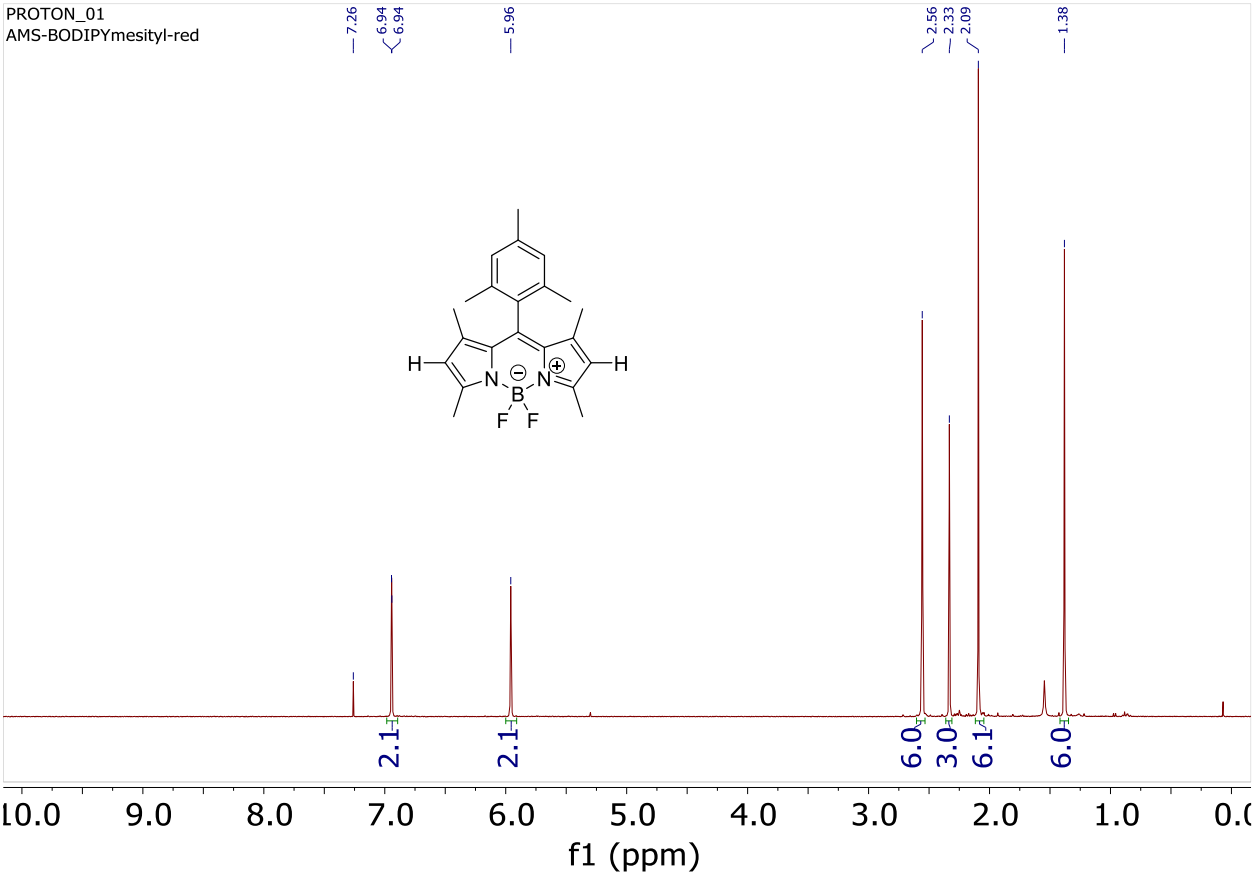


**Figure S34.** $^1$H NMR of **Mes-H** (**S1**) BODIPY in $CDCl_3$

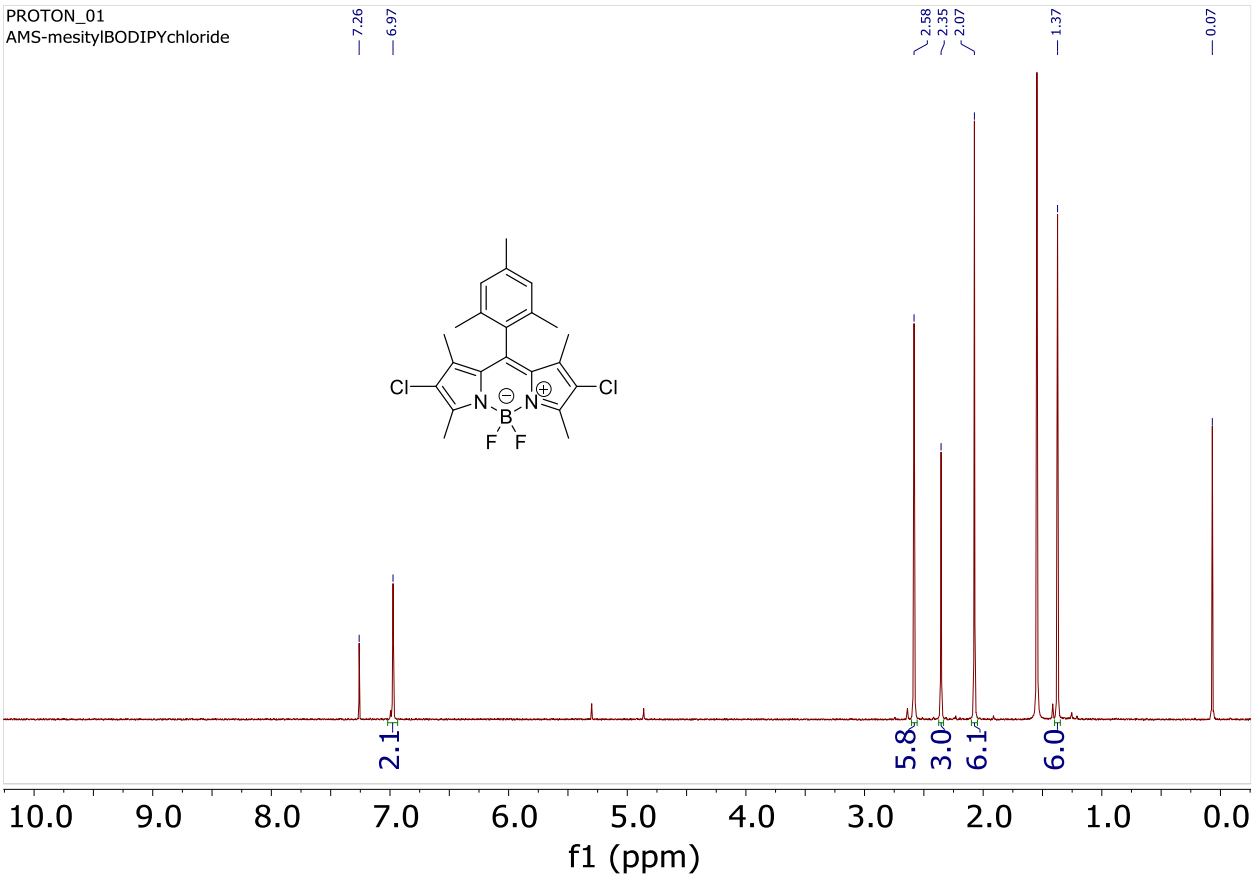


**Figure S35.** $^{1}H$ NMR of **Mes-Cl** (**S2**) BODIPY in $CDCl_3$

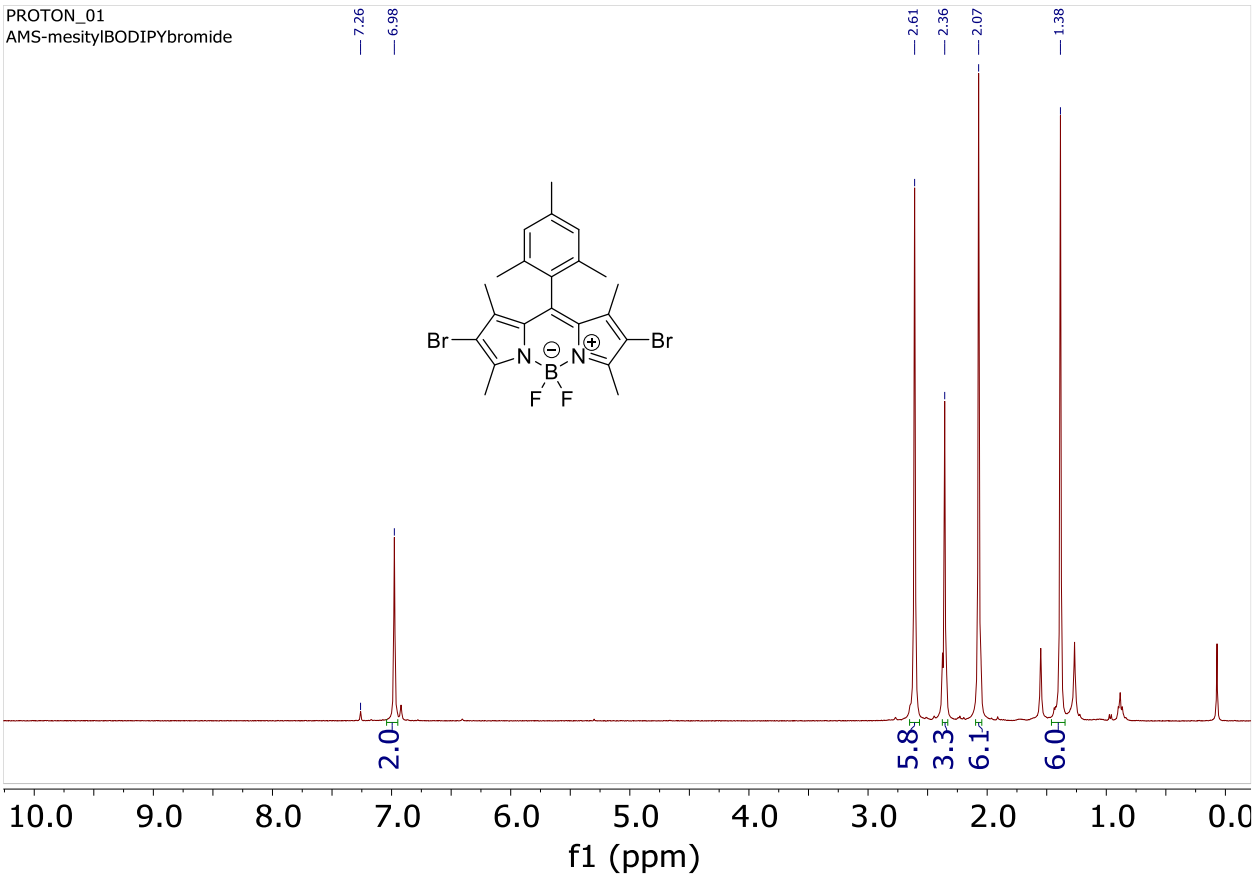


**Figure S36.** $^{1}$H NMR of **Mes-Br** (**S3**) BODIPY in $CDCl_3$

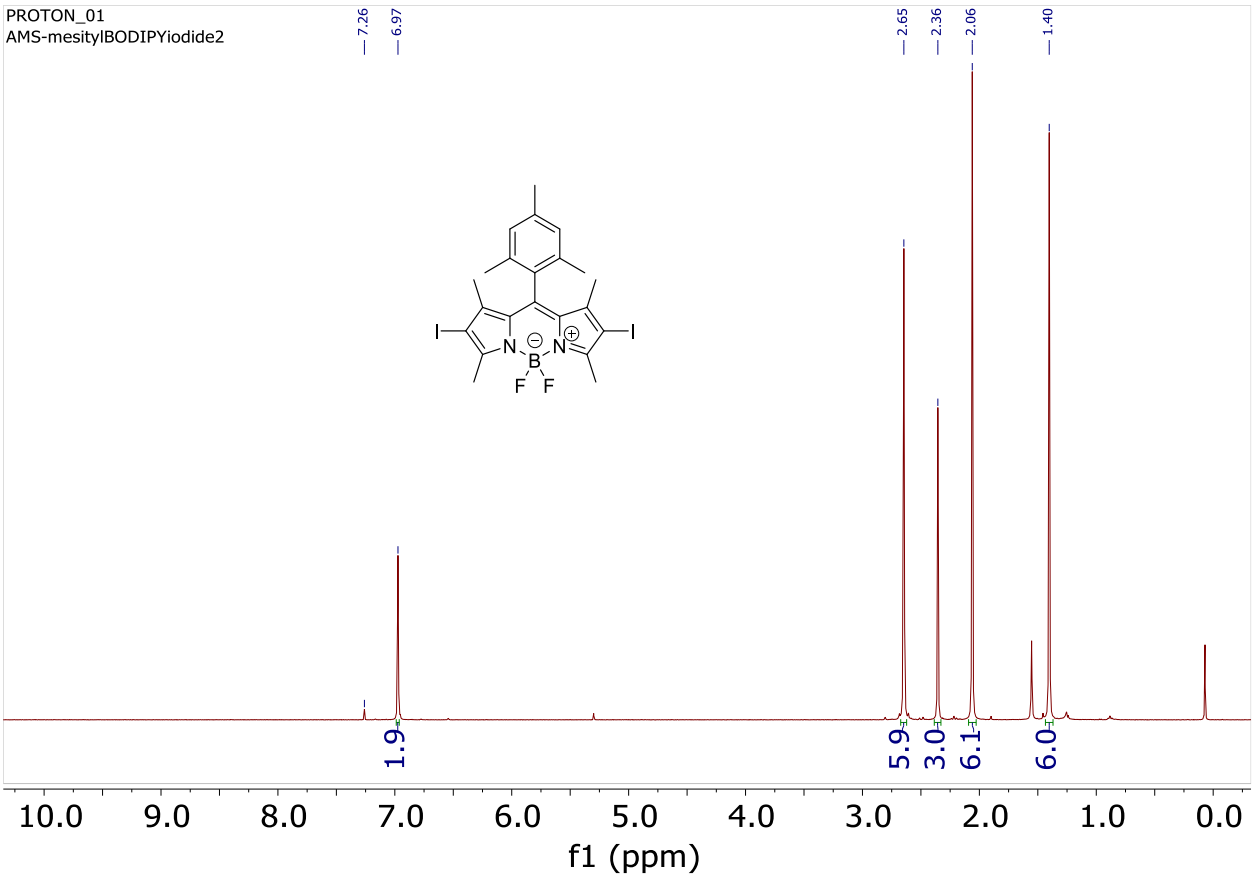


**Figure S37.** $^{1}H$ NMR of **Mes-I** (**S4**) BODIPY in $CDCl_3$

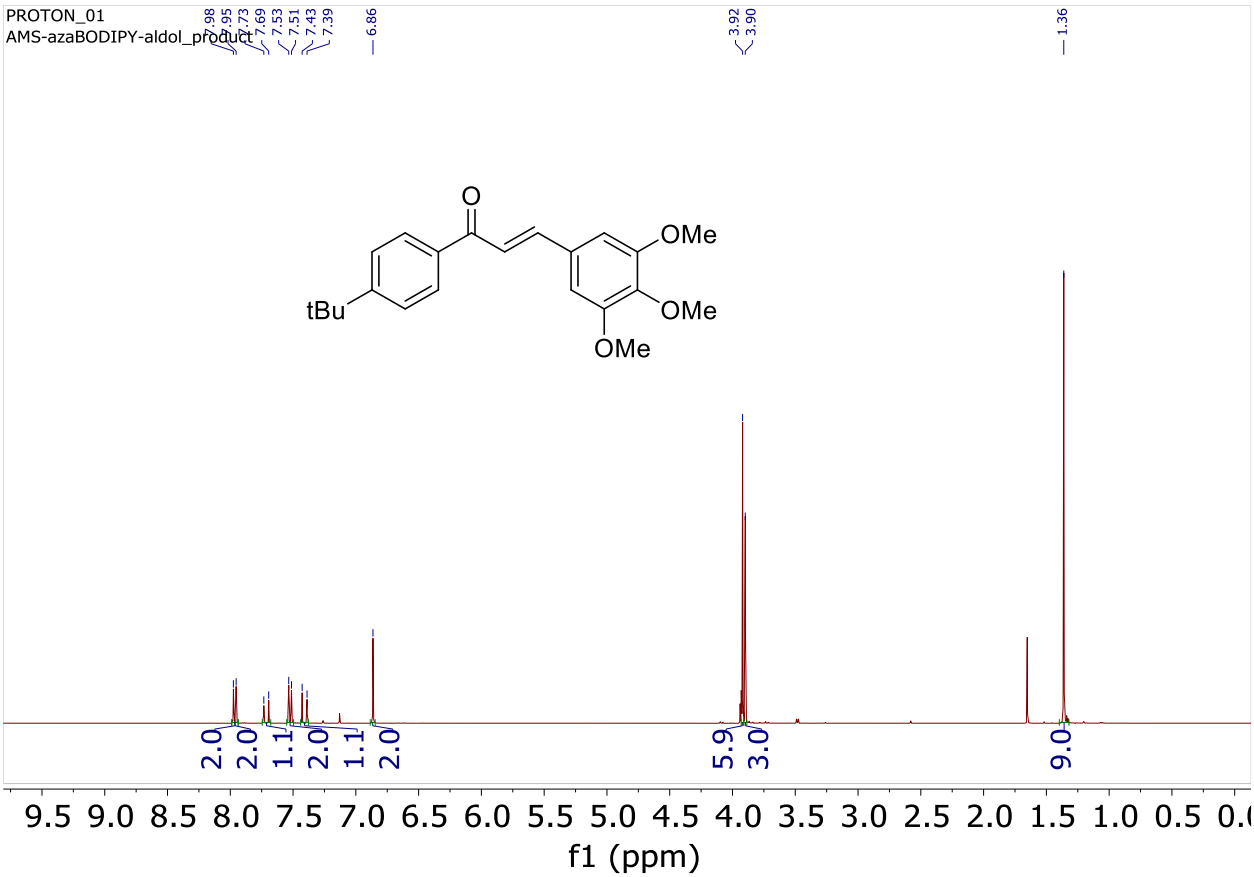


**Figure S38.** $^{1}H$ NMR of Aldol Intermediate (**S5**) in $CDCl_3$

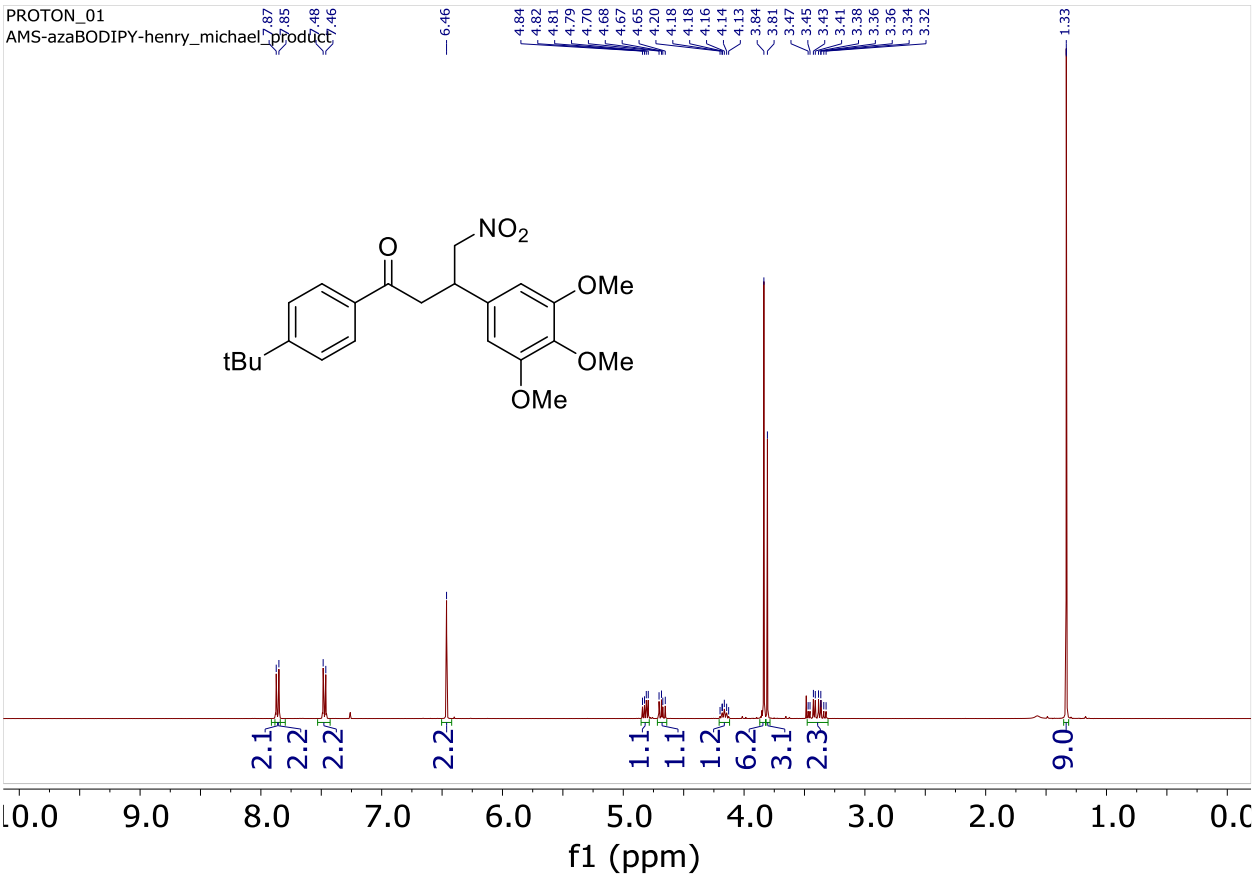


**Figure S39.** $^{1}H$ NMR of Henry-Michael intermediate (**S6**) in $CDCl_3$

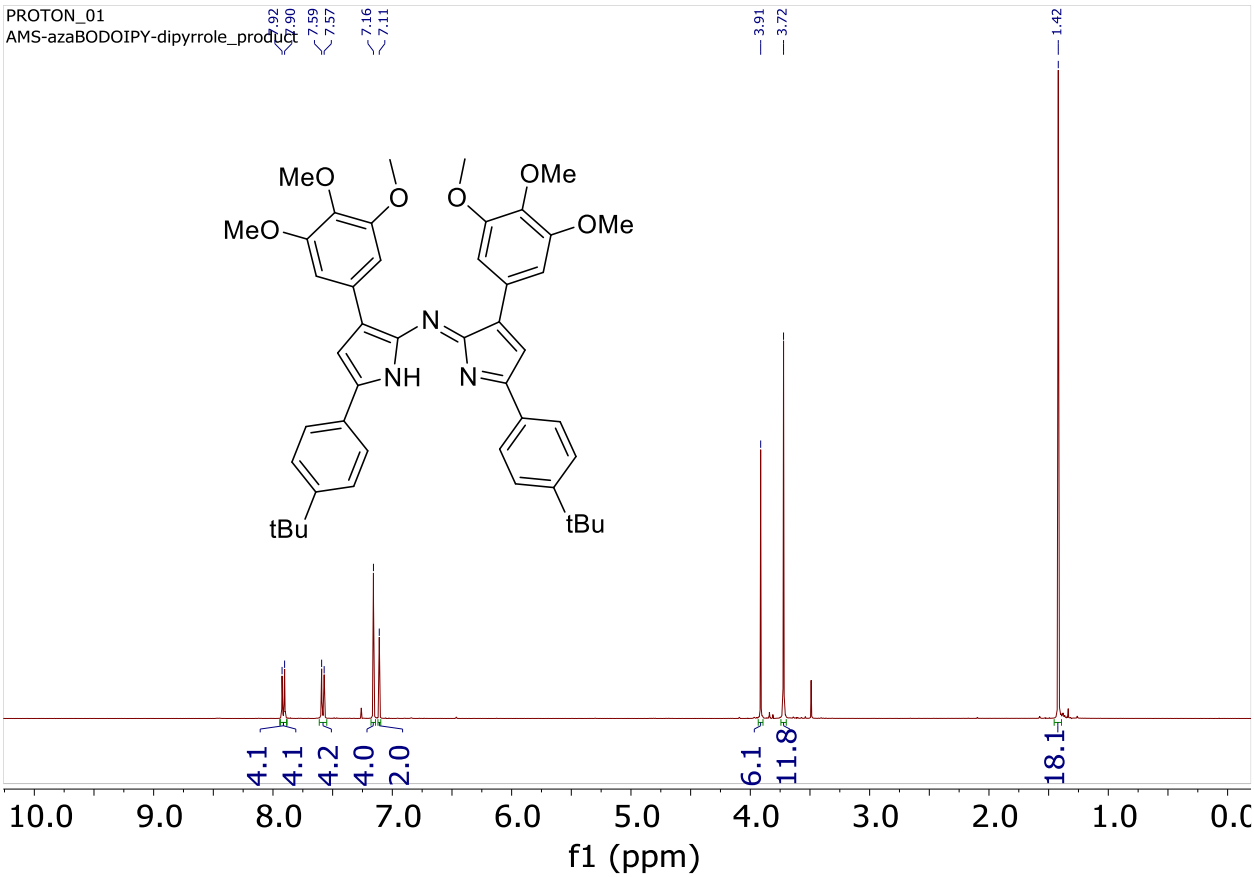


**Figure S40.** $^{1}$H NMR of aza-dipyrrole intermediate (**S7**) in $CDCl_3$

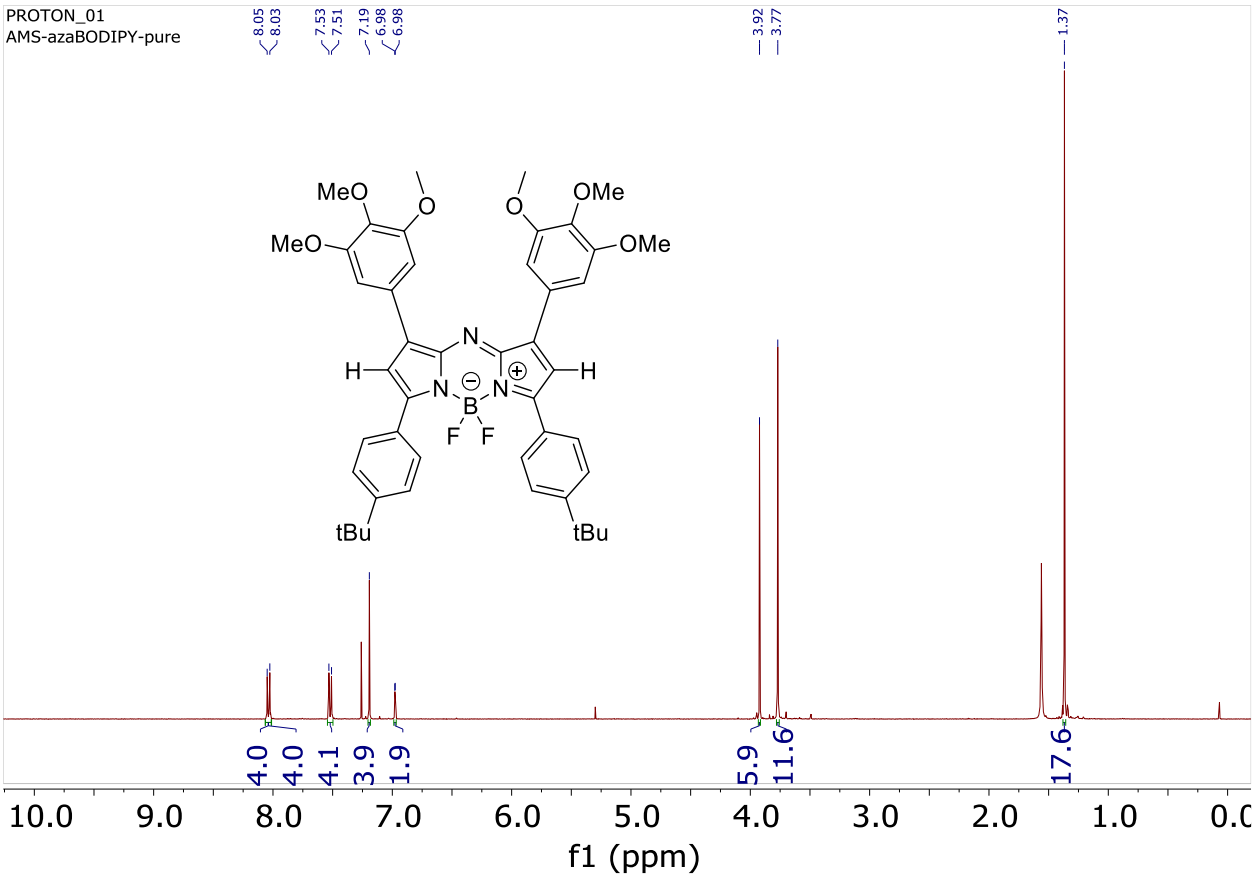


**Figure S41.** $^{1}H$ NMR of **aza-H** BODIPY (**S8**) in $CDCl_3$

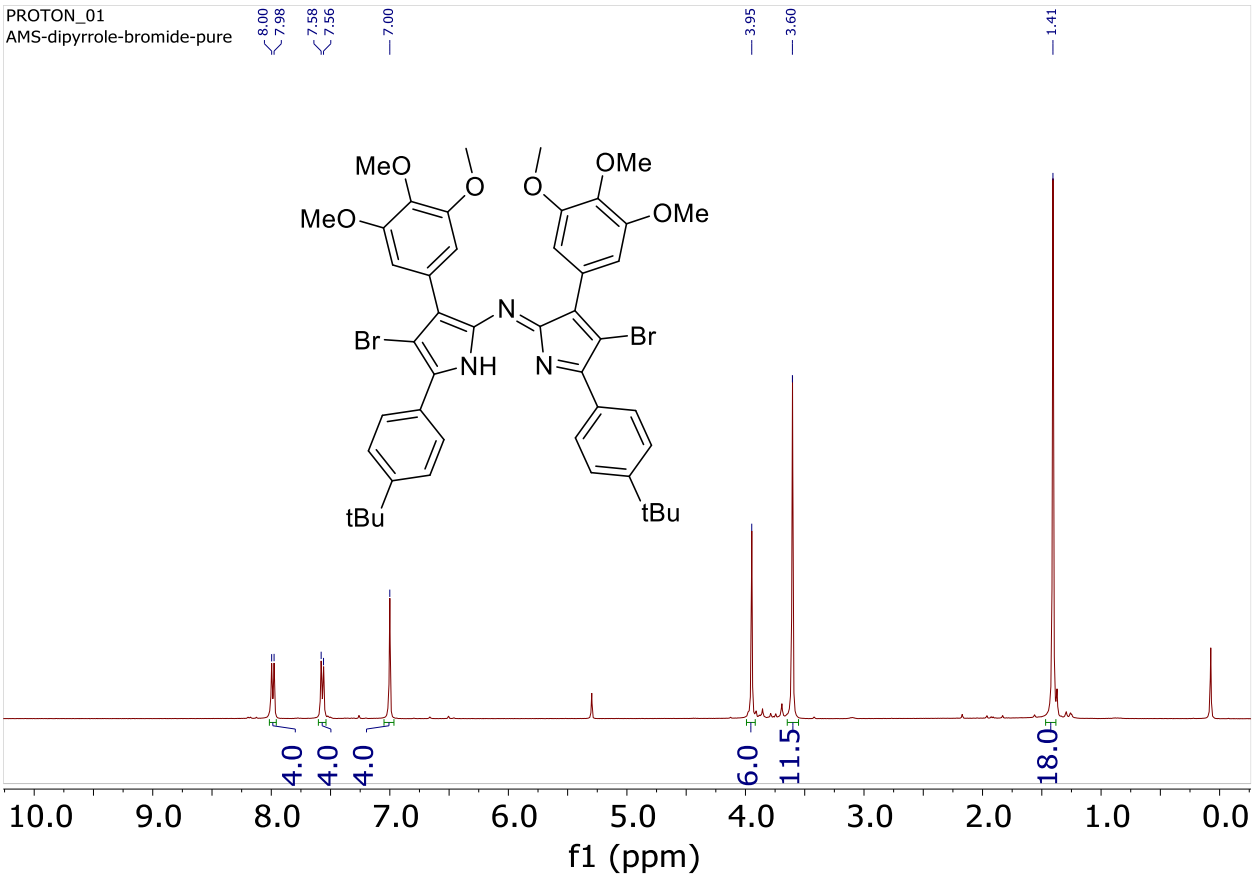


**Figure S42.** $^{1}H$ NMR of aza-Br-dipyrrole intermediate (**S9**) in $CDCl_3$

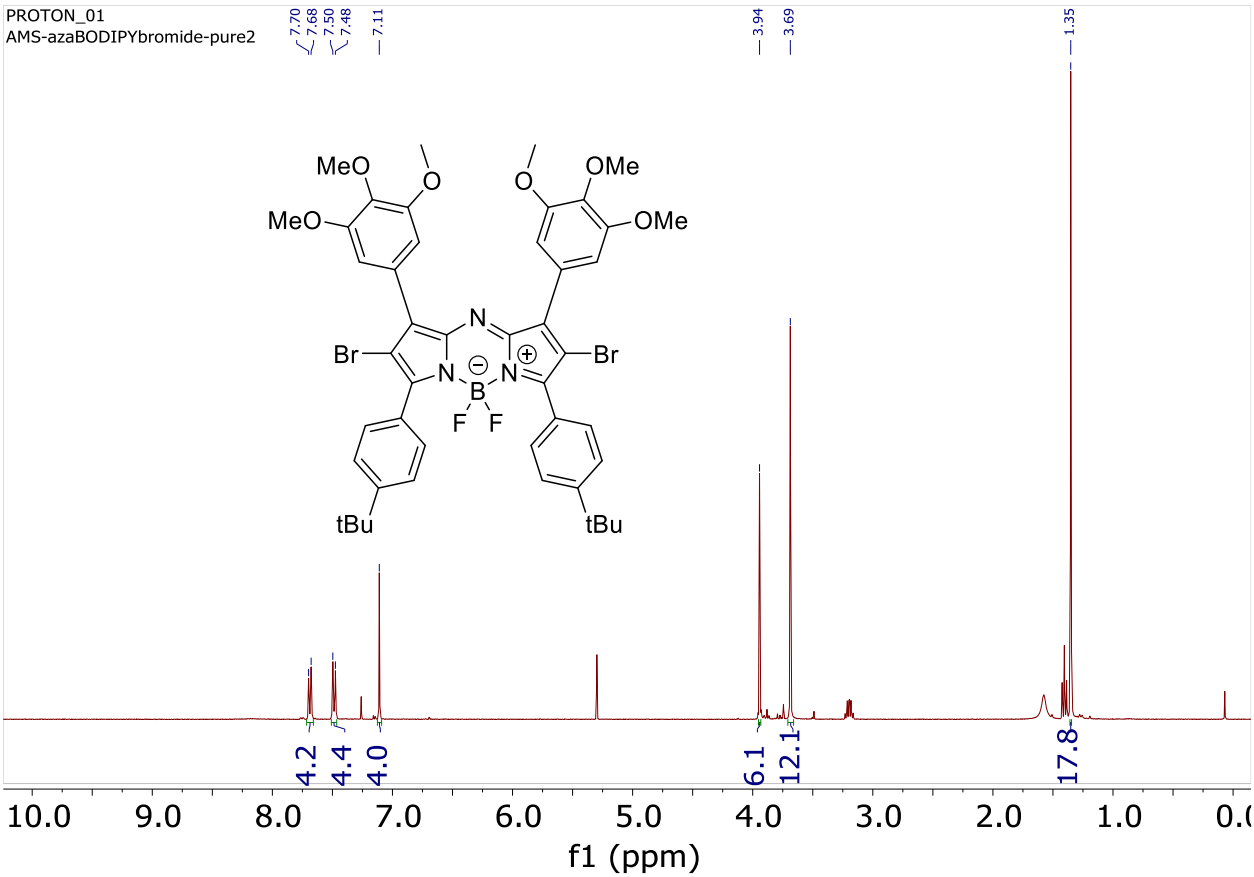


**Figure S43.** $^{1}$H NMR of **aza-Br** BODIPY (**7**) in $CDCl_3$

## REFERENCES


(1) Allen, M. J.; Page, Z. A. Tracking Photocuring via ATR-FT-IR with Illumination through the ATR Element. *Spectrosc. Appl. Noteb.* **2020**, *35* (2), 78.

(2) Le, A. K.; Bender, J. A.; Arias, D. H.; Cotton, D. E.; Johnson, J. C.; Roberts, S. T. Singlet Fission Involves an Interplay between Energetic Driving Force and Electronic Coupling in Perylenediimide Films. *J. Am. Chem. Soc.* **2018**, *140* (2), 814–826.

(3) Azzaro, M. S.; Le, A. K.; Wang, H.; Roberts, S. T. Ligand-Enhanced Energy Transport in Nanocrystal Solids Viewed with Two-Dimensional Electronic Spectroscopy. *J. Phys. Chem. Lett.* **2019**, *10* (18), 5602–5608.

(4) Thorat, K. G.; Kamble, P.; Ray, A. K.; Sekar, N. Novel Pyrromethene Dyes with N-Ethyl Carbazole at the Meso Position: A Comprehensive Photophysical, Lasing, Photostability and TD-DFT Study. *Phys. Chem. Chem. Phys.* **2015**, *17* (26), 17221–17236.

(5) Wang, X. F.; Yu, S. S.; Wang, C.; Xue, D.; Xiao, J. BODIPY Catalyzed Amide Synthesis Promoted by BHT and Air under Visible Light. *Org. Biomol. Chem.* **2016**, *14* (29), 7028–7037.

(6) Lu, H.; MacK, J.; Yang, Y.; Shen, Z. Structural Modification Strategies for the Rational Design of Red/NIR Region BODIPYs. *Chem. Soc. Rev.* **2014**, *43* (13), 4778–4823.

(7) Adarsh, N.; Avirah, R. R.; Ramaiah, D. Tuning Photosensitized Singlet Oxygen Generation Efficiency of Novel Aza-BODIPY Dyes. *Org. Lett.* **2010**, *12* (24), 5720–5723.

(8) Sheng, W.; Wu, Y.; Yu, C.; Bobadova-Parvanova, P.; Hao, E.; Jiao, L. Synthesis, Crystal Structure, and the Deep Near-Infrared Absorption/Emission of Bright AzaBODIPY-Based Organic Fluorophores. *Org. Lett.* **2018**, *20* (9), 2620–2623.

(9) Lovell, L. G.; Berchtold, K. A.; Elliott, J. E.; Lu, H.; Bowman, C. N. Understanding the Kinetics and

Network Formation of Dimethacrylate Dental Resins. *Polym. Adv. Technol.* **2001**, *12* (6), 335–345.
(10) Würth, C.; Grabolle, M.; Pauli, J.; Spieles, M.; Resch-Genger, U. Relative and Absolute Determination of Fluorescence Quantum Yields of Transparent Samples. *Nat. Protoc.* **2013**, *8* (8), 1535–1550.
(11) Zimbron, J. M.; Passador, K.; Gatin-Fraudet, B.; Bachelet, C. M.; Plazuk, D.; Chamoreau, L. M.; Botuha, C.; Thorimbert, S.; Salmain, M. Synthesis, Photophysical Properties, and Living Cell Imaging of Theranostic Half-Sandwich Iridium-4,4-Difluoro-4-Bora-3a,4a-Diaza-s-Indacene (BODIPY) Dyads. *Organometallics* **2017**, *36* (18), 3435–3442.
(12) Marenich, A. V.; Cramer, C. J.; Truhlar, D. G. Universal Solvation Model Based on Solute Electron Density and on a Continuum Model of the Solvent Defined by the Bulk Dielectric Constant and Atomic Surface Tensions. *J. Phys. Chem. B* **2009**, *113* (18), 6378–6396.
(13) Romańczyk, P. P.; Kurek, S. S. The Reduction Potential of Diphenyliodonium Polymerisation Photoinitiator Is Not −0.2 V vs. SCE. A Computational Study. *Electrochim. Acta* **2017**, *255*, 482–485.
(14) Romańczyk, P. P.; Kurek, S. S. Reliable Reduction Potentials of Diaryliodonium Cations and Aryl Radicals in Acetonitrile from High-Level Ab Initio Computations. *Electrochim. Acta* **2020**, *351*, 136404.
(15) Sabatini, R. P.; McCormick, T. M.; Lazarides, T.; Wilson, K. C.; Eisenberg, R.; McCamant, D. W. Intersystem Crossing in Halogenated Bodipy Chromophores Used for Solar Hydrogen Production. *J. Phys. Chem. Lett.* **2011**, *2* (3), 223–227.
(16) Lee, Y.; Malamakal, R. M.; Chenoweth, D. M.; Anna, J. M. Halogen Bonding Facilitates Intersystem Crossing in Iodo-BODIPY Chromophores. *J. Phys. Chem. Lett.* **2020**, *11* (3), 877–884.
(17) Whited, M. T.; Djurovich, P. I.; Roberts, S. T.; Durrell, A. C.; Schlenker, C. W.; Bradforth, S. E.; Thompson, M. E. Singlet and Triplet Excitation Management in a Bichromophoric Near-Infrared-Phosphorescent BODIPY-Benzoporphyrin Platinum Complex. *J. Am. Chem. Soc.* **2011**, *133* (1), 88–96.
(18) Rachford, A. A.; Ziessel, R.; Bura, T.; Retailleau, P.; Castellano, F. N. Boron Dipyrromethene (Bodipy) Phosphorescence Revealed in [Ir(Ppy) 2(Bpy-C - C-Bodipy)]+. *Inorg. Chem.* **2010**, *49* (8), 3730–3736.
(19) Roberts, S. T.; Schlenker, C. W.; Barlier, V.; McAnally, R. E.; Zhang, Y.; Mastron, J. N.; Thompson, M. E.; Bradforth, S. E. Observation of Triplet Exciton Formation in a Platinum-Sensitized Organic Photovoltaic Device. *J. Phys. Chem. Lett.* **2011**, *2* (2), 48–54.
(20) Van Stokkum, I. H. M.; Larsen, D. S.; Van Grondelle, R. Global and Target Analysis of Time-Resolved Spectra. *Biochim. Biophys. Acta - Bioenerg.* **2004**, *1657* (2–3), 82–104.
(21) Miao, X.; Hu, W.; He, T.; Tao, H.; Wang, Q.; Chen, R.; Jin, L.; Zhao, H.; Lu, X.; Fan, Q.; et al. Deciphering the Intersystem Crossing in Near-Infrared BODIPY Photosensitizers for Highly Efficient Photodynamic Therapy. *Chem. Sci.* **2019**, *10* (10), 3096–3102.